Universität Bremen

ALFRED-WEGENER-INSTITUT
HELMHOLTZ-ZENTRUM FÜR POLAR- UND MEERESFORSCHUNG

Determination of acute protein biosynthesis rates in the blue mussel *Mytilus edulis*: The role of hemolymph parameters in temperature-dependent growth

Master's Thesis

by Franziska Kupprat

submitted to the Department 2 Chemistry/Biology

at the University Bremen

in Bremen, April 2014

Title picture © Alexander Semenov

Master's thesis

in the course of the M. Sc. program "Marine Biology"

at the University of Bremen

supervised by

1. Prof. Dr. Hans-Otto Pörtner

Department for Integrative Ecophysiology
Alfred Wegener Institute Helmholtz Centre for Polar and Marine Research

2. Prof. Dr. Wilhelm Hagen

Marine Zoology
University of Bremen

direct supervision by

Dr. Christian Bock

Department for Integrative Ecophysiology
Alfred Wegener Institute Helmholtz Centre for Polar and Marine Research

Contents

Abstract

Climate change leads to increasing water temperatures and the question how that may effect marine ectothermic communities needs to be answered. It is commonly known that marine ectothermic animals have an optimum temperature range and grow less efficient at higher temperatures. For a better understanding and to model potential population dynamics, not only ecological, but also physiological data are needed. Therefore, this study aimed to investigate cause and effect relation of temperature-dependent growth. The temperature itself is not the only factor causing temperature-dependent growth, since it affects body fluid parameters, such as extracellular PO_2, PCO_2 and pH as well as other parameters of the carbonate system. It is unclear, which of these factors is/are the main factor(s) determining temperature-dependent growth in marine ectotherms. This study investigated the specific effects of temperature and pH, while specifically controlling PO_2 and PCO_2, on protein biosynthesis as a measure for somatic growth of the blue mussel *Mytilus edulis*, which serves as a model organism for marine ectotherms. Protein biosynthesis was measured directly via ^{13}C- phenylalanine incorporation into proteins of isolated gill tissue of *M. edulis* using ^{13}C- NMR spectroscopy. The control incubation led to extremely variable protein biosynthesis rates and was therefore neglected for further interpretation of the results. The remaining four treatments revealed significant differences between those treatments that differed PO_2 and PCO_2 ($p<0.05$). Increased temperature, independent of other hemolymph parameters, though, did not affect protein biosynthesis when the other hemolymph parameters were constant ($p>0.05$). Further, pH was most likely not the determining factor for temperature-dependent growth, although some samples still need to be measured in order to further confirm this preliminary evidence. These findings led to the conclusion that PO_2, PCO_2 and/or bicarbonate concentrations are most likely the main factors to trigger temperature-dependent growth.

Figures &Tables

Figures

Tables

Tables in Appendix

Abbreviations

°C	Degree Celsius
^{1}H	Hydrogen isotope with atomic weight of 1 u
^{13}C	Carbon isotope with atomic weight of 13 u
^{15}N	Nitrogen isotope with atomic weight of 15 u
AU	Arbitrary unit
$CaCl_2$	Calcium chloride
cAMP	Cyclic adenosinemonophosphate
CO_2	Carbon dioxide molecule
DO	Dissolved oxygen/Oxygen saturation
D_2O	Deuteriumoxide, deuterated water
h	Hour
HCl	Hydrogen chloride
HEPES	4-(2-hydroxyethyl)-1-piperazineethanesulfonic acid (buffering agent)
hPa	Hectopascal
IPCC	Intergovernmental Panel on Climate Change
KCl	Potassium chloride
km	Kilometer
KOH	Potassiumhydroxide
µL	Microatmosphere
$MgCl_2$	Magnesium chloride
$MgSO_4$	Magnesium sulfate
Milli Q	Purified water
min.	Minute
µL	Microliter
mL	Milliliter
mm	Millimeter
N_2	Nitrogen molecule
NaCl	Sodium chloride
$NaHCO_3$	Sodium bicarbonate
NMR	Nuclear magnetic resonance
NaOH	Sodiumhydroxide
O_2	Oxygen molecule
OCLTT	Oxygen- and capacity limited thermal tolerance
PCA	Perchloric acid ($HClO_4$), also Hyperchloric acid
pH	Potentia Hydrogenii (*lat.* "power of hydrogen")
pH_e	Extracellular pH
pH_i	Intracellular pH
P_{air}	Atmospheric pressure of air
PCO_2	Partial pressure of carbon dioxide
PO_2	Partial pressure of oxygen
ppm	Parts per million
psu	Practical salinity unit
sAC	Soluble adenylyl cyclase
SEM	Standard error of the mean
TSP	3-(trimethylsilyl) propionic 2,2,3,3d4 acid sodium salt

1. Introduction

1.1 Global warming and thermal tolerance

Temperature is one of the crucial abiotic factors in life on our planet since it affects all biological processes from the effects on enzyme kinetics on cellular level to the distributional patterns of species on ecosystem level. Atmospheric global temperature is increasing due to anthropogenic emissions of greenhouse gases, mainly carbon dioxide (CO_2). The Intergovernmental Panel on Climate Change (IPCC) recently stated, that global temperature has already increased by 0.78°C from the average of the period 1850-1900 to the average of the period 2003-2012 and are likely to increase further by at least 1.5°C by the end of the 21st century (IPCC 2013). One of the main heat absorbance systems of our planets are the oceans and thereby temperature of the global upper ocean (upper 75 m) increased by an average of 0.11°C per decade from 1971 to 2010 (IPCC 2013). Further increase of temperature is considered to significantly affect marine ecosystems by narrowing the ecological temperature niches of animals, which have specialized to certain temperatures over millions of years in the course of evolution. Naturally, increasing temperatures will primarily affect species, which already live on their upper thermal tolerance limit (IPCC 2014). For instance, species distributional ranges will narrow or shift towards colder regions, either horizontally towards colder habitats in the north or south or vertically into deeper water layers. Examples are the poleward shifting populations of the Atlantic cod *Gadus morhua* (Perry *et al.* 2005) and the retreating populations of the blue mussel *Mytilus edulis* by 7.5 km per year at the southern distributional range at the East coast of the USA (Jones 2009, 2010). As a consequence of changes in species distribution, species richness may be decreased due to keystone species removal or decimation in ecosystems and changes in community structures are likely (IPCC 2014). For instance, experimentally removing mussel patches of a *Mytilus edulis* bed markedly reduced the abundance of epibenthic crustaceans in Scotland (Ragnarsson and Raffaeli 1999). Inevitably, the question arises, how marine ectothermic animals can cope with the expected changes. The answer to this question lies in an animal's potential for metabolic adjustment to temperature changes, which can occur on different time scales. The definitions for these different levels of adjustments will be used in this thesis according to Clarke (1991):

- ACCLIMATION is the adjustment of an organism to new conditions in the laboratory, e.g. acute adjustment to new temperatures in a laboratory experiment (short-term response to experimental temperature)
- ACCLIMATIZATION is the adjustment of an animal to environmental changes in tidal, daily, seasonal or inter-annual intervals, e.g. temporary adjustment to survive high

temperatures during low tide or daily sunshine exposure, hot summer conditions or El Niño events (adjustment for limited time)

- ADAPTATION is the evolutionary adjustment of physiology to environmental conditions (this may include acclimatization), e.g. the genetic evolution of heat responses like heat shock proteins.

In the course of evolutionary adaptation competition led to animals distributing over the globe in different thermal niches and adapting to them in sometimes very specialized ways, e.g. the adaptations of stenothermic marine ectothermic animals to very cold, but relatively stable temperatures in the Antarctic.

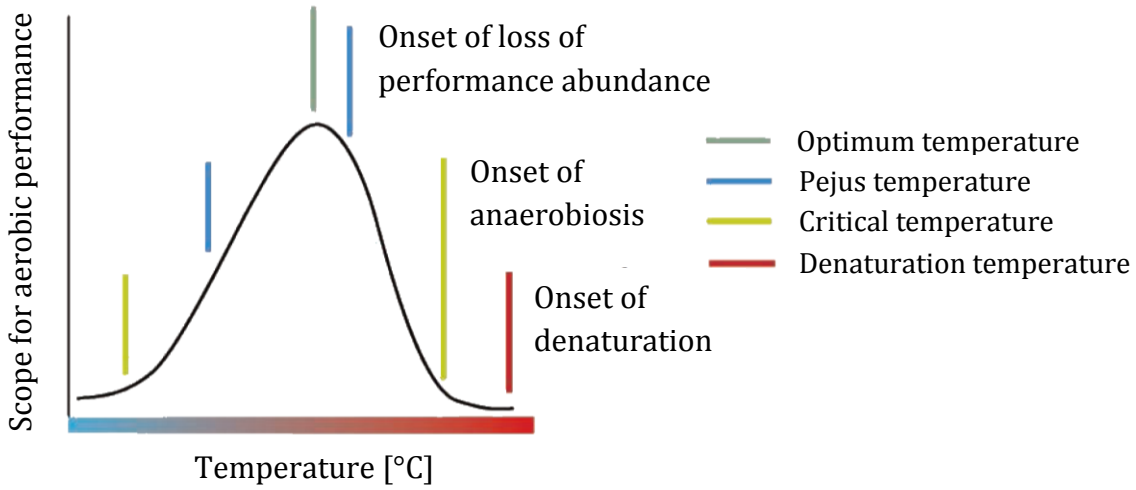

Figure 1 Visualization of the OCLTT theory. Scope for aerobic performance (e.g. somatic growth or exercise etc.) as a function of temperature [°C]. The optimum temperature range is depicted in gray, pejus temperatures in blue, critical temperatures in yellow and the red line indicates the temperature, at which denaturation starts (modified after Pörtner and Farrell 2008).

The theory of oxygen- and capacity-limited thermal tolerance (OCLTT) is based on "Shelford's Law of tolerance" and can be used to explain the adaptations to ecological temperature niches (Frederich and Pörtner (2000), further developed by Pörtner 2001, 2002, 2010, 2012, for a review see Pörtner and Farrel 2008). The OCLTT concept (Figure 1) states, that animals have a species-specific optimum temperature range for aerobic performance, which can be measured e.g. as somatic growth, reproduction, exercise, immune capacity, behaviors and/or specific dynamic action (Pörtner and Farrel 2008). Scope for performance is highest in the optimum temperature range, which is limited by the pejus temperatures in both directions, i.e. higher or lower temperatures. Beyond pejus (meaning "getting worse") temperatures, performance is decreasing due to a less efficient oxygen supply, measurable as decreasing partial pressure of

oxygen (PO_2). Further, beyond high and low critical temperatures, performance is limited to a passive existence due to anaerobic metabolism and is therefore time-limited (Pörtner and Farrel 2008). According to the Van't Hoff equation, enzymatic processes are decelerated or accelerated by the factor of 2-3 when temperatures decrease or increase, respectively, by 10°C (Q10 temperature coefficient). Hence, with decreasing temperature metabolism slows and as a consequence performance is decreasing, explaining the lowered scope of aerobic performance at low temperatures in the OCLTT model (Figure 1). In contrast, increasing temperatures induce an increase in metabolic rates in marine ectothermic animals, which naturally leads to a higher oxygen demand of the animal. The lowered performance at high temperatures is caused by a mismatch in oxygen availability and oxygen demand, because oxygen availability decreases with increasing temperatures due to decreased physical solubility in the body fluids while capacities of ventilation and/or circulation of marine ectothermic animals are limited. Warming temperatures thereby cause a decrease in the partial pressure of oxygen (PO_2) and an increase in the partial pressure of carbon dioxide (PCO_2) in the body fluids (like hemolymph) of marine ectotherms. An increase of body fluid PCO_2 is closely linked to a decrease in body fluid pH due to enhanced proton generation from the reaction of CO_2 with water (H_2O) into bicarbonate (HCO_3^-) and protons (H^+). Therefore, while body fluid pH decreases, bicarbonate ion concentrations ($[HCO_3^-]$) increase and carbonate ion concentrations ($[CO_3^{2-}]$) decrease with increasing temperatures. The strength of these effects depends on the buffer capacity of the animal's body fluid (Pörtner *et al.* 2004). Most marine ectotherms possess at least a non-bicarbonate buffer system, e.g. by partially protonating amino acid side chains. Bicarbonate itself can also act as a buffer and can be actively accumulated by many marine ectotherms (e.g. Michaelidis *et al.* 2005) to higher concentrations than caused by increased PCO_2 (discussed by Melzner *et al.* 2009).

1.2 The role of hemolymph parameters in temperature-dependent growth

It is still not fully understood, which and how these body fluid parameters or their combination might control temperature-dependent performance and associated trade-offs in the energy budget of marine ectotherms. The energy budget of marine ectotherms consists of maintenance costs and several other parameters, such as reproduction and growth, which can only occur with a surplus of energy when maintenace costs are covered (Sokolova *et al.* 2012). Maintenance costs increase under stress in the pejus temperature range leading to an associated decrease in surplus energy for growth, which may be caused by changes in body fluid parameters. All body fluid parameters, including temperature itself, can affect oxygen transport and energy availability. In this chapter, each hemolymph parameter (Temperature *per se*, PO_2, PCO_2, pH and $[HCO_3^-]$) will be discussed with respect to increasing temperatures and the concomitant effects

on energy budget. In this thesis, PO_2, PCO_2, pH and $[HCO_3^-]$ always refer to the body fluid, i.e. extracellular parameters within the animal or in experiments, if not explicitly stated elsewise.

Temperature itself, independent of the other above mentioned body fluid parameters, has an impact on all enzymatic processes (Q10 temperature coefficient) and can affect secondary and tertiary structure of enzymes as well as their stability. By altering important mitochondrial enzymes, body fluid temperature could affect metabolic processes on cellular level. All proteins and enzymes, including mitochondrial enzymes involved in the generation of oxidative energy, function at a marginal balance of stability and flexibility (Fields 2001). Stability is important for proper ligand binding and to avoid denaturation on the one hand. Flexibility, on the other hand, is crucial for different levels of substrate affinity in different conformational microstates of enzymes (Fields 2001). This marginal balance makes proteins vulnerable to warming above the normally experienced temperatures since temperature can influence secondary and tertiary structure of proteins and increased temperatures can lead to degradation (Somero 2012). The effect of temperature *per se*, independent of its associated changes in body fluid parameters, on somatic growth or other performance parameters, still needs further investigations.

Oxygen supply plays a crucial role in most marine ectotherms since ATP production, as the general energy provider in all cells, is most productive in the aerobic TCA cycle. The role of body fluid PO_2 in temperature-dependent performance was revealed in a study on mammalian hepatocytes, in which hypoxia led to a decreased *in vitro* protein synthesis (Surks and Berkowitz 1971). Further, this relation has been studied on the Antarctic bivalve *Laternula elliptica*: Hemolymph PO_2 was shown to decrease slightly when temperatures increase from optimum to pejus temperatures with a simultaneous increase in oxygen consumption and heartbeat rate. With further increasing temperatures, oxygen consumption as well as heart beat rate collapsed while hemolymph PO_2 decreased dramatically (Peck *et al.* 2002). However, some organisms can cope with anaerobic conditions for a limited time under anaerobic conditions by specialized anaerobic pathways, which can at least partially compensate for ATP generation under a lack of oxygen.

An increase in body fluid PCO_2 (hypercapnia) can be caused either by high PCO_2 in the surrounding seawater or by respiration with insufficient removal of the generated CO_2, either due to a lack of circulation or ventilation, as it is the case when temperatures rise. Effects of temperature-induced hypercapnia were recently investigated for *Mytilus edulis* from a North Sea population: At acutely increased temperatures an increase of hemolymph PCO_2 and a decline in hemolymph pH was coupled to increased oxygen consumption and heart beat rate until critical temperatures, at which heart beat rates decreased (Zittier *et al., submitted*). Investigations of hypercapnia effects on the metabolism of marine ectotherms usually combine increased body

fluid PCO_2 with the associated changes in pH and [HCO_3^-] explained above. However, so far only few studies investigated the specific effects of the parameters independently of each other. For instance, a study by Walsh *et al.* (1988) showed that body fluid PCO_2, pH and [HCO_3^-] each independently of the other parameters affected the hepatic lactate metabolism of rainbow trout *Oncorhynchus mykiss* with stronger specific PCO_2 effects than specific pH or [HCO_3^-] effects. However, in contrast to that, protein biosynthesis of isolated muscle tissue of the marine worm *Sipunculus nudus* was proven to be affected only by decreased hemolymph pH, but not by increased PCO_2 (Langenbuch *et al.* 2006). These findings are in accordance with an earlier study on *S. nudus*, which already suggested extracellular pH (pH_e) to play a key role in metabolic depression (Reipschläger and Pörtner 1996). An impact of pH_e on the metabolism of marine ectotherms is likely, because changes in body fluid pH cause changes in the intracellular pH (pH_i). These changes in pH_i causes an increase in energy demand, because acid-base status needs to be re-established in order to avoid alteration of secondary and tertiary structures, which could result in malfunctions of enzymes (Pörtner 1987, Pörtner *et al.* 2004). Moreover, a regulatory role of pH_i in the selection of amino acids used by catabolism was found in *S. nudus* (Langenbuch and Pörtner 2002). Further, severe acidosis led to inhibited protein biosynthesis rates in hepatocytes of Antarctic fish, which was thought to be mediated by the intracellular pH (Langenbuch and Pörtner 2003). These two studies show the effects a drop in pH_i may have.

To compensate for changes in extracellular pH, most marine ectothermic animals possess a buffer system in the body fluids including non-bicarbonate buffers or bicarbonate itself as described above (chapter 1.1). Michaelidis *et al.* (2005) observed increasing hemolymph PCO_2 and decreasing hemolymph pH resulting in a lowered metabolic rate on whole animal level in the Mediterranean mussel *Mytilus galloprovinciales* with the pH_e being buffered by increased bicarbonate levels, probably dissolved from the shells under high PCO_2. Intracellular pH in that study was re-established after 4 days of high CO_2 exposure. In contrast, Thomsen *et al.* (2010) did not find increased bicarbonate concentrations buffering hemolymph pH under increased PCO_2 in *M. edulis* from the Baltic Kiel Fjord, but found increased metabolic rates under moderate levels of PCO_2 (Thomsen and Melzner 2010). The effects of increased bicarbonate levels on energy metabolism, independent of pH, is linked to an intricate signaling cascade: Bicarbonate levels are involved in intracellular pH sensing (Tresguerres *et al.* 2010a) and can stimulate soluble adenylyl cyclase (sAC) (Chen *et al.* 2000, Tresguerres *et al.* 2010b), which activates cyclic adenosine monophosphate (cAMP), which again induces phosphorylation of protein kinase A (PKA). PKA, at the end of this cascade, phosphorylates, i.e. activates, several proteins of the electron transfer chain, such as Complex I and IV, which leads to an increased ATP synthesis (Zippin *et al.* 2001, Tresguerres *et al.* 2010b). This cascade from elevated bicarbonate levels over sAC over cAMP to PKA activation was fully confirmed in a study on hepatic mitochondria

isolated from mice (Acin-Perez *et al.* 2009). In accordance, the Antarctic fish *L. squamifrons* and *N. rosssii* revealed decreased mitochondrial capacity under chronic hypercapnia, which was partially compensated for by increased capacity of Complex I of the electron transport chain only in *L. squamifrons* (Strobel *et al.* 2013a). Further studies by Strobel *et al.* (2013b) also suggested Complex I activities to define ATP synthesis capacities under hypercapnia through the above-described signaling cascade in the Southern nototheniid *Notothenia angustata*. Hence, changes of bicarbonate levels might be an important process in temperature-dependent growth.

In summary, the results of these studies do not allow the identification of one single parameter that clearly triggers temperature-dependent performance in marine ectotherms. Therefore, a more detailed approach with controlling each body fluid parameter independently of the other parameters is necessary for a deeper understanding of the mechanisms behind thermal tolerance limits. For this study it was assumed, that one of the hemolymph parameters is the main factor to trigger temperature-dependent performance of marine ectothermic animals. I investigated the relevance of hemolymph pH in temperature-dependent protein biosynthesis as a proxy for somatic growth, an important performance parameter, in the model organism *Mytilus edulis* (Mytilidae, Linnaeus 1758). The blue mussel *M. edulis* was chosen since its distribution patterns have recently been reported to be negatively affected by global warming (Jones *et al.* 2009, 2010) and numerous studies on the physiology of *M. edulis* enables very precise and accurate setting of hemolymph parameters (Bayne *et al.* 1976a) (also see chapter 1.3.1). For this study a population from the Baltic Sea was chosen (see chapter 1.3.2). pH was proposed to have the largest effect on protein biosynthesis compared to the other hemolymph parameters, since several studies on marine ectotherms already suggested that extracellular pH may play a key role in metabolic depression (Reipschläger and Pörtner 1996, Langenbuch and Pörtner 2002, 2003, Pörtner *et al.* 2004, Langenbuch *et al.* 2006). PO_2 was considered less likely to determine temperature-dependent growth in *M. edulis* since the species is known to be well adapted to anoxic conditions during shell closure by numerous anaerobic pathways (reviewed in de Zwaan and Mathieu 1992).

1.3 The blue mussel Mytilus edulis

1.3.1 *M. edulis* as a model organism for marine ectotherms

The blue mussel *Mytilus edulis* (Mytilidae, L.) is an important fouling organism, usually occuring on flat or gently sloping coastal areas in boreo-temperate latitudes of the Northern and the Southern hemisphere (Lewis 1964, Suchanek 1985, Seed and Suchanek 1992). They are building dense mussel banks, which form the foundation for a variety of diverse shore communities, which makes it a keystone species in its habitats (Suchanek 1985). For example, Tsuchiya and

Nishihira (1985, 1986) found 69 associated species in *M. edulis* beds in Japan, providing substrate and shelter especially for annelids, arthropods and molluscs. Norling and Kautsky (2008) found 24 associated macrofauna species within *M. edulis* patches in the Baltic Sea, of which 11 did not occur outside the patches. Further, in the Western Baltic, *M. edulis* can make up more than 90% of the macrofauna biomass and up to 99% of the biomass (Enderlein and Wahl 2004) only controlled by the main predators *Carcinaus maenas*, *Asterias rubens* and *Littorina littorea* (Reusch and Chapman 1997, Enderlein and Wahl 2004). Besides its ecological value, *M. edulis* is highly sensitive to pollutants (Donkin *et al.* 1997, Tuffnail *et al.* 2009) and therefore used as a biomonitor in environmental management of coastal areas (Philips 1976a, 1976b, Widdows and Donkin 1989). Furthermore, *M. edulis* serves as an important food resource in many countries and due to this economical importance it is successfully produced in aquaculture (reviewed in Hickman 1992). Consequently, *M. edulis* has served as a marine ectothermic model species for numerous physiological, biochemical and genetic investigations (e.g. Bayne and Worrall 1980; Hawkins et al. 1983, 1985, 1986, 1987, 1989; Hilbish and Zimmerman 1988; Seed and Richardson 1990) and has recently been used to illustrate physiological patterns and mechanisms concerning global climate change in a comprehensive case study (Somero 2012). As they often occur in intertidal zones, blue mussels can withstand relatively wide fluctuations in salinity, temperature, desiccation and oxygen availability (Seed and Suchanek 1992). For example, it is well adapted to short-term hypoxic conditions, which are frequently experienced e.g. during low tides when mussels close their shells to avoid internal desiccation, by the development of several anaerobic pathways (de Zwaan 1983, Zandee *et al.* 1986), generally using malate as the main carbohydrate-derived fuel compared to pyruvate under aerobic conditions (de Zwaan and Mathieu 1992). Therefore, *M. edulis* can compensate for a lack of oxygenic energy production and can cover maintenance costs at least for a while under hypoxic conditions (Sokolova *et al.* 2012).

1.3.2 Temperature-dependent growth in *M. edulis*

Somatic growth of *M. edulis* populations in the North Sea is known to be temperature-dependent. The highest scope for growth was found between 10°C and 20°C for different feeding rations with a strong decline in scope for growth between 20 and 25°C (Bayne et al. 1976b). In accordance, Bayne and Widdows (1978) determined the scope for growth for an estuarine and a fully marine population for different seasons and found the maximum scope for growth between 10 and 20°C during summer compared to decreased scope for growth at lower temperatures in winter. These findings are further confirmed by shell growth analysis depicting maximum growth rates between 15-20°C with a sharp decline at temperatures beyond 20°C (Almada-Villela *et al.* 1982).

Besides its relatively wide thermal tolerance, *M. edulis* displays a remarkable tolerance to salinities ranging between 4 psu like in the inner Baltic (Kautsky 1982) to fully marine salinities at around 40 psu (Lutz and Kennish 1992), e.g. in the Mediterranean Sea. Although reduced salinities below 20 psu have been shown to negatively affect somatic growth (Kautsky 1982, Almada- Vilella 1984), shell thickness (Kautsky 1982, Nagarajan *et al.* 2006) and reproduction (Hrs-Benko 1973, Lutz and Kennish 1992, Westerbom *et al.* 2002) of *M. edulis*, the species seems to favor brackish estuaries and lagoons, most likely due to an increased food availability in these habitats by eutrophication and lowered top-down control due to less tolerant predators (Seed and Suchanek 1992).

For this study a subtidal population of *M. edulis* from the western Baltic Sea (Kiel Fjord) was chosen. Throughout the year, the subtidal population experiences temperatures from 2 to 20°C, a salinity variation between 12 to 20 psu and high nutrient availability due to eutrophication in the Kiel Fjord (HELCOM 2009, Thomsen *et al.* 2013). The population is also exposed to irregular CO_2 upwelling events from anoxic bottom waters in the Kiel Fjord (Hansen *et al.* 1999, Thomsen *et al.* 2010) reaching maximum PCO_2 values of 2500 µatm at the surface (2.5 hPa) during summer and fall (Thomsen *et al.* 2013). Food availability, though, is the more crucial factor for growth and calcification of blue mussels in the Kiel Fjord and can outweigh potential effects of high CO_2 concentrations (Thomsen *et al.* 2013). As mentioned before, the ecological importance of *M. edulis* in the Kiel Fjord is vast, since *M. edulis* makes up a large percentage of the biomass. In Kiel Fjord, *M. edulis* is commonly colonized by the barnacle *Amphibalanus improvisus* and has been shown to out-compete the barnacle under high PCO_2 (Thomsen *et al.* 2013). The main predators in this habitat are the shore crab *Carcinus maenas*, the starfish *Asterias rubens* and the periwinkle *Littorina littorea,* which are top-down controlling *M. edulis* abundances (Reusch and Chapman 1997, Enderlein and Wahl 2004).

Due to the negative effects of reduced salinity on growth the Baltic population of *M. edulis* from the Kiel Fjord population may be more sensitive to other stressors like ocean warming. Moreover, this population is subtidal and therefore not regularly exposed to extreme temperatures, which also may have caused a loss in thermal tolerance.

1.3.4 Size and growth assessment in blue mussels

Several parameters can be used to determine animal size of blue mussels. The easiest and commonly used method is measuring the one-dimensional shell parameters length (maximum anterior-posterior dimension), height (maximum ventral-dorsal dimension) and width (maximum inner-outer dimension of one valve). The relation of two of these parameters can be used for allometric size parameters, for example for an extrapolation of gill surface size (Jones *et al.* 1992). Another parameter to assess animal size can be weight, which may be measured as

whole animal wet or dry weight or the separated weights of shell and soft tissue. Further, the shell cavity volume can be determined by subtracting the replacement volume of the whole closed animal and of the opened shell with all soft tissue removed. Size parameters can be used to assess the condition of mussels. The condition index is a measure for the fitness of the animal and is defined differently in many studies. For mussels and oysters, this was summarized and evaluated by Baird (1958), who suggested, that the best way to determine bivalve condition is the relation of soft tissue wet weight and shell cavity. This condition index has been simplified further by many studies, e.g. Lander *et al.* (2012), who used the ratio of soft tissue dry weight to shell dry weight.

Growth can either be assessed by measuring animal size over time or by the determination of growth increments in the shell via counting growth rings or with the optical laser diffraction technique (Strømgren 1975). On cellular level, growth is strongly coupled to protein biosynthesis (Houlihan 1991) and therefore, as a physiological approach for growth assessment, protein biosynthesis can be determined on isolated cells or tissues as a measure for somatic growth. The physiological approach of growth measurement is much more elaborate, but also much faster and was used in this study on isolated gill tissue of *M. edulis*.

Besides water, proteins make up the second largest part of animal body mass (Houlihan 1991). They are generated through protein synthesis and are constantly degraded, recycled and re-synthesized, a process generally referred to as protein turnover, which is important for maintaining a cell's flexibility and ability to adjust to potential changes in the environment. For marine ectothermic animals protein turnover is generally highest in gill tissue with very high protein synthesis rates coupled to high degradation rates. This has been reported e.g. for fish, octopus and crabs (for review see Houlihan 1991). In contrast, white muscle tissue is one of the most efficient protein synthesizing tissues with rather slow protein synthesis rates, but as well slow degradation. In *M. edulis* gill tissue proteins are mainly composed of mucous glycoproteins (Ahn *et al.* 1988), a fibrillar protein responsible for the musculoskeletal structure (Brown 1952) and dynein proteins responsible for cilia beating (ciliary ATPase dynein) (Stephens and Prior 1992). Further, gill tissue contains large portion of metallothioneins, a protein class specialized to eliminate and metabolize accumulated organic contaminants and can therefore bind heavy metals and free radical scavengers (Gosling 2003). When investigating thermal stress, heat-shock proteins like HSP70 or HSP90 should also be taken into account as well as proteins synthesized for proteolysis (i.e. protein degradation) such as ubiquitin, sequestromal proteins, T-complex proteins and amino acid transporters (Lyons *et al.* 2003, Anestis *et al.* 2007, for review see Somero 2012).

An essential amino acid in animal protein is phenylalanine, which is mainly used for protein biosynthesis and plays only minor roles in other metabolic pathways. For example, it can be transformed into tyrosine by hydroxylation of the aromatic ring. Phenylalanine is an unpolar molecule and large extracellular quantities lead to a quick accumulation in the cytosol. Garlick *et al.* (1980) harnessed this characteristic when developing the method of flooding-dose used to follow phenylalanine incorporation into proteins using radioactive ^{14}C- tracers. It was also shown that phenylalanine is superior over lysine for this method due to lowered side effects on other metabolic processes (McNurlan *et al.* 1979, Garlick *et al.* 1980). This method has been further developed by using stable isotopes, i.e. ^{13}C- phenylalanine which can be traced in nuclear magnetic resonance (NMR) spectroscopy. The flooding-dose method is based on four assumptions, which need to be considered when applying this method (Garlick *et al.* 1980, 1983; Houlihan *et al.* 1995; Owen *et al.* 1999):

(1) The highly concentrated free amino acid rapidly diffuses into the cell along the concentration gradient
(2) The high concentration of the free amino acid itself does not affect protein biosynthesis
(3) The intracellular pool of the free amino acid stays stable over time or declines slightly; and
(4) The incorporation of the amino acid into proteins is linear over time.

The proteins in the tissue samples can be separated from the cytosolic free amino acids by applying a gradient of a strong acid, e.g. Perchloric acid $HClO_4$ and measuring ^{13}C concentrations in both fractions as it has been applied on rats by Garlick *et al.* (1980) and developed further by e.g. Owen *et al.* (1999), Langenbuch *et al.* (2006) or Wittmann *et al.* (2008). The latter two studies both applied the flooding-dose method with ^{13}C- phenylalanine investigating protein biosynthesis on isolated muscle tissue of the marine worms under different PCO_2 and pH levels or different temperatures, respectively. These experiments showed linearly increasing incorporation of the ^{13}C- labeled amino acid into proteins over seven hours. Protein extracts of these samples were analyzed by ^{13}C-spectroscopy with a multiplet signal for ^{13}C-labeled phenylalanine at 129 ppm (parts per million). Furthermore, Stapp (2011) analyzed protein biosynthesis of isolated hepatocytes of *Pachycara brachycephalum* at different temperatures. Cytosolic and protein extracts of the isolated cells were analyzed by ^{1}H-NMR spectroscopy detecting the hydrogen bound to ^{13}C atoms with a multiplet signal at 7.37 ppm (Stapp 2011). ^{1}H-NMR spectroscopy has the advantage that measurements are much faster compared to the less sensitive ^{13}C-NMR spectroscopy.

1.4 Aim of this study and working hypotheses

The aim of the study was to shed light on the mechanisms behind temperature-dependent growth. The specific effects of temperature and pH on the protein biosynthesis rates of *M. edulis* from the Kiel Fjord population were determined applying the flooding-dose method using ^{13}C-labeled phenylalanine as a tracer. For this, isolated gill tissue of *M. edulis* was incubated for 9h with ^{13}C- phenylalanine with an intermediate sample at 6h and a non-incubated control at 0h to study temperature-dependent protein biosynthesis at different temperatures and pH values. ^{13}C-phenylalanine incorporation into proteins was followed by high-resolution NMR spectroscopy and thereby protein synthesis rates were determined as a measure for somatic growth. Gill tissue was chosen since it is metabolically highly active and is not involved in reproduction processes. Further, the tissue is very thin and therefore oxygen and nutrient supply during the incubations is most likely better than in denser tissue like mantle, muscle or foot. This study analyzed the specific effects of increased temperature independent of the correspondent hemolymph parameters PO_2, PCO_2 and pH and the specific effect of decreased pH independent of temperature, PO_2 and PCO_2 on protein biosynthesis of *M. edulis* from the Kiel Fjord population.

Data on the mechanisms of temperature-dependent protein biosynthesis can provide relevant information on the limiting factors for the scope for somatic growth of *M. edulis* and can be used in individual-based population models (Grimm and Railsback 2005) to estimate an effect of global warming on the population of the ecologically and economically important species. So far individual-based modeling has been applied for an off-shore *Mytilus galloprovinciales* farm and mainly focused on carbon nitrogen and phosphorous fluxes (Brigolin *et al.* 2009).

For this study, the following two hypotheses were formulated, both against the background of the general hypothesis, that one determining factor triggers the mechanism of temperature-dependent growth in marine ectotherms.

1. ^{13}C- phenylalanine incorporation into proteins of isolated muscle tissues will decrease with decreasing pH and constant PCO_2, PO_2 and temperature, indicating decreased somatic growth.
2. Protein biosynthesis rates will not decrease at elevated temperatures when PO_2, PCO_2 and pH will be kept constant.

2. Material & Methods

2.1 Determination of hemolymph PO_2 *during acute temperature increase*

The values for hemolymph PO_2 at different temperatures were determined in a pre-experiment within this study since there is no reliable data available on hemolymph PO_2 of *M. edulis*. For this purpose, twenty individuals of *M. edulis* (size range: 60-80 mm shell length), collected from Kiel Fjord (54°20'N, 10°10'E) were cultivated at 10°C with a salinity of 16 psu for one week with daily water exchange and feeding. After one week, hemolymph samples were extracted from the posterior adductor muscle (PAM) of each mussel with a gastight Hammilton ® syringe and PO_2 was subsequently measured within the syringe using a TX micro- optode (PreSens Precision Sensing GmbH, Germany). The water temperature was then increased with a rate of 0.2°C/h to 16°C and stayed at 16°C for five more days. Hemolymph samples from the same individuals were extracted again and hemolymph PO_2 was determined. The same procedure was then operated for 22°C and 25°C. The TX micro- optodes were calibrated every day of measurement at the respective temperature according to the protocol given by the producer with a two- point calibration in $NaSO_4$ for 0% oxygen and in an air cushion above seawater (16psu) equilibrated with air for 100% oxygen. Oxygen content (in % air saturation) was measured every second over several minutes. Two typical measurement courses over time are displayed in Figure M1. The micro- optode always needed a little time to equilibrate to the surrounding medium, which is represented in an initial decline of oxygen content (Figure 2). Hence, the first 30 measurement values after exposing the optode to the hemolymph were neglected and the subsequent 30 values were analyzed as oxygen content in the hemolymph (gray shaded area in Figure 2). Some measurements drifted slightly upwards (Figure 2A) or downwards (Figure 2B) after initial stabilization and in order to minimize the influence of this drift only 30 values were analyzed as oxygen content after neglecting the first 30 values after exposure of the optode to the hemolymph. The oxygen content (in % air saturation) was converted into partial pressure of oxygen (PO_2 [hPa]) via Equations 1 and 2.

Equation 1: $PO_{2\ hemolymph} = DO/100 * PO_{2\ air}$, whereas

Equation 2: $PO_{2\ air} = (P_B - P_{H_2O}) * \varphi_{O_2}$

$PO_{2\ hemolymph}$: partial pressure of oxygen in the hemolymph of *M. edulis* [hPa]

DO: dissolved oxygen [% air saturation]

$PO_{2\ air}$: partial pressure of oxygen in the atmosphere [hPa], calculated from the vapor pressure of seawater at the respective temperature and from the barometric pressure of the respective day

φ_{O2}: percent by volume of oxygen in atmosphere (fixed value of 0.209)

P_B: barometric pressure [hPa] in the atmosphere at the respective day of measurement (wetter.com)

P_{H2O}: vapor pressure of seawater [hPa] depending on the respective temperature (see Table 1)

Table 1 Vapor pressure of seawater [hPa] at different temperatures [°C] (Dejours 1975, values for 22°C extrapolated from values for 20°C and 25°C).

Temperature [°C]	Vapor pressure of seawater [hPa]
10	12.266
16	18.318
22	25.331
25	31.731

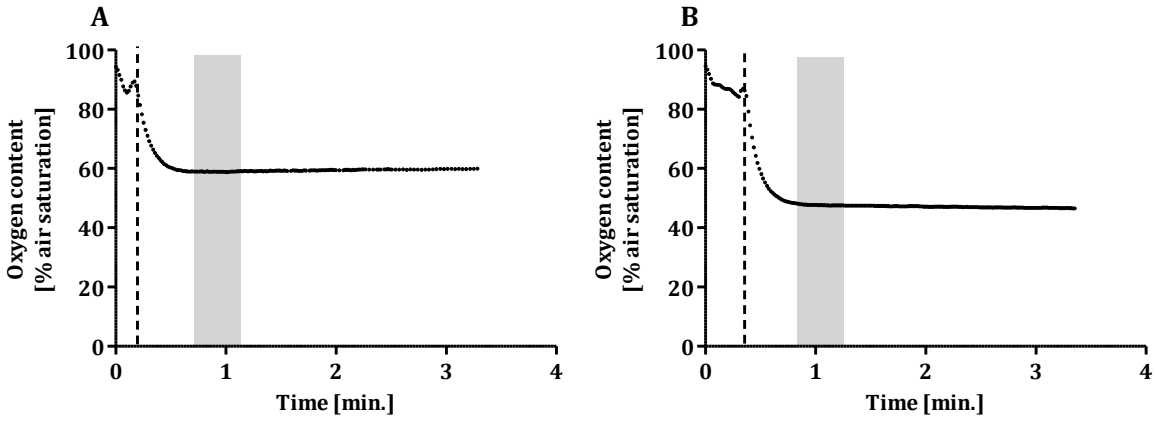

Figure 2 Two typical time courses of oxygen measurements in the hemolymph samples of *M. edulis* at 22°C with **A)** a slight upward drift after an initial decline and **B)** with a slight downward drift. The dashed lines indicate the time points when the optode was introduced to the hemolymph sample. The gray shades indicate the area, that was used for analysis of oxygen content.

2.2 Cultivation before and during main incubation experiments

Individuals of *M. edulis* were collected from the Kiel Fjord (54°20'N, 10°10'E) and transported to the Alfred Wegener Institute (AWI) in Bremerhaven, where they were cultivated at 16°C and at a salinity of 16 psu in a 100 l tank with regular water exchange and daily feeding with live marine phytoplankton (20 ml DT's Premium Reef Blend, Innovative Marine Aquaculture, USA).

Ammonium and nitrite water values were checked regularly as a measure for water quality, which remained generally stable with ammonium (NH_4^+) values below 0.5 mg/L and nitrite (NO_2^-) values below 0.1 mg/L.

For every animal in the incubation experiments the shell parameters length, width and height (in mm) as well as the wet weight of the whole animal and the dry weight of the shell and the soft tissue (in g) were measured. Since the gill tissue was used for the experiments, the dry weight could only be determined for the soft tissue without gills, which was corrected by the experimentally determined factor of 0.12 (unpublished data, Stapp) to extrapolate the dry weight of the entire soft tissue. The condition index was then calculated by dividing the dry weight of the soft tissue by the shell weight according to Baird (1958) modified by Lander *et al.* (2012) (Equation 3).

Equation 3: DW_{tissue}/DW_{shell}, whereas DW: dry weight

2. 3 Determination of protein biosynthesis rates

2.3.1 Incubations with ^{13}C- phenylalanine

Isolated gill tissue of *M. edulis* was incubated with ^{13}C- labeled phenylalanine for 6h and 9h in replicates of four at six different setups varying temperature, PO_2, PCO_2 and pH (Table 2). A control tissue sample was taken before the incubation. The incorporation of ^{13}C-phenylalanine into proteins was used as a measure for protein biosynthesis. Since all replicates were incubated in one chamber, technically they were "pseudo-replicates", but for the sake of readibility are always referred to simply as "replicates" in this study.

Temperature tolerance curves for *M. edulis* so far have only been investigated on the whole animal level for North sea populations (Bayne *et al.* 1976b, Almada-Villela *et al.* 1982). To test whether temperature tolerance windows investigated on whole animal level are also valid for isolated gill tissue, incubations of gill tissue were conducted at 16°C with the hemolymph parameters as they occur at 16°C in the whole animal and at 26°C with the hemolymph parameters as they occur at 26°C in the whole animal and protein biosynthesis rates were determined (Incubations 1 and 2 in Table 2). These incubations were necessary because tolerance limits of marine ectotherms may vary between tissue or cellular level and whole animal level as it has been shown for the Antarctic eelpout, which has an upper critical temperature at 9°C at whole animal level (van Dijk *et al.* 1999), but isolated hepatocytes, supplied with enough oxygen and energy, can withstand temperatures until 21°C and probably even further (Mark *et al.* 2005). To investigate the isolated impact of temperature or hemolymph parameters on protein biosynthesis two incubations were conducted where the gill tissue was

exposed to 16°C with the hemolymph parameters for 26°C on the one hand and at 26°C with the hemolymph parameters as they occur at 16°C on the other hand (Incubations 3 and 4 in Table 2). The last two incubation setups investigated the specific effect of pH by exposing the gill tissue to 16°C and the accordant PO_2 and PCO_2 but with a pH as it is found in the hemolymph at 26°C and vice versa (Incubation 5 and 6 in Table 2).

Table 2 Setups for the six different incubations varying temperature [°C], PO_2 [hPa], PCO_2 [hPa] and pH (NBS scale) indicating the number of replicates for each incubation and the time points for each incubation. hemolymph parameters as they occur in the whole animal at different temperatures were estimated according to (a) the data of Thomsen *et al.* (2013), who investigated *in situ* hemolymph PCO_2 and pH in the *M. edulis* population from the Kiel Fjord at different temperatures during the year and (b) the data of Zittier *et al.* (*submitted*), who investigated hemolymph pH and PCO_2 for acute temperature increase for a *M. edulis* population from the North sea. The hemolymph PO_2 for the *M. edulis* population from the Kiel Fjord was determined under acute temperature increase as part of this study.

Incubation number	Temperature [°C]	PO_2 [hPa]	PCO_2 [hPa]	pH	replicates	Time points [h]
1	16	PO_2 at 16°C	1.6[(a)]	7.55[(a)]	4	0, 6, 9
2	26	PO_2 at 26°C	5.2[(b)]	7.20[(b)]	4	0, 6, 9
3	16	PO_2 at 26°C	5.2	7.20	4	0, 6, 9
4	26	PO_2 at 16°C	1.6	7.55	4	0, 6, 9
5	16	PO_2 at 16°C	1.6	7.20	4	0, 6, 9
6	26	PO_2 at 26°C	5.2	7.55	4	0, 6, 9

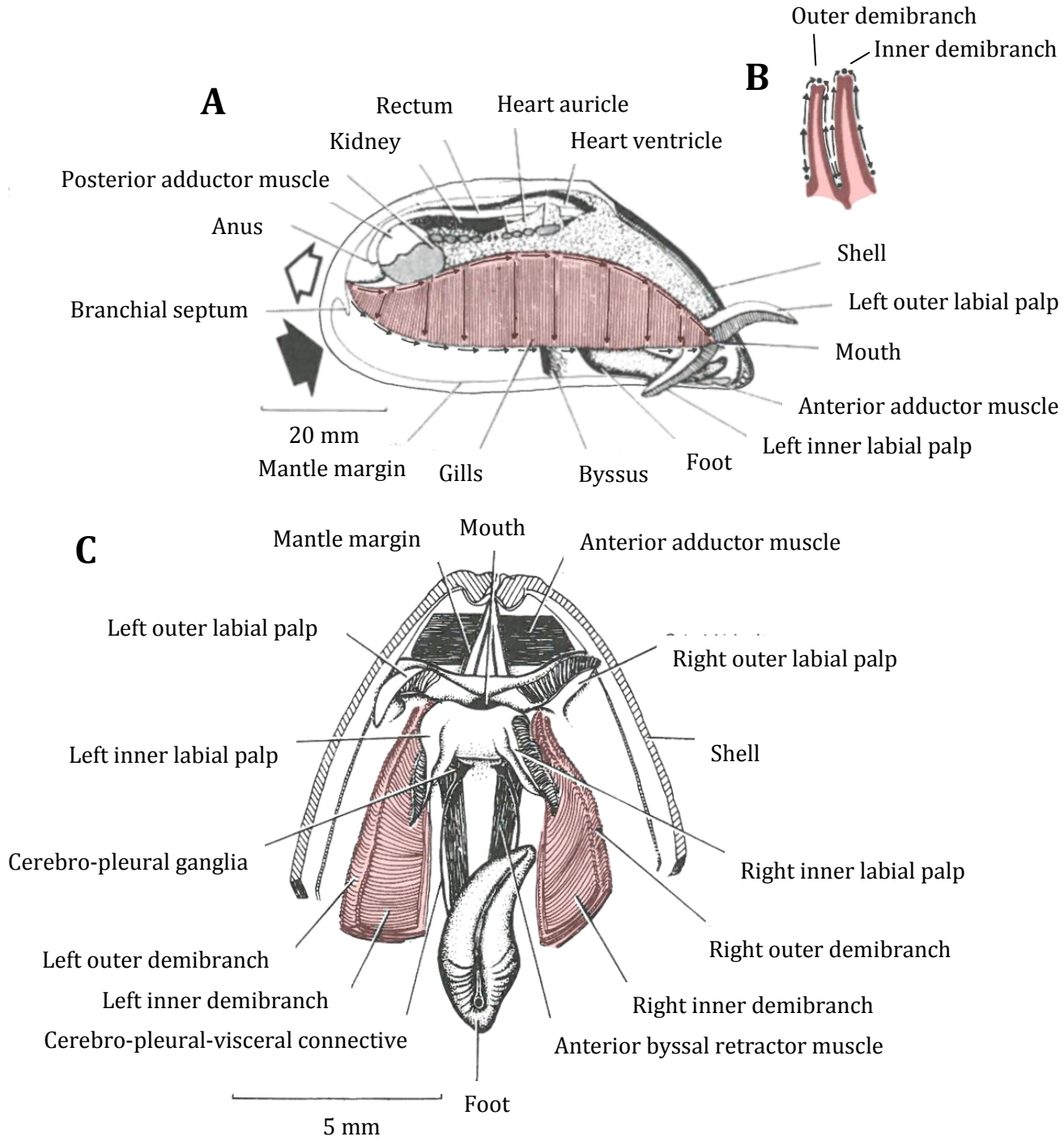

Figure 3 The anatomy of *M. edulis.* **A)** The organs and ciliary currents (→) as seen from the right side. The large arrows represent the filtration current. **B)** A diagrammatic section through a gill showing the ciliary currents (→) and the food grooves (•). **C)** The organs as seen from the ventral surface. The gills consist of one right and one left part each dividing into an inner and an outer demibranch. The gills as they were cut out for the experiments are highlighted in red (modified after Morton 1992).

For the incubations of isolated gill tissue with ^{13}C- phenylalanine, the two gills (left and right half) consisting of two demibranches each (Figure 3) were removed with scissors from the mussel in filtered seawater (16 psu) on ice (highlighted area in Figure 3). The demibranches were separated and placed into small dishes filled with filtered seawater on a shaking table (GFL 3005, 75/min) on ice for a "recovery phase" of 30-60 minutes. Each gill demibranch then represented one time point (control, 6h or 9h). The fourth demibranch of each mussel was cut into three pieces and one third was added to each time point. With only one individual mussel per replicate, there was not enough tissue to end up with a highly enough concentrated extract and ^{13}C- phenylalanine was not detectable in NMR spectroscopy. Hence, three mussels were pooled in order to achieve reliable detection of the ^{13}C- labeled phenylalanine in NMR spectroscopy. Consequently, one time point of one replicate consisted of 1⅓ gill demibranches each from three different mussels. Each of the six incubation experiments consisted of four replicates, named A-D. Prior to shock- freezing the tissue in liquid nitrogen (N_2) the remaining incubation medium (6h and 9h), was dapped off from the gill tissue samples on tissue paper (KimWipe ®) to avoid contamination of the cytosolic extract with ^{13}C- labeled phenylalanine from the medium. Control samples were also dapped off on paper tissue, so that all tissue was exposed to the same level of handling stress. The samples were then immediately shock-frozen in liquid nitrogen and stored at -80°C. All gill tissue was handled with spring steel tweezers to minimize mechanical stress.

The incubation medium simulated the chemical hemolymph composition as close as possible (Table 3). Bayne *et al.* (1976a) summarized the composition of hemolymph of *M. edulis* and listed the concentrations of the different compounds for fully marine populations and brackish water populations. Ion composition was mixed according to these data (Bayne *et al.* 1976a, ion composition for 16 psu, see Table 3) and to guarantee energy supply during the incubations, glucose was added in a concentration of 2 mM (Bayne *et al.* 1976a). A flooding-dose of $^{13}C_9$-^{15}N-L-phenylalanine (98% uniformly labeling of all carbon isotopes; Sigma Aldrich Chemie GmbH, Germany) was added in a concentration of 3 mM (Langenbuch *et al.* 2006, Stapp 2011). ^{13}C-^{15}N-phenylalanine was chosen over ^{13}C- phenylalanine because it is more economical. The ^{15}N- label was not necessary for the experiments, but also had no obvious effect on the ^{13}C-NMR spectra (tested in pre-measurements, data not shown).

Table 3 Compounds of the incubation medium simulating the hemolymph of *M. edulis* indicating concentration [mM], the quality of the chemicals and the supplying producer of the chemicals.

Compound	Concentration [mM]	Quality	Producer
Sodium chloride (NaCl)	213.00	Pure Ph. Eur. USP	AppliChem GmbH, Darmstadt, Germany
Potassium chloride (KCl)	7.50	Pure Ph. Eur. USP	AppliChem GmbH, Darmstadt, Germany
Calcium chloride ($CaCl_2$)	5.80	Pure Ph. Eur. BP, USP, Food grade	AppliChem GmbH, Darmstadt, Germany
Magnesium chloride ($MgCl_2$) (hexahydrate)	11,.30	Pure Ph. Eur. USP	AppliChem GmbH, Darmstadt, Germany
Magnesium sulfate ($MgSO_4$) (heptahydrate)	13.20	Pure Ph. Eur. USP	AppliChem GmbH, Darmstadt, Germany
HEPES	20.00	Cell culture grade	AppliChem GmbH, Darmstadt, Germany
D(+)-Glucose (monohydrate)	2.00	Pure Ph. Eur.	AppliChem GmbH, Darmstadt, Germany
Sodium bicarbonate ($NaHCO_3$)	1.70	Cell culture grade	AppliChem GmbH, Darmstadt, Germany
$^{13}C_9$-^{15}N-L-Phenylalanine	3.00	98% uniformly labeling of all carbon isotopes	Sigma Aldrich Chemie GmbH, Germany

The incubation medium was always mixed one day prior to the experiment. The pH of the medium was buffered with 20 mM HEPES and adjusted to the required value with HCl (1 M) and NaOH (1 M). The medium was then filtrated through a 0.2 µm filter (Sartoris stedim biotech) to avoid bacteria contamination and then stored in the fridge over night. On the next day, the incubation chamber (VWR, 115 mm Boro 3.3) was filled with 200 mL of incubation medium and was placed in a tempered water bath to ensure a constant temperature during the incubation. The medium was bubbled with the respective gas mixture from a mass flow controller (input N_2, O_2 and CO_2; HTK, Vögtlin Instruments AG, Switzerland) for at least one hour prior to the incubation, during which the mussels were dissected. After pre-bubbling of the medium, the pH was re-adjusted to the respective value and the tissue was transferred to the medium. The two time points (6h and 9h) with four replicates each were incubated in the same incubation

chamber and were separated by a net with nine compartments, of which one compartment was used for bubbling (Figure 4). After placing the net into the chamber and placing each replicate or time point, respectively into one compartment of the net, the chamber was sealed with laboratory film (Parafilm ® M, Pechiney Plastic Packaging, Chicago, USA) leaving only one chimney- shaped outflow built out of a blue pipette tip for gas outflow (Figure 4).

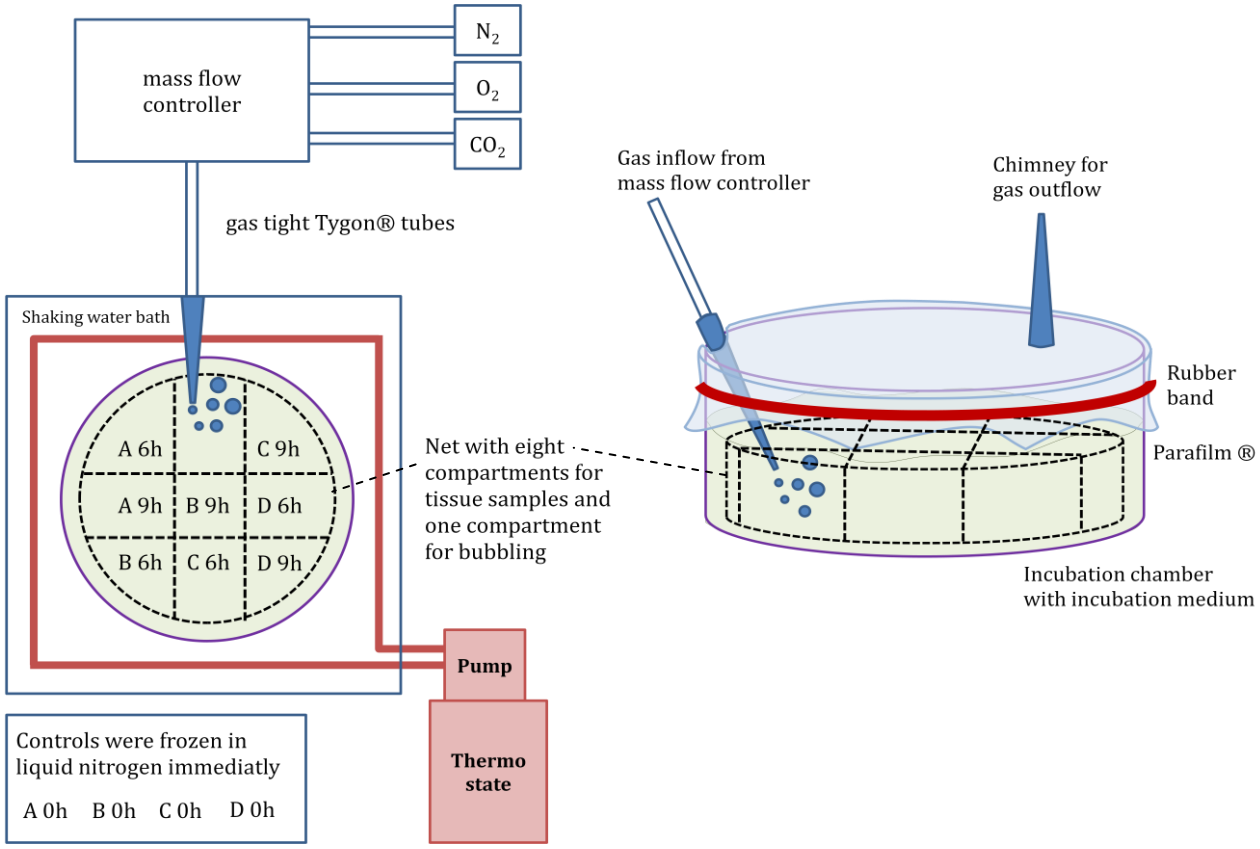

Figure 4 Schematic sketch of the experimental setup. Replicates for each incubation were named A, B, C and D.

The gas mixing was implemented using a mass flow controller (HTK, Vögtlin Instruments AG, Switzerland), which was connected to the incubation chamber with a flexible, gas tight tube (Tygon ®, Saint-Gobain Corporation, France) ending in a 1 mL pipette tip into the incubation medium with a constant rate of bubbling. The gas parameters and their stability over time were ensured for each incubation setup prior to all incubations. Temperature was checked several times during each incubation and remained stable with an error of ±0.5°C. pH was checked and re- adjusted before every incubation and checked again after 9h. pH did not decrease more than 0.05 units over 9h. For PCO_2 measurements a CO_2 analyzer (CA-10a, 10-series Gas Analyzer, Sable Systems, USA) was used, which was calibrated with a two point calibration with pure nitrogen for a PCO_2 of 0 µatm (=0 hPa) and a calibration gas mixture with a PCO_2 of 5000 µatm (≈5.07 hPa). PO_2 analysis was implemented using a TX micro- optode (PreSens Precision Sensing GmbH, Germany), which was calibrated the same way as for the hemolymph PO_2 measurements

(see above). pH measurements were conducted using a pH/ION METER electrode (PHM240 Meter lab, Radiometer, Copenhagen), which was calibrated weekly with calibration buffer solutions at pH 7.00 and 10.01 (Mettler-Toledo GmbH, Analytical Schwerzenbach, Switzerland) at the respective temperature. Temperature was controlled in a shaking water bath (Grant OLS 200, 56/min.), which was cooled or heated, respectively, by a thermostate (LAUDA master PROLINE RP845, Dr. R. Wobser GmbH&Co. KG, Lauda-Königshafen, Germany).

2.3.2 Protein extraction with Perchloric acid (PCA)

Proteins from the frozen samples were extracted with Perchloric acid (PCA) according to Langenbuch *et al.* (2006). All solutions used for the extraction were pre-cooled on ice and all centrifugations (5417R, Eppendorf) were conducted with 6000 g at 0°C if not stated differently. Tissue was grinded under liquid nitrogen and the tissue powder was weighed. 0.6 M PCA was immediately added in 5 times the amount of the weighed tissue powder (v/m [µL/mg]). The tissue solution was homogenized in a processor homogenizer disruptor sonicator (UltraSonic Sonifier 450, Branson, duty cycle 40%) for 10 min. at 0°C. After homogenization, samples were centrifuged for 15 min. Then the pH of the watery phase was adjusted with 0.6 M PCA and 5 M KOH to pH 7.5 using special pH indicator paper ranging between pH 6.4 and 8.0 (Merck, Darmstadt, Germany). The precipitated KCl_4 was removed by another centrifugation for 10 min. and the supernatant containing the cytosolic compounds was dried in a rotation vacuum concentrator (Christ RVC 2-18, Martin Christ Gefriertrocknungsanlagen GmbH, Germany) at 30°C. The pellet from the first centrifugation was re- dissolved in PCA (same amount as for the first extraction) and centrifuged again for 15 min. The supernatant was neglected and the washed pellet was dissolved in Milli Q (3 times the weight of tissue powder v/m [µL/mg]). After thorough mixing the pH was adjusted with 0.6 M PCA and 5 M KOH to pH 7.5 using the special indicator paper. Afterwards, the solution was centrifuged for 10 min. and the supernatant containing water-soluble proteins and the pellet containing water-insoluble proteins were also dried in the rotation vacuum concentrator at 30°C. After drying, the two protein fractions were recombined and diluted in 1 M NaOH (3 times the weight of tissue (v/m [µL/mg]). To hydrolyze the proteins, the solution was shaken at 99°C with 400 rpm in a ThermoMixer comfort® (Eppendorf) for 45 min. in total with thorough mixing for 15 seconds in between after 15 min. Then, the solution was centrifuged for 10 min. at 20°C and the supernatant containing all hydrolyzed proteins was dried in the rotation vacuum concentrator at 30°C. This extraction method separated the amino acids bound to proteins from the free cytosolic amino acids and therefore ^{13}C- labeled phenylalanine, which is freely in the cytosol is separated from ^{13}C- labeled phenylalanine, which is incorporated into proteins.

2.3.3 NMR spectroscopy

The relative amounts of ^{13}C- labeled phenylalanine in both the cytosolic and the protein fraction were detected via nuclear magnetic resonance (NMR) spectroscopy to determine uptake rates into the cytosol of gill tissue and incorporation rates into proteins. NMR spectroscopy is mainly used for structural analyses of organic compounds. However, it is more and more also used in physiological analyses to determine the composition of organic compounds in cells and tissues, also known as metabolic profiling.

The method is based on the nuclear spin characteristics of atoms with odd numbers of protons and/or neutrons in their nucleus. The nuclides ^{1}H and ^{13}C, for example, which were analyzed in this study, both have a core spin of $I = 1/2$ and a magnetic dipole moment. Put into a static magnetic field two values for a magnetic quantum number are possible (m=+1/2 and m=-1/2), which leads to two possible and equally probable energetic states. With a second superimposed magnetic field transitions are induced between these two energetic states. A transition, i.e. a reversal of spin orientation, from the lower to the upper energy level leads to an absorption of energy; a transition from upper to lower energy level creates an emission of energy. Due to the population excess in the lower level, absorption of energy is the dominant process and can be observed as a signal. This signal is proportional to the total number of spins in the sample and therefore also to the concentration. With the pulsed NMR method a radiofrequency pulse excites all nuclei of one species (^{1}H or ^{13}C) simultaneously. The absorption is detected in NMR spectroscopy and depends on the type of atom and on the chemical environment. Signals split up when the nuclei are distracted by other nuclear spins in the close environment of the same molecule. The chemical shift also results from the chemical environment, which shields a nucleus. Nuclei are differently shielded depending on the position they have within the molecule. The signal intensity represents the relative amount of nuclei with an identical chemical environment. In ^{13}C- NMR spectroscopy the carbon nuclei of the stable ^{13}C- isotopes are detected and in ^{1}H- NMR spectroscopy the nuclear spins of all hydrogen protons are detected. Since hydrogen is the most numerous component of all organic molecules, ^{1}H spectra are usually more comprehensive than ^{13}C spectra. In ^{1}H spectra ^{12}C- bound protons can be distinguished from ^{13}C-bound protons, since the molecular configuration of the metabolite changes the molecular environment of the protons and therefore the protons are distracted differently. Even in ^{1}H spectra without artificially added ^{13}C-labels, the natural frequency of stable ^{13}C- isotopes is often visible as little "satellite" signals right and left of the correspondent ^{12}C- bound proton signal. In conclusion, ^{1}H measurements have the advantage that they are much more sensitive than ^{13}C-measurements and contain information on many different metabolites, but are also only an indirect measurement of ^{13}C content. In contrast, ^{13}C measurements directly measure ^{13}C content

in the samples directly, but reveal fewer signals and are much less sensitive, i.e. measurements take much longer.

In Fourier transform NMR spectroscopy, which is the method of choice due to its enhanced signal-to-noise ratio, the signal intensity is displayed as a function of frequency with the unit ppm (parts per million). Due to this transformation of the "pure" signal, NMR spectroscopy is no absolute quantitative method, but just detects relative quantities to one arbitrary reference signal. That is why all concentrations in the results are presented in an arbitrary unit (AU).

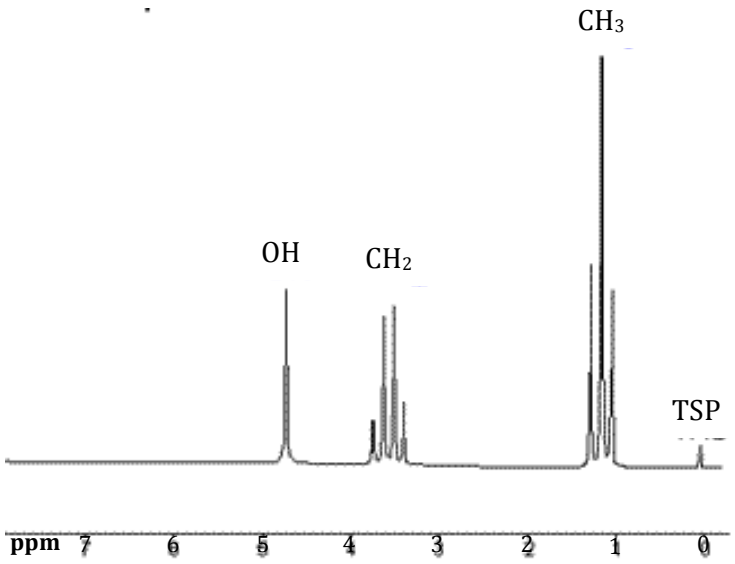

Figure 5 Example of an ^{1}H-NMR spectrum of a pure ethanol solution with trimethylsilyl propionate (TSP) as an internal standard. **OH-** hydroxyl group; **CH_2-** methylene group; **CH_3-** methyl group. The chemical shift [ppm] is shown on the x-axis (source: alevelchem.com).

A simple example to explain how NMR spectra are generated is the ethanol ^{1}H NMR spectrum. Ethanol (CH_3-CH_2-OH) generates three signals in ^{1}H- NMR spectroscopy (Figure 5), each representing the group of identical protons bound to one carbon or oxygen atom, respectively. The methyl group (CH_3-) creates the least chemically shifted (at 1.19 ppm) signal and is distracted by two protons from the methylene group (-CH_2-) and therefore creates a signal with three peaks (a triplet). The methylene group (–CH_2-) is distracted by three protons from the methyl group (CH_3-) and creates a signal with four peaks (a quadruplet at 3.65). This signal is not distracted by the proton, which is bound to the oxygen atom, because the oxygen atom is very large and does not enable this single proton to influence other protons. Therefore, the proton from the hydroxyl group (-OH) is a single unsplit signal with the biggest chemical shift at 5.00 ppm. It is also the signal with the smallest intensity, i.e. the smallest integral, since it is only generated by one single proton. The quadruplet of the methylene group (–CH_2-) accordingly generates a signal with twice the intensity of the hydroxyl signal (–OH) since it is generated by two identical protons. The methyl group (CH_3-), hence, creates the largest signal with three

times the size of the hydroxyl group (–OH). The integral beneath the signal represents the amount of core spins from one chemically coherent group of one molecule. Chemical shifts may vary depending on the pH of the measured solution and on the presence of other compounds in the solution. Figure 5 shows an example ^{1}H-NMR spectrum of a pure ethanol solution with trimethylsilyl propionate (TSP) as internal standard (set to 0 ppm).

^{1}H spectra were generated to relatively quantify not only the uptake of ^{13}C- phenylalanine but also to analyze changes of other metabolites over time. For ^{1}H NMR experiments an automated routine (developed in house), consisting of four experiments (zgpr, cpmg, noesy and jres), was run for each sample. Zgpr NMR spectra usually display all compounds, which results in complex spectra with overlaying signals. The cpmg experiments, on the contrary, filter long-chained molecules such as fatty acids, so that these spectra reveal a cleaner baseline and less overlaying signals. The noesy experiments typically display a better resolution of the molecules bound to bigger complexes such as proteins and the jres experiment is a two-dimensional measurement, which facilitates signal assignment. The cpmg NMR spectra were most suitable for processing and analysis, showing the best signal separation and lowest baseline changes and were therefore chosen for semi- quantitative analysis.

For the NMR analysis the dried extracts were suspended in 70 µl (for cytosolic extracts) or 90 µl (for protein extracts) deuterated water (D_2O) with 1% (w/w) TSP (3-(trimethylsilyl) propionic-2,2,3,3-d_4 acid sodium salt (Sigma Aldrich Chemie GmbH, Germany) for internal calibration and vortexed. The assembled rotor was injected into a triple tunable ^{1}H- ^{13}C- ^{31}P- HRMAS probe of a 9.4 T Avance 400 WB NMR spectrometer (Bruker Biospin GmbH, Germany) operating at a ^{1}H resonance frequency of 400 MHz and fully relaxed high-resolution one-dimensional (1D), one pulse ^{1}H- and ^{13}C- NMR spectra were generated (for details on the acquisition parameters of the NMR experiments see Table A1 in the Appendix). Prior to all NMR measurements, field homogeneity was optimized using a standard shim protocol resulting in typical line width of 1-2 Hz.

2.4 Data analysis

All data are depicted as means and standard errors of the mean (SEM). Plots, linear regressions and curve fittings as well as all statistical tests were performed in Prism 5 (Version 5.03, GraphPad Software Inc., 2009). The significance level for all statistical analyses was set to α=5%.

Hemolymph PO_2 data were analyzed with a repeated measures one-way analysis of variance (rANOVA) and the data were fitted using the Hill equation for dose and response relationships with a built-in feature of Prism 5 (Equation 4).

NMR spectroscopy is a powerful tool for relative quantification of metabolites, but absolute quantification is difficult. Therefore, the amount of incorporated ^{13}C- labeled phenylalanine was determined in relation to the other samples by referring the spectra to each other and integrating the relevant signals. The ^{13}C- phenylalanine signal was integrated between 6.9 and 7.8 ppm in the ^{1}H NMR spectra and between 124.7 and 131.7 ppm in the ^{13}C NMR spectra. Spectra from protein and cytosolic spectra, respectively were calibrated on a separate scale each, as well as ^{1}H and ^{13}C spectra. ^{13}C- spectra were normalized dividing the integral by the tissue weight (used for extraction). For the ^{1}H- spectra this method was not feasible, because it resulted in very unrealistic time courses of cytosolic metabolites and therefore, the spectra were normalized to a broad multiplet at 1.74 ppm, which is a fatty acid signal and was assumed to be constant among all samples. All integrals were multiplied with the factor 10, as it has been done by Langenbuch *et al.* (2006), so that the results were comparable to literature data. Relative concentrations of ^{13}C- labeled phenylalanine in each sample of the cytosolic fractions were plotted over time (0h, 6h and 9h) and fitted with Equation 6 (One-Site total binding fit in Prism 5). For the protein fractions linear regressions were calculated and the slopes were perceived as the protein biosynthesis rates. Other analyzed metabolites from the cytosolic ^{1}H spectra included anaerobic end products, amino acids and osmolytes.

3. Results

3.1 Determination of hemolymph PO_2 during acute temperature increase

Hemolymph PO_2 was determined at 10°C (n=20) and under increased temperatures at 16°C (n=18), 22°C (n=18) and 25°C (n=17) after five days of acclimation at each temperature (Figure 6). One sample from the 10°C mixed with seawater during extraction and was neglected. Two other animals died during hemolymph extraction at 10°C and one died during the 22°C measurements. Data from these animals were completely neglected from the analysis, so that in total data from 16 animals were used for a repeated measurements analysis of variance (rANOVA) of hemolymph PO_2 and for a regression of these data using the Hill equation, which is commonly used for dose-response relations of inhibitors (Equation 4).

Equation 4: Y = Bottom + (Top - Bottom)/(1 + 10^((LogIC50 - X) * HillSlope))

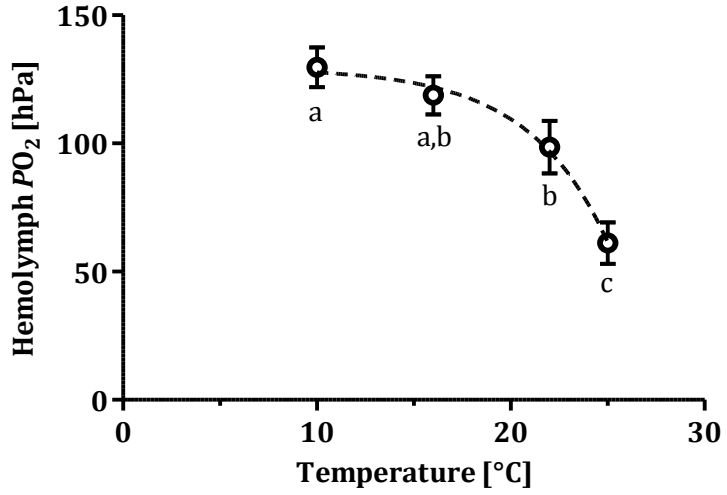

Figure 6 Partial pressure of oxygen (PO_2)[hPa] in the hemolymph of the blue mussel *M. edulis* (population from Kiel Fjord) at four different temperatures. Temperature was acutely increased with 0.2°C/h and the animals were acclimated to the new temperature for five more days. All animals were investigated at all temperatures (n=16). The circles with error bars indicate means ± SEM. The dashed line indicates the regression using the Hill equation with R^2=0.36. Different letters indicate significant differences between groups determined via an rANOVA.

Hemolymph PO_2 was 129.7±7.8 hPa at 10°C and decreased slightly to 120.8±7.4 hPa at 16°C. With further increase to 22°C hemolymph PO_2 decreased further to 98.6±10.2 hPa and decreased further to 61.2±8.1 hPa at 25°C. The rANOVA revealed a highly statistically significant effect of temperature (F=20.68, p<0.0001). The *post hoc* Tukey's multiple comparison tests

revealed significant differences between the PO_2 at 10°C and 22°C ($p<0.01$) and 25°C ($p<0.001$) and between 22°C and 25°C ($p<0.01$) (Table A2 in Appendix). The PO_2 at 16°C only differed statistically significant from the PO_2 at 25°C ($p<0.001$). The best-fit values for the regression of the hemolymph PO_2 data are displayed in Table 4 resulting in Equation 5, representing a moderate fit with $R^2=0.36$. The hemolymph PO_2 for 16°C was chosen as 126.7 hPa for the 16°C treatments in the following incubations, a value determined by including all measurements at 16°C (also the ones that were neglected from the rANOVA). Using Equation 5 the hemolymph PO_2 for 26°C was calculated to be 42.96 hPa and was rounded to 40 hPa in the following experiments resulting in the final experimental setup (Table 5).

Equation 5: PO_2 [hPa] = -4.646*10^6 + (129.4 - (-4.646*10^6)/(1+ (10^((70.5 – T[°C]) * (-0.1063)))

Table 4 Best- fit values (estimates indicated by ~) for the Hill equation as calculated with Prism 5 for the hemolymph PO_2 values displayed in Figure R1.

Best-fit values	
Bottom	~ -4.646*10^6
Top	129.4
LogIC50	~ 70.50
HillSlope	~ -0.1063
IC50	~
Span	~ 4.646*10^6
Std. Error	
Bottom	~ 1.174*10^12
Top	18.48
LogIC50	~ 1.033*10^6
HillSlope	~ 0.2960
Span	~ 1.174*10^12
Goodness of Fit	
Degrees of Freedom	60
R square	0.3873
Absolute Sum of Squares	68649
Sy.x	33.83
Number of points analyzed	64

3.2 Cultivation of M. edulis

The average condition index of the experimental animals (n=72) was 14.01±4.85. Another batch of mussels (n=9), which was cultivated ca. 2 months longer at AWI under the same conditions had an average condition index of 3.74±1.18 and was thereby significantly lower. The "older" (i.e. longer in cultivation) batch was not used for experiments, but these results hold important information on the effect of the cultivation on the conditions of the animals.

3.3 Incubations

Unfortunately, not all samples could be measured within the time frame of this thesis due to the unavailability of the NMR spectrometer from January 2014 onwards. For the cytosolic fraction three incubations were analyzed (incubation 1: n=4; incubation 2: n=4; incubation 3: n=3) and for the protein fraction five incubations were analyzed (incubation 1: n=4; incubation2: n=3; incubation 3: n=3; incubation 4: n=3; incubation 5: n=2). The remaining samples are still available, and are planned to be measured as soon as the NMR spectrometer is ready for use again. An overview of the experimental setup (including the determined PO_2 values) and the respective analyzed samples is displayed in Table 5.

Table 5 Updated table M2 (see above) indicating the six different incubation setups including the PO_2 values [hPa] estimated from values determined in this study and also indicating the replicates of the cytosolic and protein fraction, that were analyzed for this thesis.

Incubation number	Temperature [°C]	PO_2 [hPa]	PCO_2 [hPa]	pH	Measured replicates cytosol	Measured replicates protein	Time points [h]
1	16	126.7	1.6	7.55	4	4	0, 6, 9
2	26	40.0	5.2	7.20	4	3	0, 6, 9
3	16	40.0	5.2	7.20	3	3	0, 6, 9
4	26	126.7	1.6	7.55	0	3	0, 6, 9
5	16	126.7	1.6	7.20	0	2	0, 6, 9
6	26	40.0	5.2	7.55	0	0	0, 6, 9

3.3.1 Validation of the ^{13}C- phenylalanine signal in ^{1}H and ^{13}C NMR spectroscopy

The solution of a pure ^{13}C- phenylalanine solution (0.5 M) revealed a series of signals with the most prominent signal between 124 and 132 ppm in the ^{13}C NMR spectrum (Figure 7A) and between 6.9 and 7.8 ppm in the ^{1}H NMR spectrum (Figure 8A), which was the signal of the aromatic ring of ^{13}C- phenylalanine confirmed by literature data (Avison *et al.* 1990, Schäfer *et al.* 1984). Besides remarkable differences between all spectra, the signal of the aromatic ring was visible in both the cytosolic and protein ^{13}C- spectra of all 6h and 9h samples (Figure 7) and in the cytosolic, but not in the protein ^{1}H spectra (Figure 8). The other, non-aromatic ^{13}C-

phenylalanine signals varied strongly in intensity amongst samples and were not feasible for analysis of ^{13}C- phenylalanine content in the cells. Additionally, the other ^{13}C- phenylalanine signals were overlain by other metabolites in the ^{1}H spectra (Figure 8B,C) and therefore only the signal of the aromatic ring was feasible for determination of uptake rates. In summary, uptake of ^{13}C- phenylalanine into the cytosol was determined via analyses of both the ^{1}H and ^{13}C NMR spectra, whereas ^{13}C- phenylalanine incorporation into proteins could only be determined by an analysis of the ^{13}C NMR spectra.

Some of the non- phenylalanine signals in the ^{1}H spectra could be assigned to amino acids, end products of anaerobic metabolism and osmolytes (Table 6) according to a comprehensive ^{1}H NMR study on salmon (Castejón *et al.* 2010). Most of these assignments were made in the cytosolic spectra whereas in the protein spectra only few amino acids could be positively identified (Table 6).

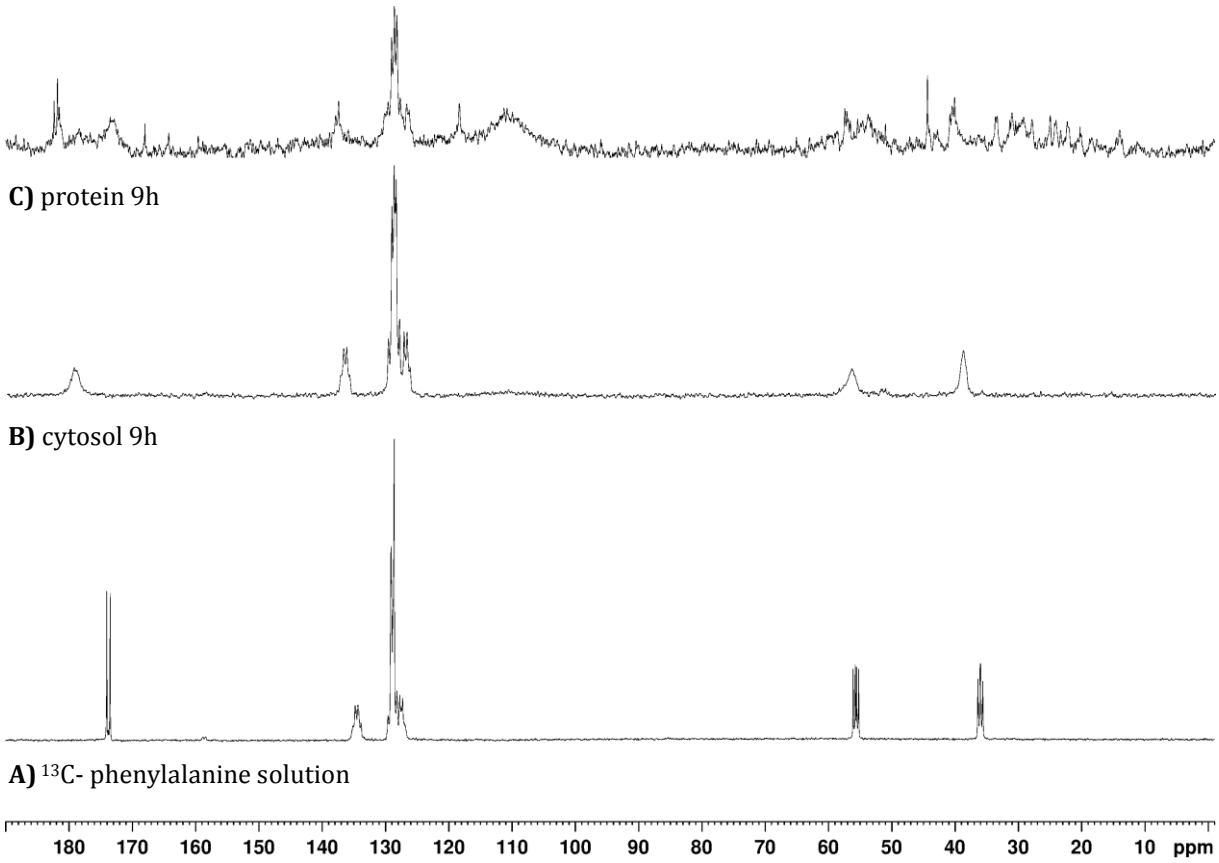

Figure 7 A) ^{13}C- NMR spectra of a pure ^{13}C- phenylalanine solution (0.5 M) compared to a spectrum of **B)** a cytosolic extract and **C)** a protein extract of gill tissue of *M. edulis* each incubated with ^{13}C- phenylalanine for 9h. Note the good concurrence of the phenylalanine signals between all spectra.

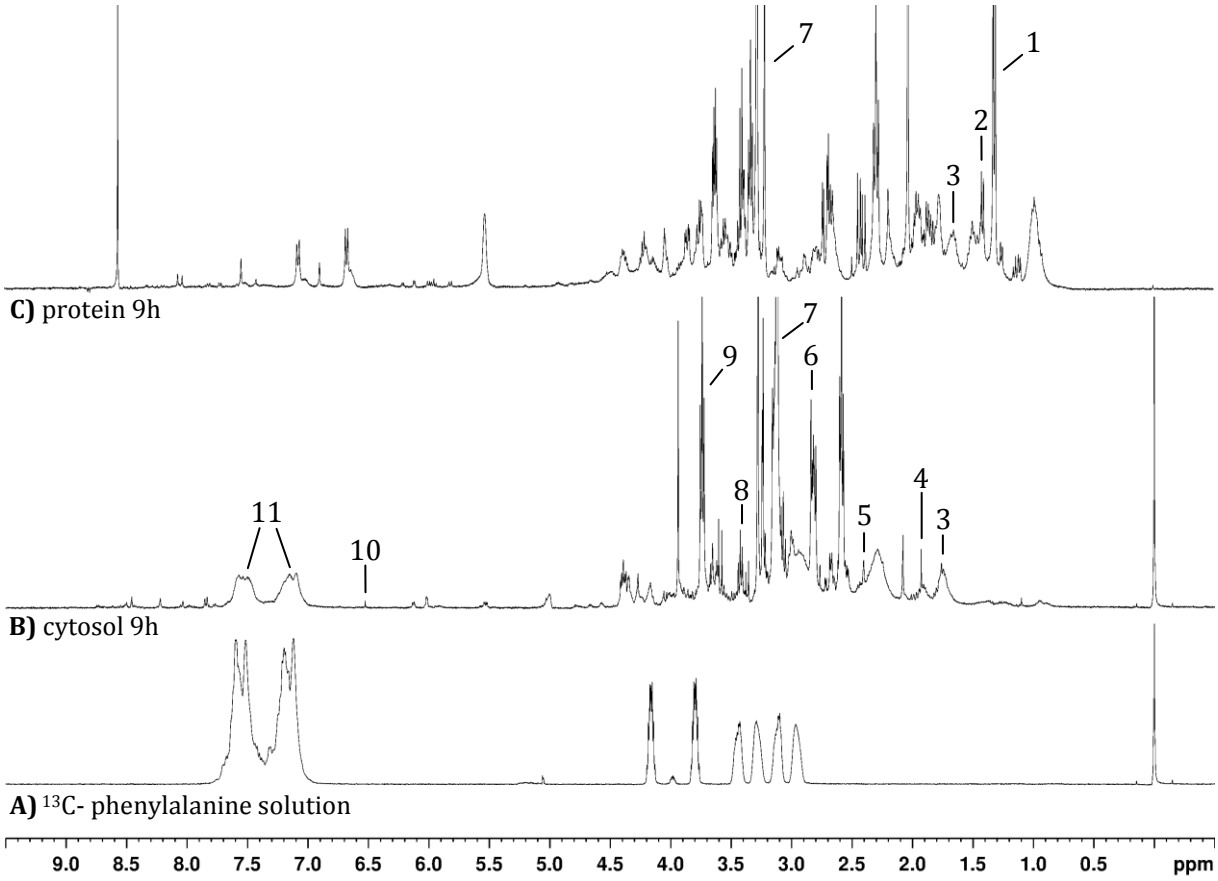

Figure 8 A) ^{1}H- NMR spectra of a pure ^{13}C- phenylalanine solution (0.5 M) compared to a spectrum of **B)** a cytosolic extract and **C)** a protein extract of gill tissue of *M. edulis* each incubated with ^{13}C- phenylalanine for 9h. Signals were assigned to the following metabolites (also listed in Table 6): **1-** Threonine; **2-** Alanine; **3-** Fatty acid; **4-** Acetic acid; **5-** Succinic acid; **6-** Tyrosine; **7-** Trimethylamine oxide (TMAO); **8-** Taurine; **9-** Lysine; **10-** Fumaric acid; **11-** ^{13}C- phenylalanine (aromatic ring).

Table 6 Additional metabolites in cytosolic and protein fraction displayed in ^{1}H- NMR spectra (cpmg).

Number	Metabolite	Chemical shift [ppm]	Visible in cytosolic ^{1}H spectra	Visible in protein ^{1}H spectra
1	Threonine	1.34		X
2	Alanine	1.48	X	X
3	Fatty acids	1.74	X	X
4	Acetic acid	1.93	X	
5	Succinic acid	2.41	X	
6	Tyrosine	3.07	X	X
7	TMAO	3.29	X	
8	Taurine	3.43	X	
9	Lysine	3.76	X	
10	Fumaric acid	6.53	X	
11	^{13}C- phenylalanine	7.33	X	

3.3.2 ^{13}C- phenylalanine uptake into the cytosol of incubated gill tissue

Figures 9 (^{13}C spectra) and 10 (^{1}H spectra) depict examples of NMR spectra, which visualize the uptake of ^{13}C- phenylalanine into the cytosol of the gill tissue of *M. edulis* before the incubation (0h) and after 6h and 9h of incubation with 3 mM ^{13}C- labeled phenylalanine.

Generally, in the control (0h) samples there was no visible signal of ^{13}C- phenylalanine. Therefore the control integration between 124.7 and 131.7 ppm in the ^{13}C spectra (Figure 9) and between 6.93 and 7.73 ppm in the ^{1}H spectra (Figure 10) led to nominal values, resulting from the noise in the spectra and were subtracted from all integrals for normalization. The integrals [arbitrary unit AU] of the ^{13}C- phenylalanine signals were plotted over time for both the ^{1}H-spectra and the ^{13}C- spectra (Figure 11). After 6h a clear increase of the ^{13}C- phenylalanine signal was observed with a further increase after 9h. Only two replicates in incubation 2 in the ^{1}H spectra and one replicate of incubation 3 in ^{1}H and ^{13}C spectra showed slightly lower levels of ^{13}C- phenylalanine after 9h compared to 6h. Additionally, one sample of incubation 1 depicted an extremely low value only in the ^{13}C spectra after 9h (Figure 11), which was not the case in the

correspondent ^{1}H- measurement. Therefore, the value from the ^{13}C NMR spectra was excluded as apparently resulting from a technical error.

One-way ANOVAs for ^{13}C and ^{1}H spectra revealed no statistically significant differences between all 6h and 9h samples for all incubations and also between incubations, neither for the analysis of ^{1}H spectra ($F=1.564$, $p=0.2298$) nor for the analysis of ^{13}C spectra ($F=0.7437$, $p=0.6022$) (Table A3 in Appendix). According to the assumptions of the flooding-dose method, the cytosolic content of the ^{13}C- label should increase very fast and stay stable (or decrease slightly) over incubation time. Therefore, the means for all time points were fitted with a curve usually used for ligand- binding relationships - the "One Site - total binding" model of Prism 5 (equation 6, Figure 12). Best- fit values are summarized in Table 7 with all $R^2 \geq 0.82$. The analysis via ^{1}H spectra revealed slightly different uptake kinetics than the analysis via ^{13}C spectra. For example, the Kd (i.e. half maximum) values differed between incubations and also between ^{1}H- and ^{13}C-spectra. Especially incubation 1 showed an almost linear relationship of cytosolic ^{13}C-phenylalanine content over time (Figure R7) when integrals were analyzed from ^{1}H- spectra. The Kd value of incubation 1 was highest for both ^{1}H and ^{13}C analysis and was 2-10 times higher than in the other incubations.

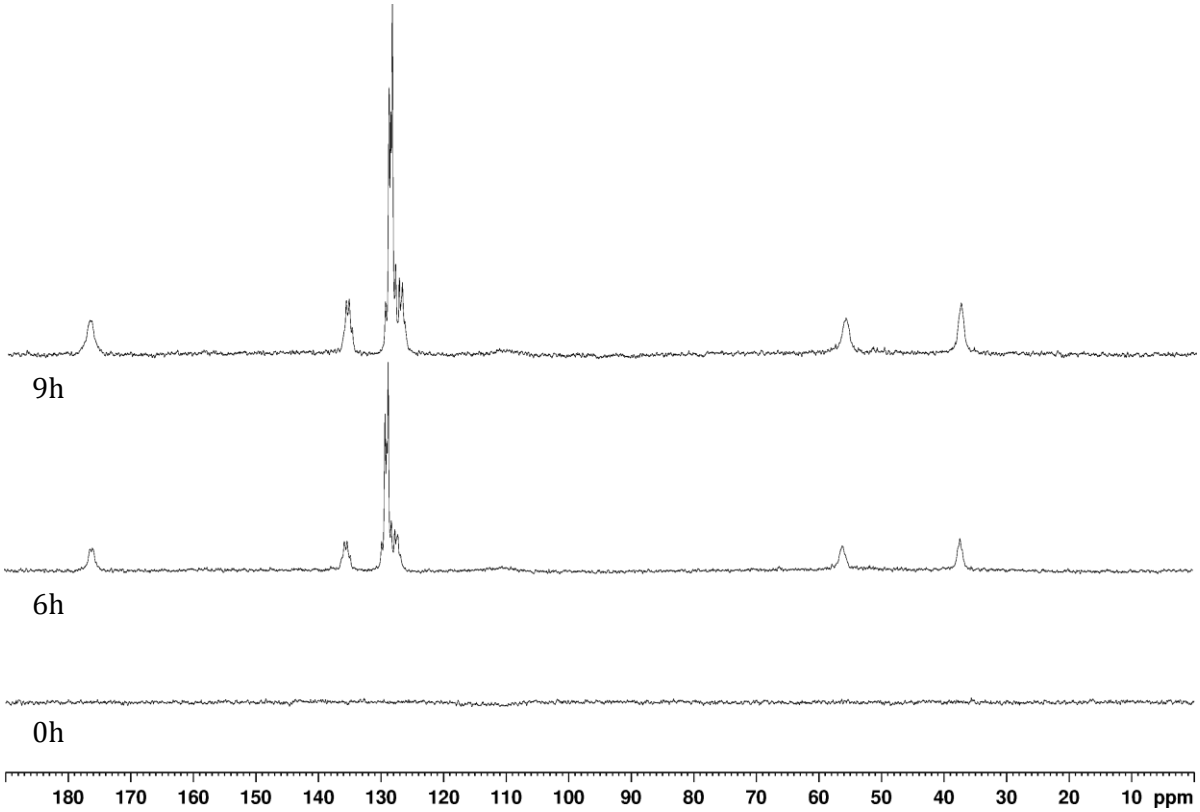

Figure 9 ^{13}C- NMR spectra of cytosolic fraction of incubated gill tissue of *M. edulis* before the incubation (0h) and after 6h and 9h, respectively.

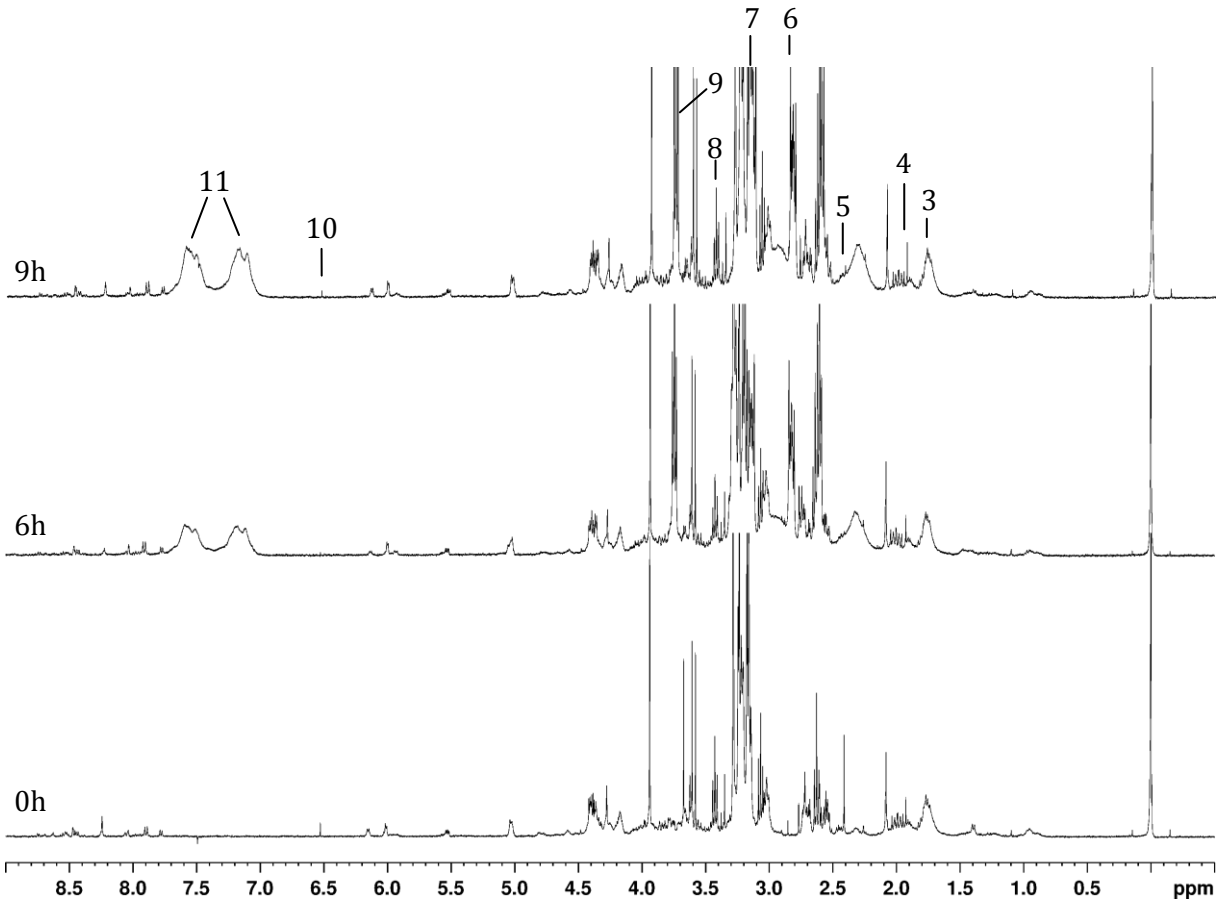

Figure 10 ^{1}H- NMR spectra of the cytosolic fraction of incubated gill tissue of *M. edulis* before the incubation (0h) and after 6h and 9h, respectively. Signals were assigned to the following metabolites (also listed in Table 6): **1-** Threonine; **2-** Alanine; **3-** Fatty acid; **4-** Acetic acid; **5-** Succinic acid; **6-** Tyrosine; **7-** Trimethylamine oxide (TMAO); **8-** Taurine; **9-** Lysine; **10-** Fumaric acid; **11-** ^{13}C- phenylalanine (aromatic ring).

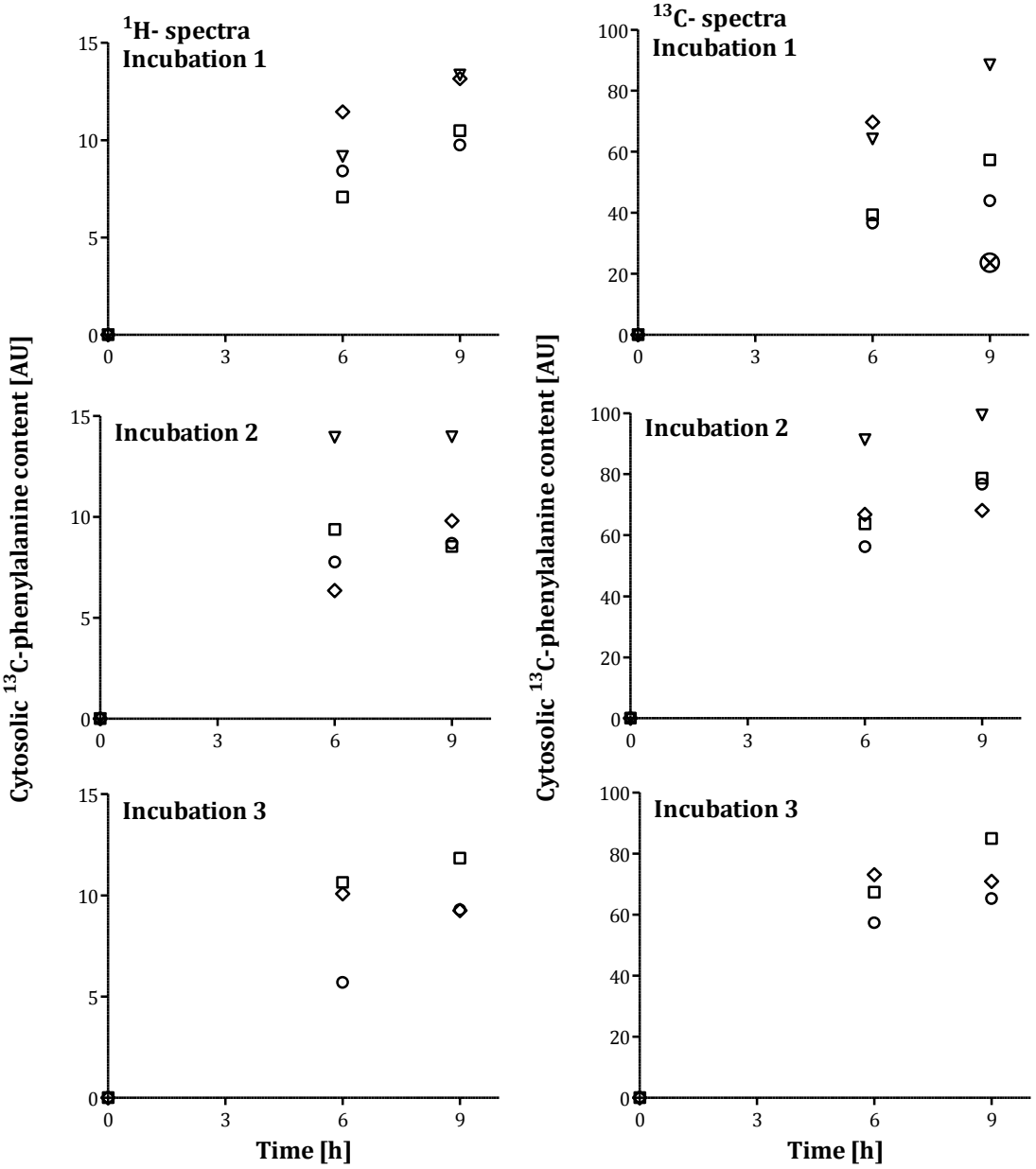

Figure 11 ^{13}C- phenylalanine content [AU] in the cytosol of gill tissue of *M. edulis* over time [h]. The integrals were analyzed from ^{1}H- (left) and ^{13}C- spectra (right), normalized to a specific scaling factor (^{1}H- spectra) or tissue powder weight from extraction (^{13}C- spectra), respectively. Circles, squares, triangles and diamonds mark the different replicates; The encircled X marks an outlier in the analysis of ^{13}C spectra in incubation 1. Incubation 1 and 2: n=4, incubation 3: n=3.

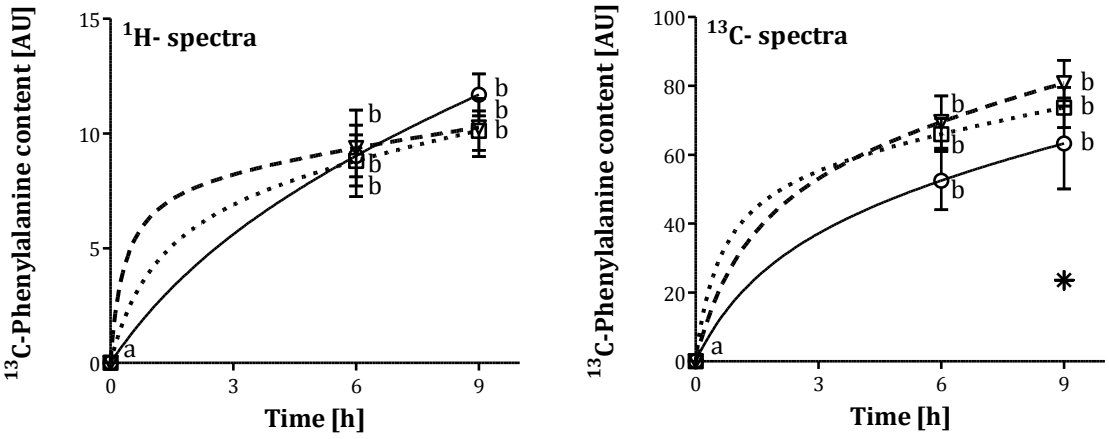

Figure 12 ^{13}C- phenylalanine content [AU] in the cytosol of gill tissue of *M. edulis* over time [h] analyzed from ^{1}H- (left) and ^{13}C- spectra (right), normalized to a specific scaling factor (^{1}H- spectra) or tissue powder weight from extraction (^{13}C- spectra). Shown are means ± SEM for each time point of each incubation. Circles: Incubation 1 (n=4) (continuous regression line); Triangles: Incubation 2 (n=4) (dashed regression line); Squares: Incubation 3 (n=3) (dotted regression line). All regressions were fitted with a model for ligand total binding (Prism 5, Equation 6) with all $R^2 \geq 0.82$. Letters indicate the statistically significant differences (ANOVA, Table A3).

Equation 6: Y=Bmax*X/(Kd+X) + NS*X + Background,

with Y=cytosolic ^{13}C- phenylalanine content [AU] and X=Time [h]

Table 7 Best- fit values for the fits of incubation 1, 2 and 3 in Figure R12 using Equation 6 (One site- total binding fit in Prism 5) for **A)** ^{1}H and **B)** ^{13}C spectra analysis.

A) ^{1}H- spectra	Incubation 1	Incubation 2	Incubation 3
Bmax	~ 10.2	~ 8.327	~ 8.465
Kd	~ 4.794	~ 0.3515	~ 1.237
NS	~ 0.5581	~ 0.2495	~ 0.2974
Background	$-1.554*10^{-13}$	$-7.753*10^{-17}$	$-1.696*10^{-16}$
Std. Error			
Bmax	$\sim 7.340*10^{15}$	$\sim 6.563*10^{15}$	$\sim 3.926*10^{16}$
Kd	$\sim 4.356*10^{15}$	$\sim 2.981*10^{15}$	$\sim 1.967*10^{16}$
NS	$\sim 2.985*10^{14}$	$\sim 4.180*10^{14}$	$\sim 2.247*10^{15}$
Background	0.8324	1.330	6.187
Goodness of Fit			
Degrees of Freedom	8	8	5
R square	0.9369	0.8322	0.9055
Absolute Sum of Squares	20.18	52.08	18.96
Sy.x	1.588	2.551	1.947
Number of points analyzed	12	12	9
B) ^{13}C- spectra	Incubation 1	Incubation 2	Incubation 3
Bmax	~ 54.51	~ 68.21	~ 59.77
Kd	~ 2.379	~ 1.483	~ 0.6419
NS	~ 2.240	~ 2.470	~ 1.991
Background	$-9.979*10^{-16}$	$-4.731*10^{-16}$	$4.831*10^{-16}$
Std. Error			
Bmax	$\sim 5.745*10^{16}$	$\sim 2.230*10^{17}$	$\sim 3.717*10^{16}$
Kd	$\sim 5.086*10^{15}$	$\sim 1.428*10^{16}$	$\sim 2.446*10^{15}$
NS	$\sim 2.908*10^{15}$	$\sim 1.241*10^{16}$	$\sim 2.283*10^{15}$
Background	9.897	6.887	5.620
Goodness of Fit			
Degrees of Freedom	7	8	5
R square	0.8170	0.9262	0.9674
Absolute Sum of Squares	1904	1220	331.6163
Sy.x	16.49	12.35	8.144
Number of points Analyzed	11	12	9

3.3.3 ^{13}C- phenylalanine incorporation into proteins of gill tissue

Figure 13 shows an example of the increasing ^{13}C- phenylalanine signal, as it was visible in the ^{13}C spectra of protein fractions. The integral of the signal between 124.7 and 131.7 ppm, i.e. the content of ^{13}C- phenylalanine in the proteins is depicted over time in Figure 14 for all incubations. According to the assumptions of the flooding dose method, a linear regression was fitted for the protein biosynthesis rates, even though eight replicates showed slightly lower values for 9h than for 6h (two replicates of each incubation except incubation 2). Nevertheless,

all linear regressions had a good fit to the data with $R^2 \geq 0.7$ and showed a positive linear relation of ^{13}C- phenylalanine content with time. Figure 15 displays the slopes of these linear regressions as protein biosynthesis rates comparing the two different temperatures at the different hemolymph parameter settings. Average protein biosynthesis rates (in arbitrary unit per hour) for incubations 2 and 3 (3.57±0.18 AU/h and 3.78±0.13 AU/h) were around 32-41% lower than for incubations 4 and 5 (6.07±0.35 AU/h and 5.80±0.44 AU/h). The average protein biosynthesis rate of incubation 1 was 0.44±1.31 AU/h (control conditions with all parameters as they occur at 16°C) and were slightly higher than protein biosynthesis rates of incubation 2 and 3, but lower than protein biosynthesis rates of incubations 4 and 5. A striking feature of the dataset (Figure 15) is the large variation of protein biosynthesis rates in incubation 1 with all parameters at control values. The data for all incubations were normally distributed (Shapiro- Wilk test, all $p>0.05$), but the homogeneity of variances was not given (Bartlett's test, $p=0.01231$) and therefore a two- way ANOVA for testing interactive effects of temperature and hemolymph parameters was not possible. A non- parametric one- way Kruskal- Wallis analysis did not reveal any significant differences between incubation treatments (Kruskal-Wallis statistics=6.238; $p=0.1821$). An outlier test performed on the coefficients of variance confirmed incubation 1 to be a significant outlier in the dataset due to its large variation (Grubb's test, $p<0.05$). When incubation 1 was disregarded, the Bartlett's test did not detect a significant difference from homogeneous variances in incubations 2-5 ($p=0.5843$) and a one- way ANOVA detected highly significant differences between the treatments ($F=22.83$, $p=0.0005$). The *post hoc* Bonferroni's multiple comparison test revealed the significances depicted in Figure 15 building two pairs of statistically not significantly different treatments, i.e. incubations 2 and 3 were significantly lower than incubations 4 and 5 ($p<0.05$, Table A5 in Appendix).

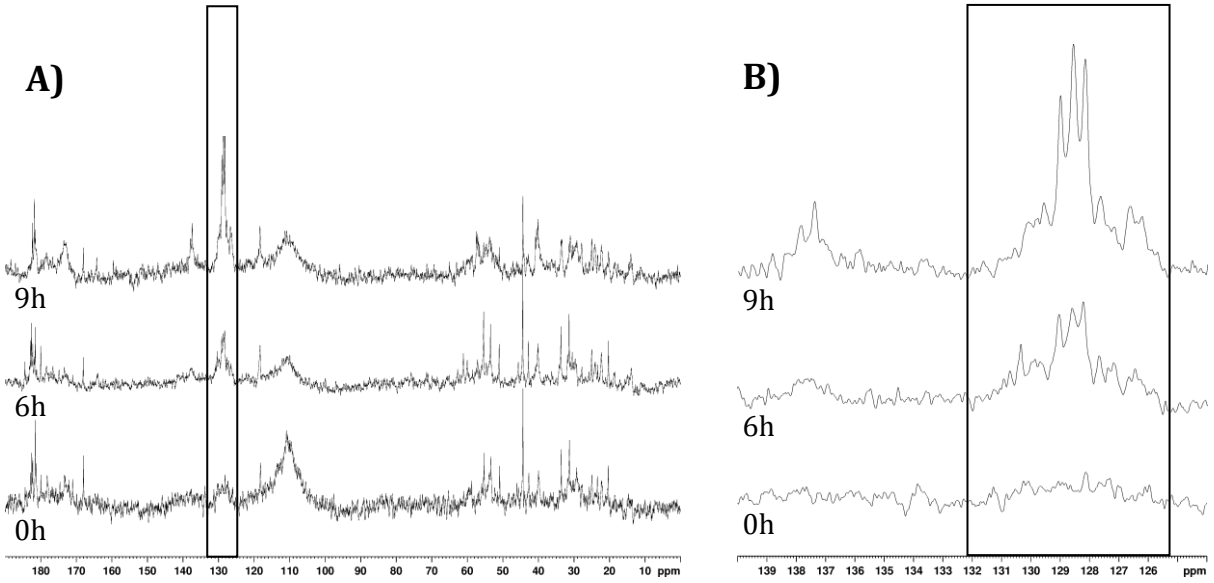

Figure 13 A) ^{13}C- NMR spectra of protein fraction of incubated gill tissue of *M. edulis* before the incubation (control) and after 6h and 9h, respectively **B)** close- up of phenylalanine signal between 124-140 ppm. The highlighted area indicates the integrated area of the ^{13}C-phenylalanine signal between 124.7-131.7 ppm.

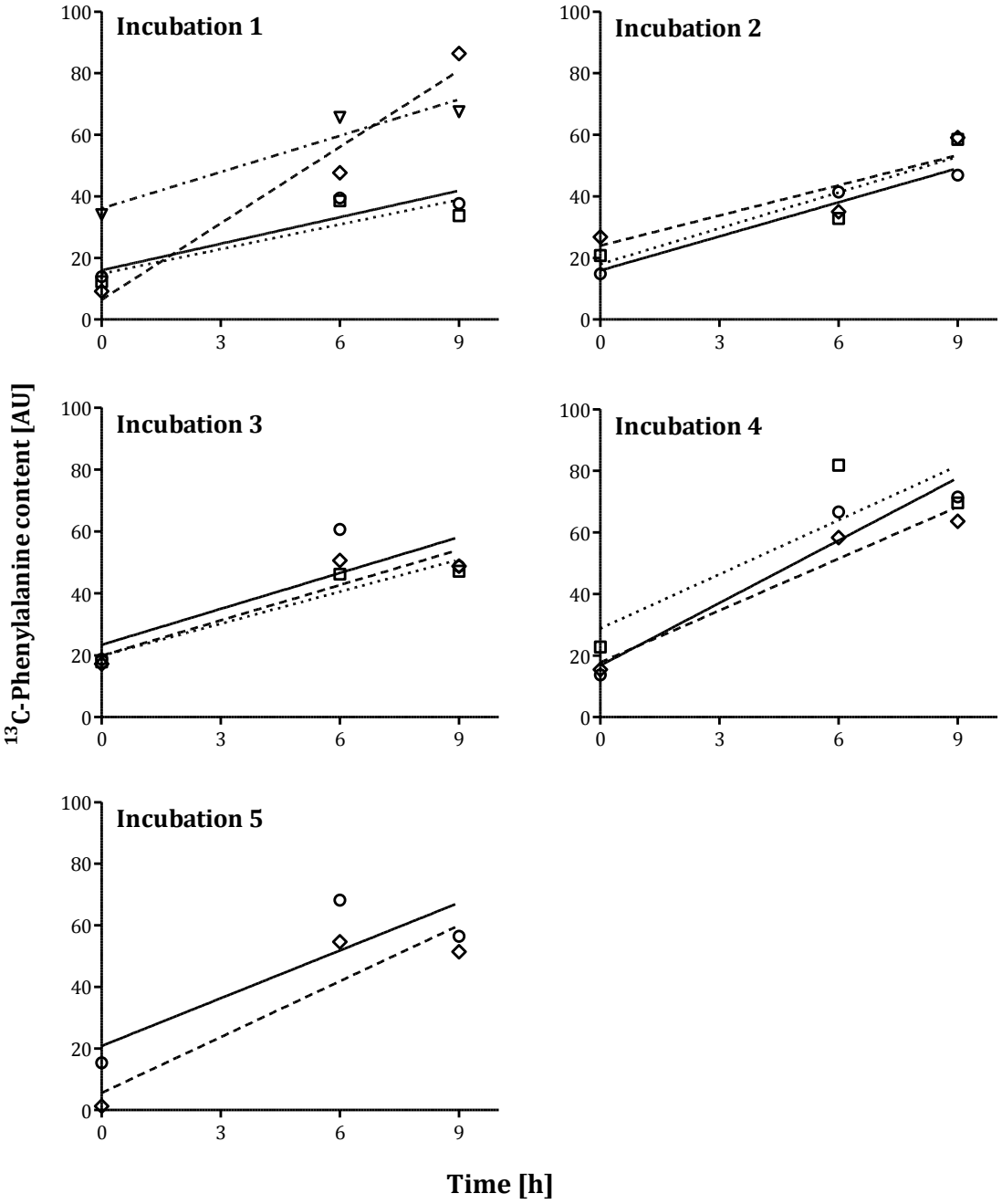

Figure 14 Integrals of the protein extracts, i.e. ^{13}C- phenylalanine content [AU]in the proteins over time and linear regressions for all replicates (different symbols and different dashing of lines) of incubations 1-5. All integrals were normalized to the weight of tissue powder used for extraction. Incubation 1: n=4, Incubation 2, 3 and 4: n=3, Incubation 5: n=2. For all linear regressions: $R^2 \geq 0.7$.

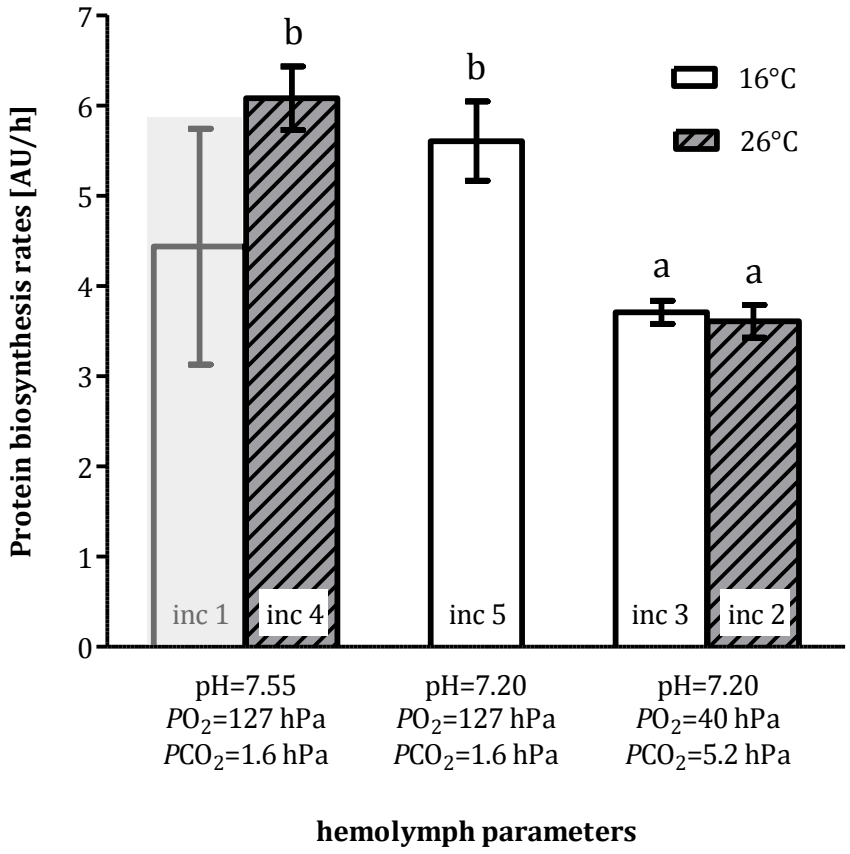

Figure 15 Protein biosynthesis rates (means of slopes of linear regressions in Figure 14) of all incubations [AU/h]. Incubation 1: n=4, Incubation 2, 3 and 4: n=3, Incubation 5: n=2. Displayed are means ± SEM. Different letters indicate the statistically significant differences between incubation treatments (One- way ANOVA with *post hoc* Bonferroni's multiple comparison test) when incubation 1 is neglected (indicated by gray shade).

3.3.4 Additional cytosolic metabolites

Besides the ^{13}C- phenylalanine signal, the ^{1}H- spectra also revealed relevant changes in other metabolites over the incubation time. The Shapiro- Wilk normality test revealed no statistically significant deviation from normal distributions for any incubation or time point (all $p>0.05$). The differences between incubations and time points were analyzed with an ANOVA and *post hoc* Bonferroni's multiple comparison test, if variances were homogeneous and with the less sensitive non- parametric Kruskal- Wallis test with Dunn's multiple comparison test, if variances were not homogeneous.

Anaerobic end products can provide information on condition of the animal or tissue before and during the incubation, respectively. Here, I focused on succinic acid (succinate) and fumaric acid (fumarate), because succinate is one of the main end products of incipient anaerobic metabolism in *M. edulis* (de Zwaan 1983, de Zwaan and Mathieu 1992). Both metabolites result in clearly

isolated signals at 2.41 ppm (succinate) and 6.53 ppm (fumarate) in the cytosolic ^{1}H- NMR spectra. Variances of succinate levels were not homogeneous and therefore the data were analyzed with a Kruskal- Wallis test, which revealed a significant difference between time points (Kruskal- Wallis statistic=22.58, $p=0.0039$) and with *post hoc* Dunn's multiple comparison test. For fumarate a one-way ANOVA with *post hoc* Bonferroni's multiple comparison test was performed ($F=27.38$, $p<0.0001$). The two signals were closely related and showed similar time courses in the different incubations (Figure 16A,B), whereupon total succinate levels were around 30 times higher than fumarate levels. In incubation 1 and 3 levels of both metabolites did not change significantly over time (all $p>0.05$), but in incubation 2 (at 26°C with all parameters as they occur at 26°C) the levels of both metabolites increased significantly (all $p<0.05$) after 6h and decreased slightly after 9h, but were not significantly different to the 6h sample (all $p>0.05$). For succinate the levels of the 6h and 9h samples of incubation 2 did not differ significantly to the overall levels of incubation 1 and 3 (all $p>0.05$, also see Table A6 and A7 in Appendix). Furthermore, in incubation 1 replicate C had a remarkably high succinic acid level in the control, although an outlier test (Grubb's test) did not indicate this value as a significant outlier compared to all other control (0h) samples ($p>0.05$).

Another interesting clear feature in the cytosolic ^{1}H NMR spectra was the lysine signal. Lysine is a crucial metabolite for protein biosynthesis since lysine is one of the main constituents of animal protein. Interestingly, the signal was only found in the incubated samples after 6h and 9h, but not in control spectra at 0h (Figure 16C). The lysine content did not differ significantly neither between 6h and 9h for all incubations nor between incubations (One-way ANOVA, $F=1.821$, $p=0.1655$, Table A8 in Appendix).

Trimethylamine oxide (TMAO) (Figure 16D) is an important osmo- regulator in all marine ectothermic invertebrates and the signals did not change significantly during all incubations (one-way ANOVA, $F=1.063$, $p=0.4200$, Table A9 in Appendix).

The ^{1}H spectra of the protein fraction revealed a very complex picture, which altered only slightly among samples, when normalized to the fatty acid signal at 1.74 ppm. Only few metabolites could be assigned with literature references (Table 6).

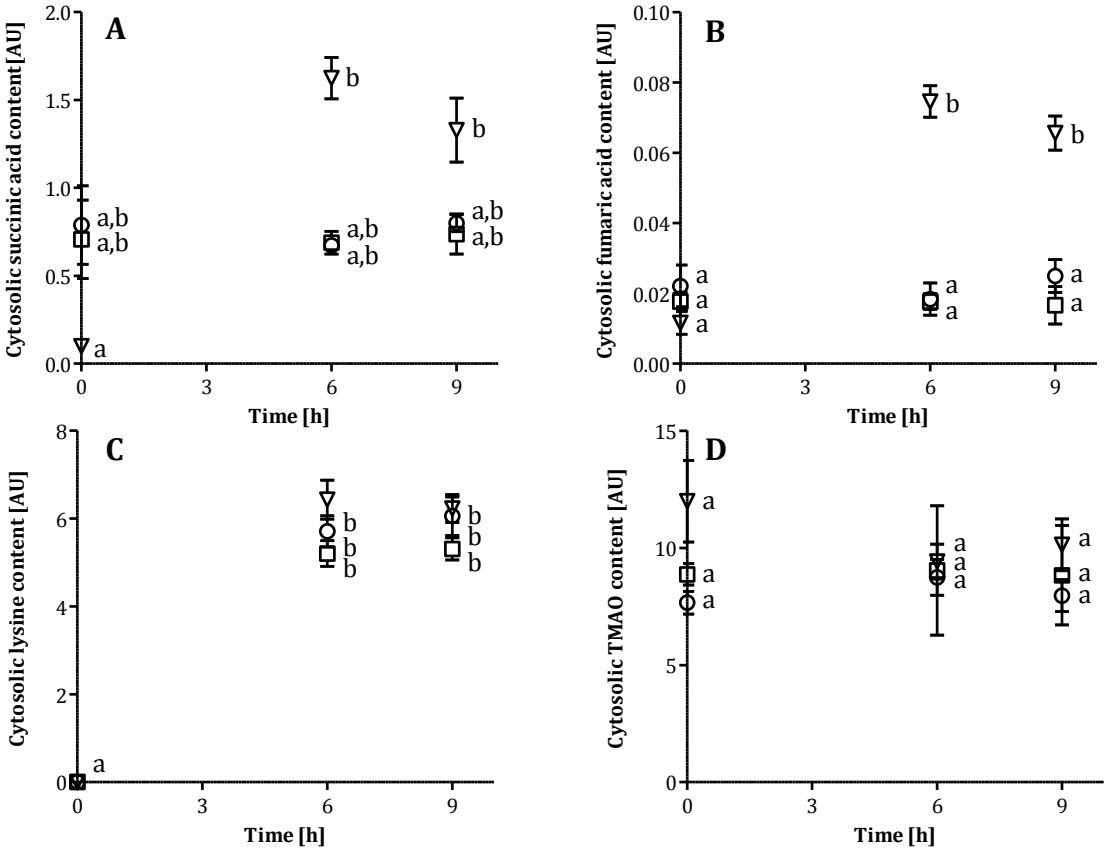

Figure 16 Changes of cytosolic content [AU] of **A)** succinic acid **B)** fumaric acid **C)** lysine and **D)** trimethylamine oxide (TMAO) in gill tissue of *M. edulis* over time [h] incubated at three different incubation treatments (Table 5). Incubation 1: Circles; Incubation 2: Triangles; Incubation 3: Squares. Different letters indicate significant differences (only comparing within each graph not between graphs; A: Kruskal- Wallis test, B & D: ANOVA, C: ANOVA for incubated samples (6h and 9h) only.

4. Discussion

In general, the flooding-dose technique was successfully applied to gill tissue of *M. edulis* in this study. The incorporated ^{13}C- phenylalanine could be validated in all cytosolic fractions in ^{1}H- and ^{13}C- NMR spectra as well as in all ^{13}C NMR spectra of the protein fractions in all incubations. The cytosolic uptake of the free amino acid was not significantly different between 6h and 9h, which means, that the cytosol was well enriched with ^{13}C- phenylalanine and a limitation of the incorporation into proteins by cytosolic ^{13}C- phenylalanine concentrations can be excluded. Protein biosynthesis rates were significantly different between incubations and the implications of the results will be discussed in chapter 4.4. Firstly, several aspects of the methodology need to be validated to fulfill the presuppositions for the main experiments.

4.1 Temperature-dependent hemolymph PO_2

As expected the hemolymph PO_2 decreased with increasing temperature, in line with the assumptions from the OCLTT model and from the literature (e.g. Peck *et al.* 2002). On the one hand, it is not entirely clear, though, if the PO_2 decrease is due to temperature increase or due to handling stress since the same mussels were used repeatedly for each temperature. On the other hand, determining the PO_2 for the same animals at each temperature reduced the inter-individual effects. Further, the mussels had one week between each extraction of hemolymph to recover from handling stress. The decreasing PO_2 values also could have been a cultivation effect, but during this experiment, only 17-20 mussels shared a tank of 100 L, water was exchanged daily and therefore the hemolymph PO_2 data determined in this study can be considered as valid. The values determined for *M. edulis* in this study were 129.7±7.8 hPa at 10°C, 118.8±7.4 hPa at 16°C, 98.56±10.2 hPa at 22°C and 61.2±8.1 hPa at 25°C (Figure 6). The data were well in range with data from other studies of bivalve hemolymph PO_2. For example, the hemolymph PO_2 values for *Laternula elliptica*, an Arctic bivalve, had oxygen levels of around 50% of ambient seawater at control temperatures (0°C) (≈105 hPa), which were lowered to 0-12% under increased temperatures (9°C) (≈0-25 hPa). The temperature-dependent relationship of hemolymph PO_2 of *M. edulis* was well in line with data determined for the Pacific oyster *Crassostrea gigas*, which has a similar distributional range as *M. edulis*. The hemolymph PO_2 of *C. gigas* was determined as 114.4±36.7 hPa at 15°C (Lannig *et al.* 2010), as 70.9±5.3 hPa at 18°C (Allen and Burnett 2008) and as 49.5±2.7 hPa at 25°C (Boyd and Burnett 1999). Beckmann (2011) determined hemolymph parameters (PO_2, PCO_2 and pH) at 10°C, which were in the range of the data determined for 25°C (Boyd and Burnett 1999), which was probably caused by prolonged shell closure before hemolymph extraction (Beckmann 2011). This shows, how important it is, that bivalves are not closed before hemolymph extraction so that

misinterpretations of the hemolymph parameters with respect to temperature can be avoided. The hemolymph PO_2 in *M. galloprovinciales* of 53±6 Torr (=70±8 hPa) at control temperature (18°C), measured by Michaelidis *et al.* (2005), is rather low around 40% of the value determined for *M. edulis* in this study and the value would correspond to a PO_2 at 24°C in *M. edulis*. Shell closure before hemolymph extraction might therefore be the explanation for the rather low hemolymph PO_2 values at control levels in *M. galloprovinciales*. It cannot be excluded, though, that a slight mixing of hemolymph with ambient seawater occurred in the posterior adductor muscle of *M. edulis*. As e.g. described by Gosling (2003) the hemolymph vessels transport the hemolymph from the gills through the heart ventricles and then the veins open into a sinus, which partly allows exchange of the hemolymph and surrounding seawater. Nonetheless, a slight overestimation of PO_2 for all values will not affect the results of this mainly mechanistic study.

4.2 Cultivation of animals

The significantly lower condition index for the batch, which had been cultivated at AWI two months longer than the batch of the experimental animals ($p<0.001$) means a decrease in mussel tissue in relation to shell weight and can be best explained by starvation effects. Considering that the experimental mussels for this study were cultivated at AWI for at least one month, the condition index, for these animals is probably decreased as well in comparison to wild mussels. These findings are in accordance with earlier studies indicating that carbohydrate and protein content of *Mytilus edulis* is reduced especially in the mantle tissue under prolonged laboratory cultivation condition (Bayne and Thompson 1970). The importance of optimal feeding of *M. edulis* during experiments has already been discussed by e.g. Bayne *et al.* (1976b) and again recently by Thomsen *et al.* (2013), who showed that sufficient food supply in the Kiel Fjord can even out-balance hypercapnia effects in *M. edulis*. For this study mussels were fed with commercial living phytoplankton once daily, which could be optimized by a flow-through system with natural brackish water from the Kiel Fjord. Determination of maximum filtration rate of the mussels would ensure optimal performance condition of the mussels before the start of the experiments. Nevertheless, since all experimental mussels experienced the same cultivation effects, a lowered condition should not affect the results.

4.3 The flooding-dose method using ^{13}C- labeled phenylalanine

All in all, the methodology is valuable for direct determination of protein biosynthesis in gill tissue of *M. edulis*. The ^{1}H-/^{13}C- NMR approach has the great advantage in comparison to e.g. radioactive tracers, that not only the tracer (i.e. ^{13}C- phenylalanine) can be followed, but also the

main intracellular metabolites. Especially the cytosolic ^{1}H spectra contain information about the condition of the animal as well as cellular information on anaerobic end products or osmoregulation.

The cytosolic ^{13}C- phenylalanine contents were not significantly different between 6h and 9h and also not between incubations, which confirms that the differences in protein biosynthesis rates are not due to differences in availability of ^{13}C- phenylalanine but are positively due to restrictions in energy budget caused by different hemolymph parameters. The uptake kinetics with a non-linear curve-fitting resulted in differences between incubation and especially incubation 1 displayed a different uptake than incubation 2 and 3 (difference of incubation 1 discussed later in 4.4.1). However, for a proper curve fitting more time points are necessary especially shortly after the start of the incubation to validate the first assumption of the flooding-dose method, that the free amino acid equilibrates quickly with the intracellular levels.

The increase of ^{13}C- phenylalanine content in proteins over time was assumed to be linear according to the basic assumptions of the flooding-dose method (Garlick *et al.* 1980). In a study on *S. nudus* protein biosynthesis rates were perfectly linear (Langenbuch *et al.* 2006). However, in this study most replicates did not depict a linear course over time since in eight of the fifteen replicates of all incubations the samples taken after 9h had lower ^{13}C-phenylalanine levels than after 6h. Therefore, 9h may already have been too long for incubating isolated gill tissue and the tissue may have started to degrade. The incubation time of 9h was chosen based on a pre-experiment (16°C, pH 7.55, bubbling with air, 0h, 1.5h, 4h, 9.5h), in which the protein ^{13}C-phenylalanine content did not decrease after 9h. For future studies more time points should be considered and incubation time may be shortened by a few hours. Fitting the curves non-linearly and taking the maximum slopes of the new curves may result in different results. The limited time for this thesis, though, did not allow further analysis in this direction. More time points could also ameliorate the linear fit. The lowered ^{13}C- content in the proteins after 9h in more than 50% of all replicates are probably due to net protein degradation resulting from lower protein synthesis than proteolysis, most likely caused by deteriorated condition of the isolated tissue, which naturally cannot survive infinitely in the isolated state. In *S. nudus* the protein biosynthesis rates were perfectly linear over 7h (Langenbuch *et al.* 2006), probably because the muscle tissue generally has lower metabolic activity, including slower protein turnover rates than the gill tissue of *M. edulis* (Houlihan 1991) and thereby less tissue was degraded.

Hence, it is desirable to have a measure for the fitness of the tissue to assess, at which time point after isolation the tissue is degrading and does no longer represent the tissue in the whole organism. One way to measure the condition of the tissue could be oxygen consumption. An experiment, in which tissue is incubated, as it was for this study, and oxygen consumption

measurements in between could answer these questions. However, this would probably lead to increased handling stress and tissue condition would decrease faster than during an undisturbed incubation. Another way to measure the condition of isolated gill tissue during the incubation could be to document the changes of cilia beating over time. A lack of energy supply in the tissue due to tissue degradation should influence the beating frequency of the gill cilia, responsible for creating the water flow through the whole animal for feeding and respiration purposes. Several earlier studies have investigated effects of neurotransmitters such as Acetylcholine (e.g. Bulbring *et al.* 1953) or Serotonin (e.g. Stommel and Stephens 1985) on the cilia and showed that ciliary movement is maintained in isolated gill tissue (Jørgensen 1974).

4.4 Temperature-dependent protein biosynthesis in Mytilus edulis

The protein biosynthesis rates determined in this study (Figure R11) were 2.3 to 3.6 times higher than the rates determined by Langenbuch *et al.* (2006) for *S. nudus*, which is generally in the same range. The higher rates in this study are not surprising because muscle tissue is commonly known to have lower protein synthesis rates than gill tissue in all marine ectotherms (Houlihan 1991). For *S. nudus* protein biosynthesis rates of muscle tissue measured with the same method was lowered by almost 60% when pH decreased by 1.2 units (Langenbuch *et al.* 2006). Changes of hemolymph parameters, as they occur at the whole animal level with a temperature increase of 10°C, caused lowered protein biosynthesis rates by around 40% (comparison incubation 4 and incubation 2, Figure 15). However, the study on *S. nudus* applied a fairly high level of hypercapnia and did not consider temperature effects (Langenbuch *et al.* 2006). Hence, a comparison between the two studies is difficult, but at the same time illustrates the importance of combined studies taking into account global warming and ocean acidification as a combined process, since both processes include similar changes and effects might add up.

Figure 15 assembles important information on the specific effects of temperature and pH, each contemplated independently of all other hemolymph parameters, on the protein biosynthesis of *M. edulis* from the Kiel Fjord population. Before these effects can be discussed, it needs to be considered, that the control incubation (incubation 1) may not be feasible for analysis of temperature and pH effects due to its large variation. Hence, reasons for the large variation in the control incubation treatment will be discussed first (4.2.1). Then, the specific effects of temperature *per se* (4.2.2), independent of the other hemolymph parameters (PO_2, PCO_2 and pH) will be discussed. Further, based on conclusions drawn from 4.2.1 and 4.2.2, further aspects of temperature- dependent growth will be discussed (4.2.3 and 4.2.4 and 4.2.5).

4.4.1 High variation in control incubation

The control incubation (incubation 1) showed an extremely high variation of protein biosynthesis rates (4.44±1.31 AU/h) with an SEM of around 30% of the mean, while the other incubations displayed SEMs between 3 to 8% of the mean values. On closer examination of the ^{13}C-phenylalanine content in the protein fraction over time (Figure 14 Inc. 1), it becomes clear, that the variation resulted from two replicates with very low protein biosynthesis rates, which were the lowest rates determined in all experiments (Figure 14 Inc. 1). Another replicate revealed a very high protein biosynthesis rate, which lied above the rates from all other incubations and the fourth replicate depicted a medium protein biosynthesis rate with a rather large integral of ^{13}C- phenylalanine in the control sample at 0h (Figure 14 Inc. 1). It cannot be fully excluded, that the observed protein biosynthesis rates of incubation 1 are simply in the range of the natural variability. For example, the isolated gill tissue may simply have a higher scope for variability under control incubations and a treatment of any kind may then narrow the variability and lead to the observed differences in variance. The condition indices for any animals used for the incubations were not particularly low and condition can therefore not be drawn upon for explaining variation. Other factors, which were not measured or documented in this study, may also play a role in protein biosynthesis rates on whole animal level, like the sex of the animal and/or gonad production. These parameters were not determined since experiments were conducted in November and gonads were not developed far enough to allow sex determination and an impact of gonad production on the animals was assumed to be minor. Moreover, the gills are not involved in any reproductive processes and therefore should not be affected by gonad development. However, expecting highest growth rates at control conditions at 16°C, the protein biosynthesis rates at this temperature should exhibit the highest rates. In accordance, with this, in a pre-experiment, gill tissue was incubated at 16°C with a pH of 7.55 in the same setup, but the medium was bubbled with air rather than defined PO_2 and PCO_2.The protein biosynthesis rate for this incubation was 7.3 AU/h, which comes close to the highest protein synthesis rate found in incubation 1 (8.27 AU/h). Consequently, the low protein biosynthesis rates found in this study under control conditions (incubation 1) are more likely to be the result of errors. The first of these replicates contained two of the largest mussels used for all incubations and since protein synthesis is thought to decrease with size (Bayne *et al.* 1976b), i.e. age (Hawkins and Bayne 1992) this might be an explanation for the exceptional low value. The other replicate with a low protein biosynthesis rate displayed high succinate levels in the control sample (0h). It is known, that *M. edulis* accumulates high levels of succinate during initial anaerobiosis, i.e. when it is closed for few hours, e.g. at the beginning of low tides (de Zwaan 1983, de Zwaan and Mathieu 1992). Therefore, the high succinate levels in one replicate of incubation 1 indicate, that the mussels of this replicate were closed at least for several hours

before the experiment started. Mussels usually close their shells when they are stressed, so at least one of the pooled mussels may have faced some sort of stress, which may have inhibited protein biosynthesis and this may explain the low rate. The fourth replicate revealed notably high levels of ^{13}C- phenylalanine in the control sample (34 AU at 0h) (Figure 14, Inc. 1), which may have been caused by carry over error of ^{13}C from an incubated sample (6h or 9h) to a control sample, either during the extraction process or in the NMR rotor. If the ^{13}C-phenylalanine content in the 0h sample of this replicate were in the same range as the other control levels (9-14 AU), the slope of the linear regression would increase and protein biosynthesis rates would fall in the expected higher range. In conclusion, the reasons for some unexpected low protein biosynthesis rates and a consequently large variation in the control incubation can only be guessed and the results remain equivocal. Therefore, in the following interpretation of the protein biosynthesis rates, incubation 1 will be neglected and the determination of an alternative control is desirable.

4.4.2 Specific effects of temperature

The comparison of incubation 2 (all parameters as they occur at 26°C) and incubation 3 (temperature at 16°C and all other parameters as they occur at 26°C) showed no significant difference ($p>0.05$) and both treatments are remarkably similar in means and also in variations. This shows, that temperature does not influence protein biosynthesis, when PO_2, PCO_2 and pH are at levels as they occur at 26°C. It was expected that the protein biosynthesis would be even a little lower in incubation 2, because proteins degrade faster beyond optimum temperatures due to less stability (Somero 2012). However, the protein biosynthesis rates in incubation 2 are only marginally lower than in incubation 3 (not significant $p>0.05$) and therefore the effect of temperature, independent of other hemolymph parameters, can be considered as not significant for this case, probably because the higher temperature is still in the pejus range and enhanced protein degradation is only momentous beyond critical temperatures. Additionally, between incubation 2 and incubation 4 (temperature at 26°C and all other parameters as they occur at 16°C) all parameters are altered except for temperature (both at 26°C) and the protein biosynthesis rates are significantly lower in incubation 2 by around 40% ($p<0.01$). Although this comparison does not positively proof, that temperature alone does not influence protein biosynthesis, it further indicates, that temperature *per se* is not the main determining factor of temperature-dependent growth, when PO_2, PCO_2 and pH are kept constant. Incubation 4 shows high protein biosynthesis rates, even though at 26°C somatic growth is decreased at whole organism level. This is apparently due to sufficient energy supply by control level PO_2, PCO_2 and pH. Earlier studies have already proven that thermal limits are much broader, when oxygen and energy supply are sufficient (Somero and DeVries 1967). For instance, isolated hepatocytes of

the Antarctic eelpout *Pachycara brachycephalum* have a much broader thermal tolerance compared to the whole animal (Mark *et al.* 2005).

All in all, these findings confirm the second hypothesis that protein biosynthesis rates will not decrease at elevated temperatures when PO_2, PCO_2 and pH are kept constant.

Assuming that temperature *per se* does not affect protein biosynthesis rates significantly, when the hemolymph parameters are kept constant, and considering, that protein biosynthesis rates for incubation 1 were expected to be largest among all treatments (see above 4.4.1), the protein biosynthesis rates for the control incubation (incubation 1) should theoretically be around the values determined for incubation 4. Therefore, in the following argumentation incubation 4 is considered as the "alternative control incubation" (incubation 1_{theory}).

Based on this argumentation, the alternative control incubation (inc. 1_{theory}=all parameters as they occur at 16°C) would be significantly higher than incubation 2 (all parameters as they occur at 26°C) (6.07±0.35 vs. 3.57±0.18; $p<0.01$). This would mean, that isolated gill tissue synthesizes proteins dependent on temperature (coupled to the correspondent hemolymph parameters) in the same way as somatic growth depends on temperature at the whole organism level. These findings indicate that the temperature-dependent performance observed at whole animal level (Bayne *et al.* 1976b, Almada-Vilella 1982, see chapter 1.2.2) is also valid for isolated gill tissue, considering the above-mentioned assumptions.

4.4.3 Specific effects of pH

Many studies on marine ectotherms investigated the effects of acidosis in the light of respirational acidosis or ocean acidification. Generally pH has been found to influence protein biosynthesis in marine invertebrates (Langenbuch and Pörtner 2002, Langenbuch *et al.* 2006), marine vertebrates (Langenbuch and Pörtner 2003), mammals (Dorovkov *et al.* 2002) and in plants (Vayda *et al.* 1995) caused by pH sensitive phosphorylation of elongation and initiation factors.

The comparison between incubation 1_{theory} (=incubation 4) and 5 (temperature at 16°C and PO_2 and PCO_2 as they occur at 16°C and pH as it occurs at 26°C) holds information on the specific effect of pH on protein biosynthesis. Incubation 5 reached around 92% of the protein biosynthesis rates of incubation 1_{theory}. The two treatments differed only by a lowered pH, while all other parameters were constant. The comparison did not reveal a significant difference ($p>0.05$) and pH may therefore not significantly affect temperature-dependent protein biosynthesis in *M. edulis* from the Kiel Fjord population. Additionally, between incubation 2 and 5 all parameters are altered except for pH resulting in significantly lower protein biosynthesis rates of incubation 2 ($p<0.05$) at levels around 36% of the rates in incubation 5 (Figure 15). This

further indicates, that pH is rather not the main factor determining temperature-dependent protein biosynthesis rates. However, low replication of incubation 5 (n=2) needs to be considered and measurements of further replicates and also the protein biosynthesis rates of incubation 6 will reveal more comprehensive information about specific pH effects on protein biosynthesis rates. Comparing incubation 2 and 6 can give a direct measure for pH effect since these two treatments only differed in pH (incubation 6 with control pH) while keeping all other parameters at the levels as they occur at 26°C.

According to these results, the first hypothesis, that a decreased pH independently of temperate, PO_2 and PCO_2 leads to decreased protein biosynthesis rates, is rather rejected. This result, though, needs to be contemplated carefully, considering, that incubation 5 only consists of n=2 and one incubation still needs to be analyzed for further validation of the results (inc. 2 vs. inc. 6) and also considering that the values for incubation 1_{theory} are hypothetical.

The indications in this study, that a decreased pH does not seem to affect protein biosynthesis rates is in contrast to findings on protein biosynthesis rates of the marine worm *S. nudus* (Langenbuch *et al.* 2006). However, the study on *S. nudus* investigated the effect of a drop in pH 4 times larger than the drop in hemolymph pH expected for a 10°C increase in temperature (Δ pH 1.2 vs. 0.3). Thus, the difference in pH may have been too small to cause a pH effect on protein biosynthesis. The differences can, of course, also derive from the different species and different tissue type.

Extracellular pH cannot be fully compensated at the whole animal level of the *M. edulis* population from the Kiel Fjord except for only slight non-bicarbonate buffering (Thomsen *et al.* 2010). A drop in extracellular pH, as caused by rising temperatures was expected to cause a specific effect on protein biosynthesis, because it will most likely cause changes in pH_i. Even though the pH_i was shown to be actively regulated in *M. galloprovinciales*, it was not fully compensated in gill tissue until after four days of exposure to hypercapnia (Michaelidis *et al.* 2005). In accordance, Beckmann (2011) found that pH_i in the Pacific oysters *C. gigas* is not regulated immediately during experiments and proposed that *C. gigas* hemocytes need at least several hours before regulating pH_i. Hence, it can be assumed that the pH_i in the experiments of this study was not fully compensated without major implications on protein biosynthesis. The pH_i homeostasis (acid-base homeostasis) is usually performed at the expense of an enhanced cellular and mitochondrial energy demand since protons have to be removed actively. An indication for increased energy demand resulting from pH_i regulation has been shown for *M. edulis* from Kiel Fjord: moderate levels of hypercapnia caused an increase in metabolic rate, which was suggested to result from increased costs for cellular homeostasis (and calicification) (Thomsen and Melzner 2010). Unfortunately, the pH_i was not determined in this study for the

incubated tissue and therefore only speculations on pH_i effects are possible. If pH_i was actively regulated during the exposure to lowered pH_e during the incubations in this study, the likely increased energy demand would not have led to decreased protein biosynthesis rates in gill tissue of *M. edulis*. This would indicate, that pH_i seems to be regulated with only little energy expenditure or at least not enough to significantly decrease protein biosynthesis rates. The regulation of pH_i in *M. galloprovinciales,* though suggests a rather slow regulation of pH_i during the acute exposure to a decreased pH_e. However, this is only a hypothetical argumentation and the questions, to which extend the pH_i was regulated during the incubations and which effects this may or may not have on protein biosynthesis rates, remain unanswered. Future studies may include the determination of pH_i as an additional factor in temperature-dependent growth. Occasional upwelling of oxygen depleted/CO_2 enriched bottom waters in the Kiel Fjord need to be taken into account as well, when addressing potential effects of intracellular and extracellular pH in the *M. edulis* population from the Kiel Fjord since the population may already have developed adaptations to an acute drop in pH.

It is most likely, that hemolymph PO_2 and/or PCO_2 cause the observed decrease of protein biosynthesis rates between incubation 1_{theory} and 2 by about 40%. In line with this conclusion is the observed difference between incubation 3 and 5 ($p<0.05$) of around 32% since only PO_2 and PCO_2 were varied between these two treatments while temperature and pH were kept constant. This will be further investigated by future comparison of incubation 4 and incubation 6. Moreover, between incubation 4 and 5 temperature and pH were altered while PO_2 and PCO_2 were kept constant. This comparison did not reveal a significant difference ($p>0.05$), which also indicates, that the hemolymph gas parameters PO_2 and/or PCO_2 are likely the determining factors for protein biosynthesis rates. Further confirmation of this conclusion will also be available when comparing incubations 3 and 6.

To sum up, based on the theoretical values for control protein biosynthesis rates, one may conclude, that a temperature increase from 16°C to 26°C, including associated changes in the other hemolymph parameters, does affect protein biosynthesis in isolated gill tissue (inc 1_{theory} vs. inc 2). Temperature *per se*, i.e. independent of other hemolymph parameters, does not influence protein biosynthesis rates significantly (inc 2 vs. 3; inc 2 vs. 4). pH is most likely not the only determining factor, either (inc 1_{theory} vs. 5; inc 2 vs. inc 5), although some measurements are still necessary to fully confirm this (inc 1_{theory} vs. inc 6; inc 2 vs. inc 6). Therefore, the determining factor is likely one of the other parameters or a combination of them. This could be PO_2 and or PCO_2, but also other parameters of the carbonate system, such as bicarbonate.

4.4.4 The role of hemolymph PO_2

M. edulis is known to be well adapted to low oxygen tension and therefore PO_2 was not considered to be a crucial factor. The PO_2 values as they occur at 26°C are low but not yet in the hypoxic range. Severe hypoxia is generally considered to start below a threshold of 0.2 mL O_2 /L (PO_2≈40 hPa), which is the lowest PO_2 applied in this study (Diaz and Rosenberg 2008). Elevated succinate and fumarate levels in incubation 2 indicate, that the oxygen tension was too low to fully support aerobic metabolism and thus a mismatch occurred between oxygen demand and oxygen supply. This mismatch was likely caused by elevated enzymatic activity due to the temperature (26°C) only, because incubation 3 had the same low oxygen tension and high PCO_2 with low pH, but at 16°C and did not reveal increased succinate and fumarate levels after 6h and 9h (Figure 16A,B). *M. edulis* is known to have different "stages of anaerobic metabolism" known from studies of anaerobic end products over the tidal cycle (de Zwaan 1983, de Zwaan and Mathieu 1992, see Figure 17). Those studies revealed succinate as the main anaerobic end product in the beginning of air exposure and the associated shell closure. After prolonged air exposure, succinate was found to be further metabolized to propionate (Figure 17). Therefore, anaerobiosis in incubation 2 can be considered as mildly or "initial" since succinate was accumulated and likely not further processed to propionate. Further, the gill tissue was able to maintain protein biosynthesis rates by anaerobic pathways because incubation 2 did not reveal significantly lower protein biosynthesis rates than incubation 3, which did not accumulate succinate. Moreover, the Pacific oyster *C. gigas* was found to accumulate succinate in the gills under hypercapnia, whereas mantle and muscle tissue did not reveal these accumulations (Lannig *et al.* 2010), thus indicating that anaerobic metabolism may already occur in bivalve gill tissue, when the whole animal is not yet experiencing hypoxic conditions. In conclusion, these findings confirm, that *M. edulis* is well adapted to low oxygen tension and therefore suggest, that the determining factor for temperature-dependent protein biosynthesis in gill tissue of *M. edulis* rather lies in PCO_2 or other parameters of the carbonate system.

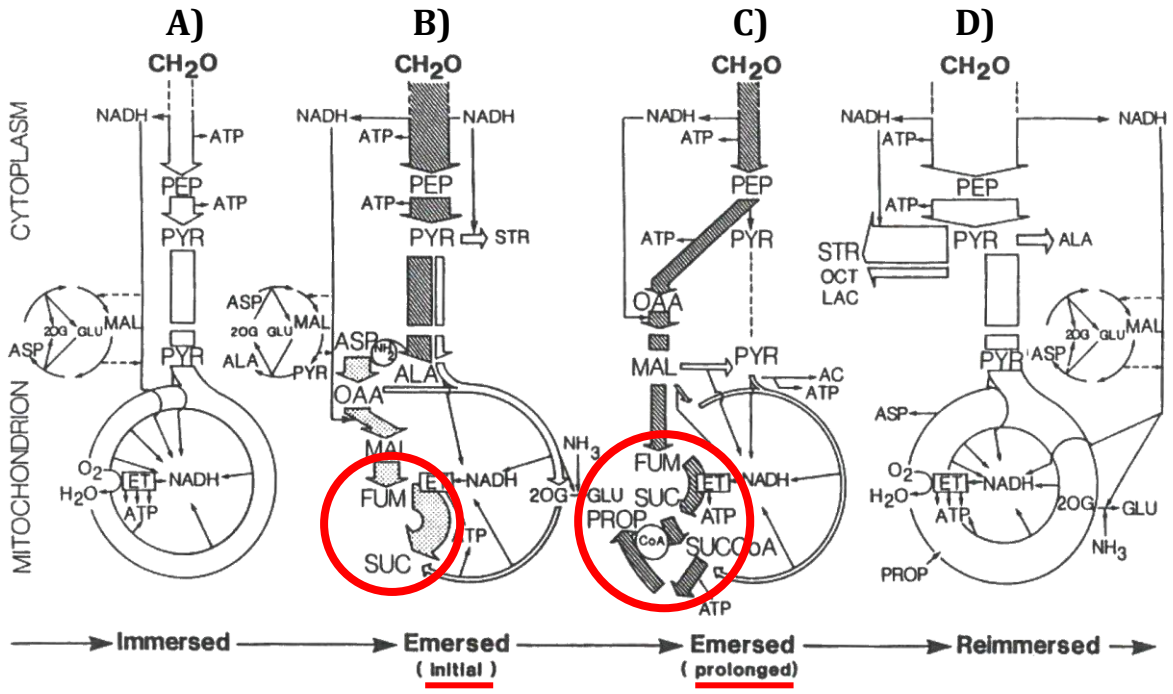

Figure 17 Schematic illustrations of the transition between metabolic pathways over the tidal cycle: **A)** Aerobiosis when mussels are immersed under water **B)** Initial anaerobiosis during beginning of air exposure **C)** Steady-state stage of anaerobiosis after prolonged air exposure **D)** Aerobiosis after reimmersion. The width of the arrow indicates the relative carbon flux through the pathways. Red circles highlight the relevant anaerobic pathways discussed in this thesis. **Abbreviations: AC-** acetate; **ALA-** alanine; **ASP–** aspartate; **CH_2O-** glycogen; **ET-** electron transfer chain; **FUM-** fumarate; **GLU-** glutamate; **LAC-** lactate; **MAL-** malate; **OAA-** oxaloacetate; **OCT-** octopine; **2OG-** 2-oxoglutarate; **PEP-** phosphoenolpyruvate; **PROP-** propionate; **PYR-** pyruvate; **STR-** strombine; **SUC-** succinate; **SUCCoA-** succinyl CoA (modified after de Zwaan and Mathieu 1992).

4.4.5 The role of hemolymph PCO_2 and bicarbonate

Only few studies investigated the specific effects of pH and PCO_2 independently from each other. Walsh *et al.* (1988) found PCO_2 to influence lactate metabolism of isolated hepatocytes from rainbow trout in the process of acidosis, independent from pH and [HCO_3^-]. In that study, pH and [HCO_3^-] also showed effects on lactate metabolism, independent from PCO_2 and from each other, but not as strong as the specific PCO_2 effects. PCO_2 may therefore be an important factor for temperature-dependent protein biosynthesis in *M. edulis*. However, Langenbuch *et al.* (2006) found no effect of PCO_2 on protein biosynthesis rates of an invertebrate and the question whether PCO_2 is the determining factor for temperature-dependent growth in *M. edulis* requires additional investigations. Further studies with targeted systematic variation of only PCO_2 while controlling all other hemolymph parameters need to address this issue in the future.

It is further unclear, which role bicarbonate concentrations play in the cellular energy generation. Unfortunately, it was not possible to specifically control [HCO_3^-] in this study. The

studies by Thomsen *et al.* (2010) suggested that the Kiel Fjord blue mussels do not regulate extracellular pH by bicarbonate accumulation and that the carbonate chemistry follows the Davenport diagram based on to the Henderson-Hasselbach equation (Melzner *et al.* 2009, Thomsen *et al.* 2010). Based on the hemolymph PCO_2 and pH values, that were chosen and controlled for 16°C and 26°C, hypothetical bicarbonate levels were read as followed from the Davenport diagram (Table 8).

Table 8 Settings for the incubation medium including theoretical bicarbonate concentrations in the different incubation treatments (1-6).

	Temperature	$\boldsymbol{PO_2}$	$\boldsymbol{PCO_2}$	**pH**	**Theoretical [$\boldsymbol{HCO_3^-}$]**
Incubation 1	16°C	127 hPa	1.6 hPa	7.55	1.7 mM
Incubation 2	26°C	40 hPa	5.2 hPa	7.20	2.2 mM
Incubation 3	16°C	40 hPa	5.2 hPa	7.20	2.2 mM
Incubation 4	26°C	127 hPa	1.6 hPa	7.55	1.7 mM
Incubation 5	16°C	127 hPa	1.6 hPa	7.20	0.5 mM
Incubation 6	26°C	40 hPa	5.2 hPa	7.55	5.5 mM

Considering these theoretical values, incubation 6 could be of utmost importance, since bicarbonate concentrations at these PCO_2/pH combination may have been very high according to the Davenport diagram. If these theoretical bicarbonate concentrations were valid, incubation 2 and 3 would have had the highest levels of bicarbonate of all analyzed incubations. Interestingly, these two incubations also show the lowest protein biosynthesis rates. Indications for an effect of bicarbonate concentrations on protein biosynthesis rates have already been found and discussed by Langenbuch *et al.* (2006). The physiological background of potentially suppressed protein synthesis by bicarbonate lies in the activation of sAC (Chen *et al.* 2000), which can cause cAMP levels to rise and can thereby suppress protein translation by PHAS proteins (Lawrence *et al.* 1997). sACs have recently been discovered in several invertebrates like molluscs, echinoderms and corals (Tresguerres *et al.* 2014) and can be assumed to play an important role in the physiology of bivalves (Fabbri and Capuzzo 2010). Moreover, cAMP has been shown to affect the dynein proteins responsible for cilia beating in gill tissue (Stommel and Stephens 1985, Tresguerres 2014).

However, bicarbonate concentrations may have differed from the theoretical values in Table 8, because HEPES was used as a buffer and the same concentrations of solid bicarbonate were added to all incubations before adjusting the pH. Therefore, it is difficult to estimate how much

bicarbonate gassed out before the incubation started. Nevertheless, bicarbonate levels, at whichever concentration, probably stayed constant over the incubation time of 9h since PCO_2 and pH values remained stable.

4.4.6 Additional cytosolic metabolites

The implications of increased succinate and fumarate levels in incubation 2 have already been discussed partially with respect to protein biosynthesis and the role of hemolymph PO_2 (chapter 4.2.4). Fumarate is the second last intermediate in the initial anaerobic pathway ending in succinate (Figure 17B). Since fumarate accumulates in incubation 2 in the same pattern as succinate over time, this might indicate, that there is excess fumarate accumulated on short-term until further procession into succinate. However, this accumulation can be considered minor since overall fumarate levels were 30 times smaller than succinate levels.

Trimethylamine oxide (TMAO) levels did not differ significantly over time and also between incubations (Figure 16D, $p>0.05$). These results suggest, that TMAO levels were constant and that no further energy was expended for osmoregulation since TMAO is the most important osmolytes of all marine invertebrates. This indicates, that incubation conditions were stable with respect to ion balance. Further, the constant TMAO levels validate the calibration method on the fatty acid signal at 1.74 ppm.

Lysine is one of the most abundant amino acids in animal proteins. The cytosolic lysine levels significantly rose after 6h and 9h incubation, which may be the result of protein degradation. This may seem contradictory at first, since ^{13}C-phenylalanine incorporation indicated protein synthesis, but in all animal tissues proteins are constantly synthesized and degraded at the same time and gill tissue is in fact the tissue type with one of the highest protein turnover rates in all marine ectotherms (Houlihan 1991). The protein turnover can even account for up to 16% of basal metabolism in *M. edulis* from southwest England (Hawkins 1985). Therefore, one explanation for the elevated lysine levels could be the degradation of proteins. If lysine levels after 6h and 9h are a measure for protein turnover, the levels should be higher in incubations 4 and 5, since these treatments resulted in higher protein synthesis rates, but the cytosolic fractions of incubations 4 and 5 could not be measured, yet. However, a decrease in protein synthesis is not necessarily coupled to a decrease in protein degradation. This has been shown by Langenbuch *et al.* for protein turnover in *S. nudus*, whereupon protein synthesis rates were decreased by 60% at a low pH_e of 6.70 (Langenbuch *et al.* 2006), but protein/amino acid degradation was only 10-15% at the same settings (Langenbuch and Pörtner 2002). Furthermore, a lysine signal was expected in the ^{1}H spectra of the protein fraction, as well as other signals of amino acids, since they are the main components of proteins. However, only few signals could positively indicate amino acids, such as alanine and threonine. This is probably a

methodological effect of the extraction (see 4.5). In any case, the meaning of increased lysine levels remain unclear until further invetigations of amino acid metabolism and protein degradation under increased temperatures are conducted for *M. edulis*.

4.5 Further methodological evaluations

Some aspects of the methodology in this study have already been discussed with respect to the results. Some further aspects are discussed in this chapter.

The ideal incubation setup would have consisted of one incubation chamber per replicate with independent gassing each, so that the pseudo-replicates in this study could be considered "true replicates". Logistically, this was not possible and the final setup used in this thesis was a compromise between the theoretical optimum and the practical possibilities with time, budget and personal capacities. Pooling of three animals per replicate might become unnecessary, when the extraction method is optimized.

Protein ^{1}H spectra revealed only few amino acid signals, probably due to the hydrolization step during extraction (boiling protein fraction in 1M NaOH for 45 min.). The pH was not adjusted again before NMR measurements and may have caused strong shifts in the ^{1}H NMR spectra, so that amino acids could not be identified. Moreover, the heating may have been too short or too long and amino acids may not have fully separated or amino acids may already have fallen apart into smaller fragments, respectively. Both arguments would result in an alteration of the chemical environment of the amino acid- associated protons and thereby the amino acids would not display the typical signals in ^{1}H NMR spectra. The differences in the chemical environment however were not strong enough to affect the ^{13}C signals. This illustrates the drawbacks of ^{1}H NMR spectroscopy, namely that protons bound to carbon atoms are less stable in molecular conformation than the carbon atoms. Consequently, ^{1}H spectra are more variable and more prone to changes. A re-adjustment of pH after boiling the protein fraction in NaOH may lead to a better result. Another enhanced way to extract proteins may be ultra centrifugation after homogenization of the tissue in an extraction buffer, similar to the incubation medium. This method may also minimize the loss of tissue. However, this method has not been applied, yet for NMR metabolic profiling and needs confirmation.

Similar results of ^{1}H and ^{13}C spectra in the ^{13}C- phenylalanine signal cytosolic fraction are proof for the validity of the method. Differences may be explained by the different means of scaling and different measuring methodology. For example, ^{1}H measurements usually experience an effect, known as the "Nuclear Overhauser effect" (NOE), which describes the effect that the spin polarization of one nuclear spin population can affect the spin of another population, which is

nearby in space, irrespective of the chemical bonds between the two populations. The scaling of the ^{1}H spectra in the vertical dimension could also be done by calibrating to e.g. TMAO levels or to other metabolites, which are assumed to be constant. However, results will likely be similar since TMAO levels were quite stable in all incubations. ^{13}C- spectra could also be scaled to a particular signal instead of normalizing to tissue weight, but therefore, other signals in the ^{13}C-spectra would have to be assigned first.

5. Conclusion

Putting everything into a nutshell, temperature-dependent growth likely also occurs at the level of isolated gill tissue of *M. edulis* from the Kiel Fjord population. The method of flooding-dose worked very well and resulted in protein biosynthesis around 3 times larger than the range already determined with the same method for isolated muscle tissue of *S. nudus* (Langenbuch *et al.* 2006). Temperature-dependent protein biosynthesis was not determined by temperature *per se* and probably neither by pH. This leaves PO_2, PCO_2 and [HCO_3^-] or a combination of these factors as the potential triggers for temperature-dependent somatic growth. The treatment of incubation 6 (not measured yet) will give further confirmation of the current findings and may also reveal indications for the effects of bicarbonate concentrations. The incubation time for isolated gill tissue was probably too long since some replicates already showed net protein degradation after 9h compared to 6h. The cytosolic spectra of incubation 2 (all parameters set as they occur at 26°C) revealed succinate and fumarate levels after 6h and 9h indicating a metabolic shift from aerobic to anaerobic metabolism at these conditions, but not in incubation 3 (16°C with all other parameters as they occur at 26°C), indicating a sole temperature effect, which was not visible in the analysis of protein biosynthesis. All incubations revealed increased lysine levels after 6h and 9h, which most likely is a sign for increased protein degradation, because lysine is a common amino acid in animal protein. Whether the increased lysine levels are caused by high cytosolic ^{13}C- phenylalanine levels remains unclear.

Outlook

The interactive effects of temperature, hemolymph pH and hemolymph gas parameters (= PO_2 + PCO_2) can be analyzed in a two- way ANOVA when all data are available. Then, more advanced multivariate statistics may reveal a clearer picture of the relationship between succinate or lysine levels and protein biosynthesis.

Future experiments concerning the mechanism behind temperature-dependent growth should systematically investigate the other parameters (PO_2, PCO_2 and [HCO_3^-]) as it has been done in this study while keeping temperature constant. The findings of this study can be further validated by measuring the protein biosynthesis rates under the given conditions indirectly. Inhibitors, such as cycloheximide, lead to a decreased oxygen consumption and such measurements are usually faster and cheaper. However, not much is known on the side effects of such inhibitors. Therefore, an extra incubation with ^{13}C-phenylalanine and an inhibitor for protein biosynthesis such as cycloheximide, could combine the direct and the indirect approach of measuring protein biosynthesis. On the one hand, the protein extracts should then show no or decreased ^{13}C-phenylalanine incorporation over time. On the other hand, this would show the

possible side effects of these inhibitors on other metabolic processes by measuring the cytosolic fraction, in which the entire cytosolic metabolome can be displayed with one ^{1}H-NMR measurement and could thereby easily identify other possibly affected metabolic processes. If extraction and NMR measurements could be improved, the method used in this study could be used more frequently instead of indirect determination of protein biosynthesis. For further investigations, bicarbonate levels should be controlled severely by e.g. measuring dissolved inorganic carbon or total alkalinity of the incubation medium before and after the respective incubation time. If [HCO_3^-] showed an effect on protein biosynthesis, further studies may focus on the signaling cascade from bicarbonate over sAC to cAMP, which could influence protein biosynthesis of dynein in the ciliary apparatus or phosphorylation of the PHAS protein family. Measurements of the ciliary beating frequency would not only allow a measure for tissue condition over incubation time, but could also reveal information about the role of protein biosynthesis in the creation of the water current by measuring the ciliary beating frequency in combination with inhibitors for protein biosynthesis.

6. References

Acin-Perez R, Salazar E, Kamenetsky M, Buck J, Levin LR, Manfredi G (2009) Cyclic AMP produced inside mitochondria regulates oxidative phosphorylation. *Cell Met.* 9: 265-276.

Ahn HY, Sue LF, Ma JKH, Pinkstaff CA, Pore RS, Overman DO, Malanga CJ (1988) Synthesis and secretion of mucous glycoprotein by the gill of *Mytilus edulis* L. Histochemical and chromatographic analysis of [14C]glucosamine bioincorporation. *Biochim. Biophys. Acta* 966: 122-132.

Allen SM, Burnett LE (2008) The effects of intertidal air exposure on the respiratory physiology and the killing activity of hemocytes in the Pacific oyster, *Crassostrea gigas* (Thunberg). *J. Exp. Mar. Biol. Ecol.* 357: 165-171.

Almada-Villela PC (1984) The effects of reduced salinity on the shell growth of small *Mytilus edulis. J. Mar. Biol. Ass. U.K.* 64:171-182.

Almada-Vilella PC, Davenport J, Gruffydd LLD (1982) The effects of temperature on the shell growth of young *Mytilus edulis* L.. *J. Exp. Mar. Biol. Ecol.* 59: 275-288.

Avison MJ, Herschkowitz ZN, Novotny EJ, Petroff OAC, Rothmann DL, Colombo JP, Bachmann C, Shulman RG, Prichard JW (1990). Proton NMR Observation of Phenylalanine and an Aromatic Metabolite in the Rabbit Brain in Vivo. *Pediatr. Res.* 27(6): 566-569.

Baird RH (1958) Measurement of condition in mussels and oysters. *J. Cons. Cons. Int. Explor. Mer* 23: 249-257.

Bayne BL, Thompson RJ (1970) Some physiological consequences of keeping *Mytilus edulis* in the laboratory. *Helgoländer Meeresun.* 20: 526-552.

Bayne BL, Widdows J, Thompson RJ (1976a) Physiology II. In: Bayne BL (ed) Marine Mussels: their ecology and physiology. *Cambridge University Press*, Cambridge, pp.207-260.

Bayne BL, Widdows J, Thompson RJ (1976b) Physiological integrations. In: Bayne BL (ed) Marine Mussels: their ecology and physiology. *Cambridge University Press*, Cambridge, pp.261-291.

Bayne BL, Worrall CM (1980) Growth and production of mussels Mytilus edulis from two populations. *Mar. Ecol.-Prog. Ser.* 3: 317-328.

Beckmann M (2011) Modulation of intracellular pH of hemocytes from the Pacific oyster *Crassostrea gigas* to changes in extracellular pH. *Master's thesis*. University of Bremen.

Boyd JN, Burnett LE (1999) Reactive oxygen intermediate production by oyster hemocytes exposed to hypoxia. *J. Exp. Biol.* 202: 3135-3143.

Brigolin D, Dal Maschio G, Rampazzo F, Giani M, Pastres R (2009) An individual-based population dynamic model for estimating biomass yield and nutrient fluxes through an off-shore mussel (*Mytilus galloprovinciales*) farm. *Estuar. Coast. Shelf* S 82: 365-376

Bulbring E, Burn JH, Shelley HJ (1953) Acetylcholine and Ciliary Movement in the Gill Plates of *Mytilus edulis. Proc. R. Soc. Lond. B* 141 (905): 445-466.

Castejón D, Villa P, Calvo MM, Santa-María G, Herraiz M, Herrera A (2010) ^{1}H-HRMAS NMR study of smoked Atlantic salmon (*Salmo salar*). *Magn. Reson. Chem.* 48: 693-703

Chen Y, Cann MJ, Litvin TN, Iourgenko V, Sinclair ML, Levin LR, Buck J (2000) Soluble adenylyl cyclase as an evolutionarily conserved bicarbonate sensor. *Science* 289: 625-628.

Clarke A (1991) What is cold adaptation and how should we measure it? *Amer. Zool.* 31: 81.92.

Diaz RJ, Rosenberg R (2008) Spreading Dead Zones and Consequences for Marine Ecosystems. *Science* 321: 926-929.

Dijk PLM van, Tesch C, Hardewig I, Pörtner HO (1999) Physiological disturbances at critically high temperatures: a comparison between stenothermal Antarctic and eurythermal temperate eelpouts (Zoarcidae). *J. Exp. Biol.* 202: 3611-3621

Donkin P, Widdows J, Evans SV, Staff FJ, Yan T (1997) Effect of neurotoxic pesticides on the feeding rate of marine mussels (*Mytilus edulis*). *Pestic . Sci.* 49: 196-209.

Enderlein P, Wahl M (2004) Dominance of blue mussels versus consumer-mediated enhancement of benthic diversity. *J. Sea Res.* 51: 145-155.

Fabbri E, Capuzzo A (2010) Cyclic AMP signaling in bivalve molluscs: An overview. *J. Exp. Zool.* 313A: 179-200

Fields PA (2001) Review: Protein function at thermal extremes: balancing stability and flexibility. *Comp. Biochem. Phys. A* 129: 417-431.

Frederich M, Pörtner HO (2000) Oxygen limitation of thermal tolerance defined by cardiac and ventilator performance in the spider crab *Maja squinado. Am. J. Physiol.* 279: R1531-R1538

Garlick PJ, McNurlan MA, Preedy VR (1980) A rapid and convenient technique for measuring the rate of protein synthesis in tissues by injection of [^{3}H]phenylalanine. *Biochem. J.* 192: 719-723.

Gosling E (2003) Bivalve Molluscs. Biology, Ecology and Culture. *Fishing New Books, Blackwell Publishing Ltd, Oxford.* pp. 1-43.

Grimm V, Railsback SF (2005) Individual-based modeling and ecology. *Princeton University Press*, Oxfordshire, UK.

Hansen HP, Giesenhagen HC, Behrends G (1999) Seasonal and long-term control of bottom-water oxygen deficiency in a stratified shallow-water coastal system. *ICES J. Mar. Sci.* 56: 65–71.

Hawkins AJS (1985) Relationships between the synthesis and breakdown of protein, dietary absorption and turnovers of nitrogen and carbon in the blue mussel, Mytilus edulis L.. *Oecologia* 66: 42-49.

Hawkins AJS, Bayne BL, Clarke KR (1983) Co-ordinated rhythms of digestion, absorption and excretion in *Mytilus edulis* (Bivalvia: Mollusca). *Mar. Biol.* 74: 41-48.

Hawkins AJS, Bayne BL, Day AJ (1986) Protein turnover, physiological energetics and heterozygosity in the blue mussel, *Mytilus edulis*: the basis of variable age-specific growth. *Proc. R. Soc. Lond.* 229:161-176

Hawkins AJS, Wilson IA, Bayne BL (1987) Thermal response reflect protein turnover in *Mytilus edulis*. *Funct. Ecol.* 1: 339-351.

Hawkins AJS, Widdows J, Bayne BL (1989) The relevance of whole-body protein metabolism to measured costs of maintenance and growth in *Mytilus edulis*. *Physiol. Zool.* 62: 745-763.

Hawkins AJS, Bayne BL (1992) Physiological interrelations, and the regulation of production (Chapter 5). In: Gosling E (ed) (1992) The mussel Mytilus: Ecology, Physiology, Genetics and Culture. *Development in Aquaculture and Fisheries Science 25. Elsevier Science Publishers B.V.,* Amsterdam, The Netherlands. pp.171-222

HELCOM (2009) Eutrophication in the Baltic Sea – an integrated thematic assessment of the effects of nutrient enrichment and eutrophication in the Baltic Sea region. *Baltic Sea Environ. Proc.*:115B.

Hickman RW (1992) Mussel cultivation (Chapter 10). In: Gosling E (ed) (1992) The mussel Mytilus: Ecology, Physiology, Genetics and Culture. *Development in Aquaculture and Fisheries Science 25. Elsevier Science Publishers B.V.,* Amsterdam, The Netherlands. pp. 465-510.

Hilbish TJ, Zimmerman KM (1988) Genetic and nutritional control of the gametogenic cycle in *Mytilus edulis*. *Mar. Biol.* 98: 223-228.

Houlihan DF (1991) Protein Turnover in Ectotherms and its Relationships to Energetics. In: Gilles R (Hrsg.) Advances in Comparative and Environmental Physiology. 7: 1-43

Houlihan DF, Carter CG und McCarthy ID (1995) Protein turnover in animals. In: Walsh P, Wright P (eds.) Nitrogen metabolism and excretion. *CRC Press Boca. Raton.*, Fla. 1-32

Hrs-Brenko M (1973) The study of mussel larvae and their settlement in Vela Draga Bay (Pula, The Northern Adriatic Sea). *Aquaculture* 2: 173-182.

IPCC (2013): Summary for Policymakers. In: Climate Change 2013: The Physical Science Basis. Contribution of Working Group I to the Fifth Assessment Report of the Intergovernmental Panel on Climate Change [Stocker TF, Qin D, Plattner GK, Tignor M, Allen SK, Boschung J, Nauels A, Xia Y, Bex V, Midgley PM(eds.)]. *Cambridge University Press*, Cambridge, United Kingdom and New York, NY, USA.

IPCC (2014): Chapter 6. Ocean Systems. In: Climate Change 2014: Impacts, Adaptation and Vulnerability. Volume I: Global and Sectoral Aspects. Contribution of Working Group II to the Fifth Assessment report of the Intergovernmental Panel on Climate Change. *Cambridge University Press*, Cambridge, United Kingdom and New York, NY, USA.

Jones HD, Richards OG, Southern TA (1992) Gill dimensions, water pumping rate and body size in the mussel *Mytilus edulis* L.. *J. Exp. Mar Biol. Ecol.* 155: 213-237.

Jones SJ, Mieszkowska N, Wethey DS (2009) Linking thermal tolerance and biogeography: Mytilus edulis (L.) at its Southern limit on the east Coast of the United States. *Biol. Bull.* 217: 73-85.

Jones SJ, Lima FP, Wethey DS (2010) Rising environmental temperatures and biogeography: poleward range contraction of the blue mussel, Mytilus edulis L., in the western Atlantic. *J. Biogeogr.* 37: 2234-2259.

Jørgensen CB (1974) On gill function in the mussel *Mytilus edulis* L.. *Ophelia*13 (1-2): 187-232.

Kautsky N (1982) Growth and Size Structure in a Baltic *Mytilus edulis* Population. *Mar. Biol.* 68: 117-133.

Lander TR, Robinson SMC, MacDonald BA, Martin JD (2012) Enhanced Growth Rates and Condition Index of Blue Mussels (*Mytilus edulis*) Held at Integrated Multitrophic Aquaculture Sites in the Bay of Fundy. *J. Shellfish Res.* 31(4):997-1007.

Langenbuch M, Pörtner HO (2002) Changes in metabolic rate and N excretion in the marine invertebrate *Sipunculus nudus* under conditions of environmental hypercapnia: identifying effective acid-base variables. *J. Exp. Biol.* 205: 1153-1160.

Langenbuch M, Pörtner HO (2003) Energy budget of hepatocytes from Antarctic fish (*Pachycara brachycephalum* and *Lepidonotothen kempi*) as a function of ambient CO_2: pH-dependent limitations of cellular protein biosynthesis? *J. Exp. Biol.* 206: 3895-3903.

Langenbuch M, Bock C, Leibfritz D, Pörtner HO (2006) Effects of environmental hypercapnia on animal physiology: A ^{13}C NMR study of protein synthesis rates in the marine invertebrate *Sipunculus nudus*. *Comp. Biochem. Physiol.* A 144 (2006) 479-484.

Lannig G, Eilers S, Pörtner HO, Sokolova IM, Bock C (2010) Impact of Ocean Acidification on energy metabolism of oyster, *Crassostrea gigas* – Changes in metabolic pathways and thermal response. *Mar. Drugs* 8: 2318-2339.

Lawrence JC, Fadden P, Haysted TAJ, Lin TA (1997) PHAS proteins as mediators of the actions of insulin growth factors and cAMP on protein synthesis and cell proliferation. *Advan. Enzyme Regul.* 37: 239-267.

Lewis JR (1964) The Ecology of Rocky Shores. *English University Press*, London, 323 pp.

Lutz RA, Kennish MJ (1992) Ecology and morphology of larval and early postlarval mussels (Chapter 3). In: Gosling E (ed) (1992) The mussel Mytilus: Ecology, Physiology, Genetics and Culture. *Development in Aquaculture and Fisheries Science 25. Elsevier Science Publishers B.V.,* Amsterdam, The Netherlands. pp. 53-85

Lyndon AR, Houlihan DF (1998) Gill Protein turnover: Costs of Adaptation. *Comp. Biochem Physiol.* 119A (1): 27-34.

Lyons C, Dowling V, Tedengreen M, Gardeström J, Hartl MGL, O'Brien N, van Pelt FNAM, O'Halloran JO, Sheehan D (2003) Variability of heat shock proteins and glutathione S-transferase in gill and digestive gland of blue mussel, *Mytilus edulis. Mar. Environ. Res.* 56: 585-597

Mark FC, Hirse T, Pörtner HO (2005) Thermal sensitivity of cellular energy budgets in some Antarctic fish hepatocytes. *Polar Biol.* 28: 805-814

McNurlan MA, Tomkins AM, Garlick P J (1979) The effect of starvation on the rate of protein synthesis in rat liver and small intestine. *Biochem. J.* 178: 373-379.

Melzner F, Gutowska MA, Langenbuch M, Dupont S, Lucassen M, Thorndyke MC, Bleich M, Pörtner HO (2009) Physiological basis for a high CO_2 tolerance in marine ectothermic animals: pre-adaptation through lifestyle and ontogeny. Biogeosciences 6: 2313-2331.

Melzner F, Thomsen J, Koeve W, Oschlies A, Gutowska MA, Bange HW, Hansen HP, Körtzinger A (2013) Future ocean acidification will be amplified by hypoxia in coastal habitats. Mar Biol 160: 1875-1888.

Michaelidis B, Ouzounis C, Palera A, Pörtner HO (2005) Effects of long-term moderate hypercapnia on acid-base balance and growth rate in marine mussles *Mytilus galloprovincialis*. Mar Ecol Prog Ser 293:109-118.

Morton B (1992) The Evolution and Success of the hetromyarian form in the Mytiloida (Chapter 2). In: Gosling E (ed) (1992) The mussel Mytilus: Ecology, Physiology, Genetics and Culture. *Development in Aquaculture and Fisheries Science 25. Elsevier Science Publishers B.V.,* Amsterdam, The Netherlands. pp. 21-52.

Nagarajan R, Lea SEG, Goss-Custand JD (2006) Seasonal variations in mussels, *Mytilus edulis* L. shell thickness and strength and their ecological implications. J Exp Mar Biol Ecol 339:241-250.

Norling P, Kautsky N (2008) Patches of the mussel *Mytilus* sp. are islands of high biodiversity in subtidal sediment habitats in the Baltic Sea. Aquat Biol 4: 75-87.

Owen SF, McCarthy ID, Watt PW, Ladero V, Sanchez JA, Houlihan DF, Rennie MJ (1999) In vivo rates of protein synthesis in Atlantic salmon (Salmo salar L.) smolts determined using a stable isotope flooding dose technique. *Fish Physiol. Biochem.*20: 87-94.

Peck LS, Pörtner HO, Hardewig I (2002) Metabolic Demand, Oxygen Supply, and Critical Temperatures in the Antarctic Bivalve *Laternula elliptica*. Physiol & Biochem Zool 75: 123-133.

Perry AL, Low PJ, Ellis JR, Reynolds JD (2005) Climate Change and Distribution Shifts in Marine Fish. *Science* 308: 1912-1915

Philips DJH (1976a) The common mussel *Mytilus edulis* as an indicator of pollution by zinc, cadmium, lead and copper. I. Effects of environmental variables on uptake of metals. *Mar. Biol.*38 (1): 59-69.

Philips DJH (1976b) The common mussel *Mytilus edulis* as an indicator of pollution by zinc, cadmium, lead and copper. II. Relationship of metals in the mussel to those discharged by industry. *Mar. Biol.*38 (1): 71-80.

Pörtner HO (1987) Contributions of anaerobic metabolism to pH regulation in animals tissues: Theory. *J. Exp. Biol.* 131: 69-87.

Pörtner HO (2001) Climate change and temperature-dependent biogeography: oxygen limitation of thermal tolerance in animals. Naturwissenschaften 88: 137-146.

Pörtner HO (2002) Climate variations and the physiological basis of temperature-dependent biogeography: systemic to molecular hierarchy of thermal tolerance in animals. Comp Biochem Physiol A Mol Integr Physiol 132: 739-761.

Pörtner HO (2010) Oxygen and capacity limitation of thermal tolerance: a matrix for integrating climate related stressors in marine ecosystems. J Exp Biol 213: 881-893

Pörtner HO (2012) Integrating climate-related stressor effects on marine organisms: unifying principles linnking molecule to ecosystem-level changes. Mar Biol Prog Ser 470: 273-290

Pörtner HO, Langenbuch M, Reipschläger A (2004) Biological Impact of Elevated Ocean CO_2 concentrations: Lessons from Animal Physiology and Earth History. J*. Oceanogr.* 60: 705-718.

Pörtner HO, Farrel AP (2008) Physiology and climate change. Science 322:690-692.

Ragnarsson SÁ, Raffaelli D (1999) Effects of the mussel *Mytilus edulis* L. on the invertebrate fauna of sediments. *J. Exp. Mar. Biol. Ecol.* 241: 31-43.

Reipschläger A, Pörtner HO (1996) Metabolic depression during environmental stress: the role of extracellular versus intracellular pH in *Sipunculus nudus*. *J. Exp. Biol.* 199: 1801-1807.

Reusch TBH, Chapman ARO (1997)Persistence and space occupancy by subtidal blue mussel patches. *Ecol. Monogr.* 67 (1): 65-87.

Schäfer J, Stejskal EO, McKay RA, Dixon WT (1984) Phenylalanine Ring Dynamics by Solid-State ^{13}C NMR. *J. Magn. Reson.* 57: 85-92.

Seed R, Richardson CA (1990) Mytilus growth and its environmental responsiveness. In: Stefano GB (Editor) Neurobiology of *Mytilus edulis*. Manchester University Press, Manchester pp. 1-37.

Seed R, Suchanek TH (1992) Population and community ecology of *Mytilus* (Chapter 4). In: Gosling E (ed) (1992) The mussel Mytilus: Ecology, Physiology, Genetics and Culture. *Development in Aquaculture and Fisheries Science 25. Elsevier Science Publishers B.V.,* Amsterdam, The Netherlands. pp. 87-169

Sokolova, Frederich M, Bagwe R, Lannig G, Sukhotin AA (2012) Energy homeostasis as an integrative tool for assessing limits of environmental stress tolerance in aquatic invertebrates. *Mar. Environ. Res.* 79: 1-15.

Somero GN, DeVries (1967) Temperature tolerance of some Antarctic fishes. *Science* 156: 257–258

Somero GN (2012) The Physiology of Global Change: Linking Patterns to Mechanisms. *Annu. Rev. Mar. Sci.* 4: 39-61.

Stapp L (2011) Einfluss der Temperatur auf den zellulären Energiestoffwechsel der antarktischen Aalmutter (*Pachycara brachycephalum*, Pappenheim 1912). Diploma thesis, Johann Wolfgang Goethe-University Frankfurt am Main.

Stephens RE, Prior G (1992) Dynein from serotonin-activated cilia and flagella: extraction characteristics and distinct sites for cAMP-dependent protein phosphorylation. *J. Cell Sci.* 103: 999-1012.

Stommel EW, Stephens RE (1985) Cyclic AMP and calcium in the differential control of *Mytilus* gill cilia. *J. Comp. Physiol.* 157: 451-459.

Strobel A, Graeve M, Pörtner HO, Mark FC (2013a) Mitochondrial acclimation capacities to ocean warming and acifdification are limited in the Antarctic nototheniid fish, *Notothenia rossii* and *Lepidonotothen squamifrons*. *Plos One* 8 (7): 1-11.

Strobel A, Mark FC, Baker DW, Oellermann M, Iftikar FI, Hickey AJR, Pörtner HO (2013b) Compensation capacities for ocean acidification in the Austral nototheniid *N. angustata*. In: Strobel A (2013) Mitochondrial plasticity in response to changing abiotic factors in Antarctic fish and cephalopods. PhD thesis University Bremen. Publication IV, pp. 155-175

Strømgren T (1975) Linear measurements of growth of shells using laser diffraction. *Limnol. Oceanogr.*20: 845-848.

Suchanek TH (1981) The role of disturbance in the evolution of life history strategies in the intertidal mussels *Mytilus edulis* and *Mytilus californianus*. Oecologia (Berl.) 50: 143-152.

Suchanek TH (1985) Mussels and their role in structuring rocky shore communities. In: Moore PG and Seed R (Editors) The Ecology of Rocky Coasts. Hodder and Stoughton, Sevenoaks, U.K., pp.70-96.

Surks MI, Berkowitz M (1971). Rat hepatic polysome profiles and in vitro protein synthesis during hypoxia. *Am. J. Physiol.* 220(6): 1606-1609.

Thomsen J, Gutowska MA, Saphörster J, Heinemann A, Trübenbach K, Fietzke J, Hiebenthal C, Eisenhauer A, Körtzinger A, Wahl M, Melzner F (2010) Calcifying invertebrates succeed in a naturally CO_2-rich coastal habitat but are threatened by high levels of future acidification. Biogeosciences 7: 3879-3891.

Thomsen J, Melzner F (2010) Moderate seawater acidification does not elicit long-term metabolic depression in the blue mussel Mytilus edulis. Mar Biol 157: 2667-2676.

Thomsen J, Casties I, Pansch C, Kortzinger A, Melzner F (2013) Food availability outweighs ocean acidification effects in juvenile *Mytilus edulis*: laboratory and field experiments. Glob Change Biol 19: 1017-1027.

Tresguerres M, Buck J, Levin LR (2010a) Physiological carbon dioxide, bicarbonate and pH sensing. *Eur. J. Physiol.* 460: 953-964.

Tresguerres M, Parks SK, Salazar E, Levin LR, Goss GG, Buck J (2010b) Bicarbonate-sensing soluble adenylyl cyclase is an essential sensor for acid/base homeostasis. *P. Natl. Acad. Sci. USA* 107 (1): 442-447.

Tresguerres M, Barott KL, Barron ME, Roa JN (2014) Established and potential physiological roles of bicarbonate-sensning soluble adenylyl cyclase (sAC) in aquatic animals. J Exp Biol 217: 663-672.

Tsuchiya M, Nishihira M (1985) Islands of *Mytilus* as habitat for small intertidal animals: effect of island size on community structure. Mar Ecol Prog Ser 25: 71-81.

Tsuchiya M, Nishihira M (1986) Islands of *Mytilus* as habitat for small intertidal animals: effect of *Mytilus* age structure on the species composition of the associated fauna community organization. Mar Ecol Prog Ser 31: 171-178.

Tuffnail W, Mills GA, Cary P, Greenwood R (2009) An environmental ^{1}H NMR metabolomic study of the exposure of the marine mussel Mytilus edulis to atrazine, lindane, hypoxia and starvation. Metabolomics 5: 33-34.

Walsh PJ, Mommsen TP, Moon TW, Perry SF (1988) Effects of acid-base variables on *in vitro* hepatic metabolism in rainbow trout. *J. Exp. Biol.* 135:231-241.

Widdows J, Donkin P (1989) The application of combined tissue residue chemistry and physiological measurements of mussels (*Mytilus edulis*) for the assessment of environmental pollution. *Hydrobiol*. 188/189: 455-461.

Wittmann AC, Schroer M, Bock C, Steeger HU, Paul RJ, Pörtner HO (2009) Indicators of oxygen- and capacity-limited thermal tolerance in the lugworm *Arenicola marina. Clim. Res.* 37: 227-240.

Zandee DI, Holwerda DA, Kluytmans JH, Zwaan A de (1986) Metabolic adaptations to environmental anoxia in the intertidal bivalve mollusk *Mytilus edulis* L.. Neth. J. Zool. 36 (3): 322-343.

Zippin JH, Levin LR, Buck J (2001) CO_2/HCO_3^- -responsive soluble adenylyl cyclase as a putative metabolic sensor. *TRENDS Endocrin. Met.* 12 (8): 366-370.

Zittier ZMC, Bock C, Lannig G, Pörtner HO (*submitted*) Impact of ocean acidification on thermal tolerance and acid-base regulation of *Mytilus edulis* (L.) from the North Sea.

Zwaan A de, Bont AMT de, Hemelraad J (1983)The role of phosphoenolpyruvate carboxykinase in the anaerobic metabolism of the sea mussel Mytilus edulis L.. *J. Comp. Physiol.* 153: 267-274.

Zwaan A de, Mathieu M (1992) Cellular Biochemistry and Endocrinology (Chapter 6). In: Gosling E (ed) (1992) The mussel Mytilus: Ecology, Physiology, Genetics and Culture. *Development in Aquaculture and Fisheries Science 25. Elsevier Science Publishers B.V.,* Amsterdam, The Netherlands. pp. 223-307.

7. Acknowledgements

Firstly, I want to thank my first supervisor Prof. Dr. Hans-Otto-Pörtner for letting me conduct my Master's thesis in the Department for Integrative Ecophysiology at the AWI and for reviewing this thesis. Further, I would like to thank Prof. Dr. Wilhelm Hagen for the second supervision of this thesis.

Special thanks go to Dr. Christian Bock for direct supervision of this study, including constructive discussions and very helpful cheer-ups!

Thank you to Dr. Gisela Lannig for constructive discussions and hands-on supervision, especially during the planning of the experimental design! Moreover, I would like to thank Laura Stapp for her amazing amount of knowledge, help and support during all parts of this thesis!

I further want to thank the technicians of the Department for Integrative Ecophysiology, especially Rolf Wittig for NMR assistance and Anette Tillmann for her assistance during the incubations and for the positive lab environment, but also Nils Koschnik and Timo Hirse for technical support and for answering a lot of annoying questions!

Further, I want to thank Prof. Dr. Stephan Frickenhaus for sharing his statistical knowledge with me and to Zora Zittier for helpful discussions and (re-)organizing my thoughts especially during the final week!

Generally, I want to thank the whole Department for Integrative Ecophysiology at AWI for helpful discussions, methodological advice, cheering ups and happy hours with special thanks to the train commuters and my office mates Andrea, Alex, Basti, Anne and Ela for taking my mind off work from time to time!

Last, but not least I want to thank my family and all my friends for listening, field trips, positive energy, music and for just being there for me, especially my fellow "Marine biology" and "EMBC" mates!

8. Declaration

I hereby declare that I have developed and written the enclosed master's thesis entitled "Determination of acute protein biosynthesis rates in the blue mussel *M. edulis*: The role of hemolymph parameters in temperature-dependent growth" entirely on my own and have not used outside sources without declaration in the text. Any concepts or quotations applicable to these sources are clearly attributed to them.

This thesis has not been submitted in the same or substantially similar version, not even in part, to any other authority for grading and has not been published elsewhere.

Bremen, April 2014

_____

Franziska Kupprat

9. Appendix

Table A1 Acquisition parameters for ^{1}H resonance cpmg experiments and ^{13}C resonance zgig experiments acquired on a 9.4 T Avance 400 WB NMR spectrometer (Bruker Biospin GmbH, Germany) with a triple tunable ^{1}H-^{13}C-^{31}P-HRMAS probe.

Experimental measurement parameters	**^{13}C experiments (cytosolic extract)**	**^{13}C experiment (protein extract)**	**^{1}H experiments (cytosolic and protein extract)**
Spinning rate	3000 Hz	3000 Hz	3000 Hz
Pulse program	zgig	zgig	cpmg with water saturation
Time Domain	32768	32768	70656
Sweep width	22 kHz resulting in 219 ppm	22 kHz resulting in 219 ppm	88 kHz resulting in 22 ppm
Acquisition time	0.74 sec	0.74 sec	4 sec
Delay between pulses	2 sec	2 sec	4 sec
Receiver gain	2050	2050	71
Number of scans	1024	20480	32
Number of dummy scans	0	0	4

Table A2 Summarized results of the rANOVA and the *post hoc* Tukey's multiple comparison test for PO_2 data of *M. edulis* at four different temperatures as calculated in Prism 5. Asterisks indicate the level of significance: * p<0.05; ** p<0.01; *** p<0.001; ns: not significant.

Shapiro-Wilk normality test					
	10°C	16°C	22°C	25°C	
P Value	0.9143	0.4732	0.1068	0.3428	
W Value	0.9752	0.9489	0.9077	0.9395	
Bartlett's test for homogeneous variances					
K-squared	1.918				
df	3				
P value	0.5896				
rANOVA					
P value	< 0.0001				
F	20.68				
R square	0.5796				
Was the pairing significantly effective?					
R square	0.3276				
F	3.477				
P value	0.0006				
ANOVA Table	SS	df	MS		
Treatment (between columns)	43665	3	14555		
Individual (between rows)	36708	15	2447		
Residual (random)	31669	45	703.7		
Total	112041	63			
Tukey's Multiple Comparison Test	Mean Difference	q	Significant? P < 0.05?	Summary	95% CI of diff
10°C vs 16°C	10.95	1.650	No	ns	-14.11 to 36.00
10°C vs 22°C	31.15	4.697	Yes	**	6.100 to 56.20
10°C vs 25°C	68.56	10.34	Yes	***	43.50 to 93.61
16°C vs 22°C	20.21	3.047	No	ns	-4.846 to 45.26
16°C vs 25°C	57.61	8.686	Yes	***	32.56 to 82.66
22°C vs 25°C	37.40	5.640	Yes	**	12.35 to 62.46

Table A3 Summarized results of the one-way ANOVA for cytosolic ^{13}C- phenylalanine of all cytosolic 6h and 9h samples from all incubations.

Shapiro-Wilk normality test				
Incubation 1	**^{1}H 6h**	**^{1}H 9h**	**^{13}C 6h**	**^{13}C 9h**
P value	0.8623	0.1985	0.1974	0.9142
W value	0.9734	0.841	0.8407	0.9821
Incubation 2	**^{1}H 6h**	**^{1}H 9h**	**^{13}C 6h**	**^{13}C 9h**
P value	0.5562	0.08842	0.3246	0.4432
W value	0.9234	0.7919	0.8767	0.9024
Incubation 3	**^{1}H 6h**	**^{1}H 9h**	**^{13}C 6h**	**^{13}C 9h**
P value	0.2012	0.02629	0.7069	0.5327
W value	0.8351	0.7618	0.9766	0.9413

Bartlett's test for homogeneity of variances		
	^{1}H- spectra	**^{13}C- spectra**
K-squared	1.9626	6.9806
df	5	5
p	0.8543	0.2221

One-way ANOVA						
P value	0.6022			0.2298		
Number of groups	6			6		
F	0.7437			1.564		
R square	0.1886			0.3427		
ANOVA Table	SS	df	MS	SS	df	MS
Treatment (between columns)	21.20	5	4.24	1801	5	360.3
Residual (within columns)	91.22	16	5.701	3455	15	230.3
Total	112.4	21		5256	20	

Table A4 Best-fit values for linear regressions of protein ^{13}C- phenylalanine incorporation [AU] over time [h] (Figure 14).

Incubation 1				
	A	B	C	D
Slope	2.871 ± 1.197	8.269 ± 1.597	2.671 ± 1.474	3.931 ± 1.148
Y-intercept when X=0.0	15.98 ± 7.475	6.395 ± 9.976	14.82 ± 9.204	36.07 ± 7.169
X-intercept when Y=0.0	-5.565	-0.7733	-5.549	-9.177
1/slope	0.3483	0.1209	0.3744	0.2544
95% Confidence Intervals				
Slope	-12.34 to 18.08	-12.03 to 28.57	-16.06 to 21.40	-10.66 to 18.52
Y-intercept when X=0.0	-78.99 to 111.0	-120.4 to 133.1	-102.1 to 131.8	-55.02 to 127.2
X-intercept when Y=0.0	-infinity to +infinity	-infinity to +infinity	-infinity to +infinity	-infinity to 4.741
Goodness of Fit				
R square	0.8519	0.964	0.7666	0.9214
Sy.x	7.757	10.35	9.551	7.44
Incubation 2				
	A	B	C	
Slope	3.686 ± 0.6403	3.262 ± 1.646	3.874 ± 1.623	
Y-intercept when X=0.0	15.92 ± 3.999	23.96 ± 10.28	17.96 ± 10.13	
X-intercept when Y=0.0	-4.32	-7.347	-4.636	
1/slope	0.2713	0.3066	0.2581	
95% Confidence Intervals				
Slope	-4.450 to 11.82	-17.66 to 24.18	-16.74 to 24.49	
Y-intercept when X=0.0	-34.89 to 66.73	-106.7 to 154.6	-110.8 to 146.7	
X-intercept when Y=0.0	-infinity to 4.150	-infinity to +infinity	-infinity to +infinity	
Goodness of Fit				
R square	0.9707	0.797	0.8507	
Sy.x	4.15	10.67	10.52	
Incubation 3				
	A	B	C	
Slope	3.866 ± 2.712	3.803 ± 1.533	3.456 ± 1.091	
Y-intercept when X=0.0	23.36 ± 16.94	19.83 ± 9.574	19.76 ± 6.816	
X-intercept when Y=0.0	-6.042	-5.214	-5.719	
1/slope	0.2587	0.2629	0.2894	
95% Confidence Intervals				
Slope	-30.59 to 38.32	-15.68 to 23.28	-10.41 to 17.32	
Y-intercept when	-191.8 to 238.6	-101.8 to 141.5	-66.83 to 106.4	

X=0.0				
X-intercept when Y=0.0	-infinity to +infinity	-infinity to +infinity	-infinity to +infinity	
Goodness of Fit				
R square	0.6702	0.8602	0.9093	
Sy.x	17.58	9.935	7.073	
Incubation 4				
	A	B	C	
Slope	6.766 ± 1.779	5.609 ± 1.324	5.867 ± 3.444	
Y-intercept when X=0.0	16.76 ± 11.11	17.77 ± 8.268	28.72 ± 21.51	
X-intercept when Y=0.0	-2.477	-3.168	-4.895	
1/slope	0.1478	0.1783	0.1704	
95% Confidence Intervals				
Slope	-15.83 to 29.37	-11.21 to 22.43	-37.90 to 49.63	
Y-intercept when X=0.0	-124.4 to 157.9	-87.29 to 122.8	-244.6 to 302.0	
X-intercept when Y=0.0	-infinity to +infinity	-infinity to +infinity	-infinity to +infinity	
Goodness of Fit				
R square	0.9354	0.9472	0.7437	
Sy.x	11.53	8.58	22.32	
Incubation 5				
	A	B		
Slope	5.165 ± 3.145	6.044 ± 2.462		
Y-intercept when X=0.0	20.81 ± 19.64	5.538 ± 15.37		
X-intercept when Y=0.0	-4.03	-0.9162		
1/slope	0.1936	0.1655		
95% Confidence Intervals				
Slope	-34.79 to 45.12	-25.23 to 37.32		
Y-intercept when X=0.0	-228.7 to 270.3	-189.8 to 200.9		
X-intercept when Y=0.0	-infinity to +infinity	-infinity to +infinity		
Goodness of Fit				
R square	0.7296	0.8577		
Sy.x	20.38	15.95		

Table A5 Summarized results of the one-way ANOVA for protein biosynthesis rates excluding incubation 1 with *post hoc* Bonferroni's multiple comparison test. Asterisks indicate the level of significance: * p<0.05; ** p<0.01; *** p<0.001; ns: not significant.

Shapiro-Wilk normality test					
Incubation	1	2	3	4	5
P value	0.08437	0.5816	0.2734	0.4087	Not possible
W value	0.7893	0.9528	0.8621	0.9072	Not possible

Bartlett's test for homogeneity of variances	Including incubation 1	Excluding incubation 1
K-squares	12.798	1.943
Df	4	3
P value	0.01231	0.5843

One-way ANOVA	
P value	0.0005
Number of groups	4
F	22.83
R square	0.9073

ANOVA Table	SS	df	MS
Treatment (between columns)	13.88	3	4.626
Residual (within columns)	1.418	7	0.2026
Total	15.30	10	

Bonferroni's Multiple Comparison Test	Mean Diff.	t	Significant? P < 0.05?	Summary	95% CI of diff
inc 2 vs inc 3	-0.01010	0.2748	No	ns	-1.437 to 1.235
inc 2 vs inc 4	-0.2473	6.730	Yes	**	-3.810 to -1.137
inc 2 vs inc 5	-0.1997	4.861	Yes	*	-3.491 to -0.5032
inc 3 vs inc 4	-0.2372	6.455	Yes	**	-3.709 to -1.036
inc 3 vs inc 5	-0.1896	4.615	Yes	*	-3.390 to -0.4022
inc 4 vs inc 5	0.04762	1.159	No	ns	-1.018 to 1.970

Table A6 Summarized results of the one-way Kruskal- Wallis test for cytosolic succinate levels in incubations 1-3 with *post hoc* Dunn's multiple comparison test comparing each time point of each incubation with each other.

Shapiro-Wilk normality test			
Incubation 1	0h	6h	9h
P value	0.5089	0.7248	0.4334
W value	0.9149	0.9514	0.9005
Incubation 2	0h	6h	9h
P value	0.08824	0.8002	0.883
W value	0.7918	0.9634	0.9768
Incubation 3	0h	6h	9h
P value	0.2477	0.7203	0.5239
W value	0.8527	0.9787	0.9391

Bartlett's test for homogeneity of variances	
K-squares	19.4616
Df	8
P value	0.01258

Kruskal-Wallis test	
P value	0.0039
Number of groups	9
Kruskal-Wallis statistic	22.58

Dunn's Multiple Comparison Test	Difference in rank sum	Significant? P < 0.05?	Summary
inc 1 0h vs inc 1 6h	1.250	No	ns
inc 1 0h vs inc 1 9h	-4.000	No	ns
inc 1 0h vs inc 2 0h	12.75	No	ns
inc 1 0h vs inc 2 6h	-15.00	No	ns
inc 1 0h vs inc 2 9h	-12.00	No	ns
inc 1 0h vs inc 3 0h	1.250	No	ns
inc 1 0h vs inc 3 6h	1.917	No	ns
inc 1 0h vs inc 3 9h	0.2500	No	ns
inc 1 6h vs inc 1 9h	-5.250	No	ns
inc 1 6h vs inc 2 0h	11.50	No	ns
inc 1 6h vs inc 2 6h	-16.25	No	ns
inc 1 6h vs inc 2 9h	-13.25	No	ns
inc 1 6h vs inc 3 0h	0.0	No	ns
inc 1 6h vs inc 3 6h	0.6667	No	ns
inc 1 6h vs inc 3 9h	-1.000	No	ns
inc 1 9h vs inc 2 0h	16.75	No	ns
inc 1 9h vs inc 2 6h	-11.00	No	ns
inc 1 9h vs inc 2 9h	-8.000	No	ns
inc 1 9h vs inc 3 0h	5.250	No	ns
inc 1 9h vs inc 3 6h	5.917	No	ns
inc 1 9h vs inc 3 9h	4.250	No	ns
inc 2 0h vs inc 2 6h	-27.75	Yes	**
inc 2 0h vs inc 2 9h	-24.75	Yes	*

inc 2 0h vs inc 3 0h	-11.50	No	ns
inc 2 0h vs inc 3 6h	-10.83	No	ns
inc 2 0h vs inc 3 9h	-12.50	No	ns
inc 2 6h vs inc 2 9h	3.000	No	ns
inc 2 6h vs inc 3 0h	16.25	No	ns
inc 2 6h vs inc 3 6h	16.92	No	ns
inc 2 6h vs inc 3 9h	15.25	No	ns
inc 2 9h vs inc 3 0h	13.25	No	ns
inc 2 9h vs inc 3 6h	13.92	No	ns
inc 2 9h vs inc 3 9h	12.25	No	ns
inc 3 0h vs inc 3 6h	0.6667	No	ns
inc 3 0h vs inc 3 9h	-1.000	No	ns
inc 3 6h vs inc 3 9h	-1.667	No	ns

Table A7 Summarized results of the one-way ANOVA for cytosolic fumarate levels for incubation 1-3 with *post hoc* Bonferroni's multiple comparison test comparing each time point of each incubation with each other.

Shapiro-Wilk normality test			
Incubation 1	0h	6h	9h
P value	0.2589	0.3018	0.9936
W value	0.8596	0.871	0.998
Incubation 2	0h	6h	9h
P value	0.007546	0.5325	0.7346
W value	0.6845	0.9192	0.9529
Incubation 3	0h	6h	9h
P value	0.1327	0.4021	0.3145
W value	0.8076	0.9052	0.8766
Bartlett's test for homogeneity of variances			
K-squares	3.486		
Df	8		
P value	0.9003		

One-way ANOVA			
P value	< 0.0001		
Number of groups	9		
F	27.38		
R square	0.9012		
ANOVA Table	SS	df	MS
Treatment (between columns)	0.01669	8	0.002086

Residual (within columns)	0.001828	24	$7.619*10^{-5}$		
Total	0.01852	32			
Bonferroni's Multiple Comparison Test	Mean Diff.	t	Significant? P < 0.05?	Summary	95% CI of diff
inc 1 0h vs inc 1 6h	0.003765	0.6100	No	ns	-0.01854 to 0.02607
inc 1 0h vs inc 1 9h	-0.002813	0.4557	No	ns	-0.02512 to 0.01949
inc 1 0h vs inc 2 0h	0.01049	1.699	No	ns	-0.01182 to 0.03279
inc 1 0h vs inc 2 6h	-0.05248	8.503	Yes	***	-0.07479 to -0.03018
inc 1 0h vs inc 2 9h	-0.04349	7.047	Yes	***	-0.06580 to -0.02119
inc 1 0h vs inc 3 0h	0.004452	0.6678	No	ns	-0.01964 to 0.02854
inc 1 0h vs inc 3 6h	0.004452	0.6678	No	ns	-0.01964 to 0.02854
inc 1 0h vs inc 3 9h	0.005512	0.8268	No	ns	-0.01858 to 0.02960
inc 1 6h vs inc 1 9h	-0.006578	1.066	No	ns	-0.02888 to 0.01573
inc 1 6h vs inc 2 0h	0.00672	1.089	No	ns	-0.01558 to 0.02902
inc 1 6h vs inc 2 6h	-0.05625	9.113	Yes	***	-0.07855 to -0.03394
inc 1 6h vs inc 2 9h	-0.04726	7.657	Yes	***	-0.06956 to -0.02495
inc 1 6h vs inc 3 0h	0.0006867	0.1030	No	ns	-0.02341 to 0.02478
inc 1 6h vs inc 3 6h	0.0006867	0.1030	No	ns	-0.02341 to 0.02478
inc 1 6h vs inc 3 9h	0.001747	0.2620	No	ns	-0.02235 to 0.02584
inc 1 9h vs inc 2 0h	0.01330	2.155	No	ns	-0.009007 to 0.03560
inc 1 9h vs inc 2 6h	-0.004967	8.048	Yes	***	-0.07197 to -0.02737
inc 1 9h vs inc 2 9h	-0.04068	6.591	Yes	***	-0.06298 to -0.01838
inc 1 9h vs inc 3 0h	0.007264	1.090	No	ns	-0.01683 to 0.03136
inc 1 9h vs inc 3 6h	0.007264	1.090	No	ns	-0.01683 to 0.03136
inc 1 9h vs inc 3 9h	0.008324	1.249	No	ns	-0.01577 to 0.03242
inc 2 0h vs inc 2 6h	-0.06297	10.20	Yes	***	-0.08527 to -0.04066
inc 2 0h vs inc 2 9h	-0.05398	8.746	Yes	***	-0.07628 to -0.03167
inc 2 0h vs inc 3 0h	-0.006033	0.9050	No	ns	-0.03013 to 0.01806
inc 2 0h vs inc 3 6h	-0.006033	0.9050	No	ns	-0.03013 to 0.01806
inc 2 0h vs inc 3 9h	-0.004973	0.7460	No	ns	-0.02907 to 0.01912
inc 2 6h vs inc 2 9h	0.008990	1.457	No	ns	-0.01331 to 0.03129
inc 2 6h vs inc 3 0h	0.05693	8.540	Yes	***	0.03284 to 0.08103
inc 2 6h vs inc 3 6h	0.05693	8.540	Yes	***	0.03284 to 0.08103
inc 2 6h vs inc 3 9h	0.05799	8.699	Yes	***	0.03390 to 0.08209
inc 2 9h vs inc 3 0h	0.04794	7.192	Yes	***	0.02385 to 0.07204
inc 2 9h vs inc 3 6h	0.04794	7.192	Yes	***	0.02385 to 0.07204
inc 2 9h vs inc 3 9h	0.04900	7.351	Yes	***	0.02491 to 0.07310
inc 3 0h vs inc 3 6h	$1.863*10^{-9}$	$2.614*10^{-7}$	No	ns	-0.02576 to 0.02576
inc 3 0h vs inc 3 9h	0.001060	0.1487	No	ns	-0.02470 to 0.02682
inc 3 6h vs inc 3 9h	0.00106	0.1487	No	ns	-0.02470 to 0.02682

Table A8 Summarized results of the one-way ANOVA for lysine levels of all cytosolic 6h and 9h samples from all incubations.

Shapiro-Wilk normality test		
Incubation 1	6h	9h
P value	0.4765	0.3049
W value	0.9089	0.8718
Incubation 2	6h	9h
P value	0.7416	0.1086
W value	0.9541	0.9541
Incubation 3	6h	9h
P value	0.3252	0.4917
W value	0.8803	0.9308

Bartlett's test for homogeneity of variances	
K-squared	1.5612
df	5
p	0.9059

One-way ANOVA (6h and 9h samples only)			
P value	0.2019		
Number of groups	6		
F	1.657		
R square	0.3412		
ANOVA Table	SS	df	MS
Treatment (between columns)	4.288	5	0.8576
Residual (within columns)	8.279	16	0.5174
Total	12.57	21	

Table A9 Summarized results of the one-way ANOVA for trimethylamine oxide (TMAO) content.

Shapiro-Wilk normality test			
Incubation 1	0h	6h	9h
P-value	0.2117	0.559	0.882
W-value	0.8454	0.9239	0.9766
Incubation 2	0h	6h	9h
P-value	0.1608	0.4054	0.8092
W-value	0.8273	0.8947	0.9648
Incubation 3	0h	6h	9h
P-value	0.2271	0.2488	0.08244
W-value	0.845	0.8531	0.7864

Bartlett's test for homogeneity of variances	
K-squared	12.234
Df	8
P-value	0.1411

One-way ANOVA			
P value	0.4200		
Number of groups	9		
F	1.063		
R square	0.2616		
ANOVA Table	SS	df	MS
Treatment (between columns)	52.07	8	6.509
Residual (within columns)	146.9	24	6.123
Total	199.0	32	